Experimental tests of Multiplicative Bell Inequalities.

by

Dilip Paneru

Thesis submitted to the University of Ottawa
in partial fulfillment of the requirements for the
Master of Science degree in Physics

Ottawa-Carleton Institute of Physics
Department of Physics
University of Ottawa

Abstract

This thesis is the synthesis of theoretical and experimental works performed in the area of quantum foundations, particularly on quantum correlations and experimental tests of multiplicative Bell inequalities. First we begin with a comprehensive theoretical work performed on the foundations of quantum mechanics, focusing on the puzzling concepts of quantum entanglement, and hidden variable theories. Specifically, we present a broad overview of different classes of hidden variable theories such as local, crypto-nonlocal, contextual and non-local theories, along with several Bell like inequalities for these theories, providing theoretical proofs based on quantum mechanics for the falsification of some of these theories. Second we present a body of experimental, and theoretical works performed on a new class of Bell inequalities, i.e., the multiplicative Bell inequalities. We experimentally report the observation of the Bell parameters close to the Tsirelson (quantum) limit, upto a large number of measurement devices (n), and compare the results with a particular deterministic strategy. We also obtain classical bounds for some n, and report the experimental violation of these classical limits. We theoretically derive new richer bounds on the CHSH inequality (named after John Clauser, Michael Horne, Abnor Shimony and Richard Holt) and the multiplicative Bell parameter for $n = 2$, based on the principle of "relativistic independence", and experimentally observe the distribution of Bell parameters as predicted by these bounds.

Acknowledgements

I am deeply grateful to my supervisor, Prof. Ebrahim Karimi for his supervision, expert scientific guidance, and continued and generous support during the course of my Master's degree. I have been extremely lucky to have a supervisor who is always available for his students, literally at any time of the day. I acknowledge the financial support of the Canada Research Chairs (CRC), Canada Foundation for Innovation (CFI), and Canada First Excellence Research Fund (CFREF).

I would also like to thank Dr. Eliahu Cohen of university of Bar-Illan university for continuous guidance in science and academia, from the start of my scientific journey, and throughout the years. I am very thankful to the entire Structured Quantum Optics (SQO) group for providing a wonderful atmosphere conducive to research. In particular, I would like to thank Yingwen Zhang for his supervision in getting me started with experimental quantum optics, helping me transition from theory to the laboratory. I am also very thankful to Florence Grenapin for numerous interesting discussions, and for the shared struggle in aligning optics, and countless hours spent in perfecting the single photon source. I am grateful to my colleagues and friends, Frédéric Bouchard, Alicia Sit, Felix Hufnagel, Alessio D'errico, Manuel Ferrer, and all other SQO members, all exemplery scientists, and most importantly great friends, for all the fun times, scientific and otherwise. I would also like to acknowledge all of my coauthors in the presented works, Amit Te'eni, Bar Y. Peled, James Hubble, Avishy Carmi, Robert Fickler, and Robert W. Boyd. I also acknowledge my wonderful friends in the Advanced Research Complex (ARC), for making work place feel like home.

Most importantly, I would like to thank my parents and my wonderful sister, back in Nepal, whose immense support permeating through the great geographical distance, has continued to push me forward. I am also greatly indebted to my friends from Nepal, for their encouragement and friendships.

Statement of originality and collaborative contributions

To the best of his knowledge, the author states that the work described in this Master's thesis constitute original research in the field of physics. E. Karimi initiated the work of Chapter 2. D. Paneru conducted the review study. All the authors contributed to the text of the manuscript. E. Karimi supervised the work. E. Karimi and E. Cohen initiated the work of Chapter 3 D. Paneru designed and performed the experiment. D. Paneru performed the data analysis. E. Cohen, A. Tee'ni, B Y. Peled, A. Carmy, and D. Paneru did the theoretical work. All the authors contributed to the manuscript. E. Karimi, and E. Cohen supervised the work.

Resume

1. Paneru D., and Cohen E., Past of a particle in an entangled state, *International Journal of Quantum Information*, **15**(08), 1740019, (2017).

2. Paneru, D., Cohen, E., Fickler, R., Boyd, R. W., and Karimi, E., Entanglement: quantum or classical?, *Reports on Progress in Physics*, **83**(6), 064001, (2020).

3. Paneru, D., Te'eni, A., Peled, B. Y., Hubble, J., Zhang, Y., Carmi, A., and Karimi, E. (2020), Experimental tests of Multiplicative Bell Inequalities, arXiv:2009.03930.

Table of Contents

List of Tables

List of Figures

Chapter 1

Introduction

1.1 Overview

The mathematical formalism of quantum mechanics was developed in the first half of the nineteenth century in order to explain physical phenomena, such as black-body radiation, Compton scattering, photoelectric effect, among several others. Since then, quantum theory has seen remarkable success in explaining the physical processes at atomic and molecular level, and has branched out to different fields such as philosophy, chemistry [1–3], biology [4–6], and computer science [7–11]. Despite its remarkable success, the foundational concepts such as the the nature of wave function, entanglement, and non-locality still remain as some of the puzzling aspects of quantum theory. The indeterministic nature of measurement outcomes in quantum physics, led scientists to speculate the incompleteness of quantum theory, with numerous attempts to augment it by the addition of new parameters called "hidden variables" [12–14]. For several of such classical theories, theoretical inequalities involving correlations, known as Bell inequalities, have been derived [13], and falsified experimentally, which reaffirms the distinction between quantum and classical physics. In addition to being integral to the study of foundations of quantum mechanics, Bell inequalities are extremely useful in quantum information science [15], providing a way of certifying quantum entanglement and randomness [16]. They are also useful in device independent cryptography, where a Bell inequality violation certifies that the production of the secret keys are random, [15]. The degree of violation of Bell-type inequalities can also serve as a metric of security for device independent quantum cryptographic protocols [17]. In the work in Chapter 2, we start with a historical overview of the development of the theory of quantum entanglement. We go over several thought experiments such as Popper's ghost diffraction, the famous Schrödinger's cat thought experiment, and the EPR paradox. This serves as a background to illustrate the puzzling nature of quantum entanglement. We also introduce local and non-local hidden variable, and contextual theories and offer simple proofs of their incompatibility with quantum mechanics. These proof involve Bell inequalities, the mathematical expressions serving to distinguish between classical and quantum worlds. We also discuss interesting manifestations of quantum mechanics in single particle non-separable states, and N00N states. Going beyond the classical predictions, it is inter-

esting to see to what extent the quantum correlations depart from the classical physics. Expressions involving quantum correlations are bounded by the Tsirelson limit [18]. Recently a new class of Bell inequalities [19] were proposed for which the quantum bound can be easily found. Chapter 3, focuses on the experiment performed on testing the classical and quantum (Tsirelson) bounds of these new inequalities. We present experimental results that are beyond classical limits where applicable and closer to the Tsirelson limit. Additionally, we also derive new richer bounds for the CHSH and the multiplicative Bell parameter $\mathcal{B}_2$, and present experimental observation of these predictions. The rest of the introduction provides brief overview of the basic concepts essential to the experimental and theoretical works in the rest of the thesis. Section 1.2 introduces photon polarisation as the degree of freedom of choice for our 2D Hilbert space. We discuss the maximally entangled Bell states in Section 1.3 , which are essential to the study of experimental and theoretical quantum foundations. We briefly summarize the concepts of quantum projective measurements, (Section 1.5), and the expectation value (Section 1.6).

1.2 Photon polarisation

Electromagnetic waves propagating along a direction (say z axis), have electric and magnetic fields oscillating in the plane transverse ($x-y$ plane) to the direction of propagation. The direction of Electric field is usually taken to be the polarisation vector of the electromagnetic wave. The polarisation space can form a two dimensional Hilbert space for a photon, and since our experiment was performed with photons it serves as a basis for our photon states in subsequent works. Say, we define horizontal polarisation $|H\rangle$ and vertical polarisation $|V\rangle$, as two orthonormal basis vectors for our 2D Hilbert space. Then we can write any single photon state in the polarisation degree of freedom,

$$|\psi\rangle = \cos\theta\,|H\rangle + \sin\theta e^{i\phi}\,|V\rangle\,. \tag{1.1}$$

Other common sets of polarisation vectors used as orthonormal basis, include the diagonally and anti diagonally polarized state, ($|D\rangle$, $|A\rangle$) and left and right circularly polarized state ($|L\rangle$, $|R\rangle$), i.e.,

$$|D\rangle = \frac{1}{\sqrt{2}}\left(|H\rangle + |V\rangle\right), |A\rangle = \frac{1}{\sqrt{2}}\left(|H\rangle - |V\rangle\right) \tag{1.2}$$

$$|L\rangle = \frac{1}{\sqrt{2}}\left(|H\rangle + i\,|V\rangle\right), |R\rangle = \frac{1}{\sqrt{2}}\left(|H\rangle - i\,|V\rangle\right). \tag{1.3}$$

1.3 Bell states

Bell states are four maximally entangled states in 2D Hilbert space, which also form a complete orthonormal basis. Historically, they have been integral to the study of quantum foundations, depicting stark departures of quantum mechanics from the classical world (for example: the EPR state [20]). Bell states also play a vital role in quantum information

science, some applications of which include quantum superdense coding, teleportation, and quantum cryptography.

$$\begin{aligned}\left|\phi^{\pm}\right\rangle &= \frac{1}{\sqrt{2}}\left(\left|H\right\rangle_A\left|H\right\rangle_B \pm \left|V\right\rangle_A\left|V\right\rangle_B\right),\\ \left|\psi^{\pm}\right\rangle &= \frac{1}{\sqrt{2}}\left(\left|H\right\rangle_A\left|V\right\rangle_B \pm \left|V\right\rangle_A\left|H\right\rangle_B\right),\end{aligned} \tag{1.4}$$

where $|H\rangle$ and $|V\rangle$ stand for horizontal and vertical linear polarisation states, and subscript A and B represent photon states for Alice and Bob, two spatially separated observers. In the density matrix formalism, the state say $|\psi^-\rangle$ is written as,

$$\begin{aligned}\rho_{\psi^-} &= \left|\psi^-\right\rangle\left\langle\psi^-\right|\\ &= \frac{1}{\sqrt{2}}\left[\left|H\right\rangle_A\left|V\right\rangle_B - \left|V\right\rangle_V\left|H\right\rangle_B\right]\frac{1}{\sqrt{2}}\left[\left\langle H\right|_A\left\langle V\right|_B - \left\langle V\right|_V\left\langle H\right|_B\right]\\ &= \frac{1}{2}\Big[\left|H\right\rangle_A\left|V\right\rangle_B\left\langle H\right|_A\left\langle V\right|_B - \left|H\right\rangle_A\left|V\right\rangle_B\left\langle V\right|_V\left\langle H\right|_B\\ &- \left|V\right\rangle_V\left|H\right\rangle_B\left\langle H\right|_A\left\langle V\right|_B + \left|V\right\rangle_V\left|H\right\rangle_B\left\langle V\right|_V\left\langle H\right|_B\Big].\end{aligned} \tag{1.5}$$

Written in a matrix form in $|H\rangle_A|H\rangle_B, |H\rangle_A|V\rangle_B, |V\rangle_A|V\rangle_B, |V\rangle_A|V\rangle_B$ basis,

$$\rho_{\psi^-} = \frac{1}{2}\begin{pmatrix}0 & 0 & 0 & 0\\ 0 & 1 & -1 & 0\\ 0 & -1 & 1 & 0\\ 0 & 0 & 0 & 0\end{pmatrix}. \tag{1.6}$$

Similarly the other three Bell states can be written as,

$$\rho_{\psi^+} = \frac{1}{2}\begin{pmatrix}0 & 0 & 0 & 0\\ 0 & 1 & 1 & 0\\ 0 & 1 & 1 & 0\\ 0 & 0 & 0 & 0\end{pmatrix},\ \ \rho_{\phi^\pm} = \frac{1}{2}\begin{pmatrix}1 & 0 & 0 & \pm 1\\ 0 & 0 & 0 & 0\\ 0 & 0 & 0 & 0\\ \pm 1 & 0 & 0 & 1\end{pmatrix}. \tag{1.7}$$

1.4 Rotational invariance of a Bell state

Let us say Alice and Bob share a pair of photons in a maximally entangled Bell state in the polarisation degree of freedom:

$$\left|\phi^+\right\rangle = \frac{1}{\sqrt{2}}\left(\left|H\right\rangle_A\left|H\right\rangle_B + \left|V\right\rangle_A\left|V\right\rangle_B\right). \tag{1.8}$$

This state is also rotationally invariant, which means it stays the same under rotation of the polarisation basis. To see how, let us consider the state in a different basis a, a', rotated by an angle θ with respect to the H, V basis. The basis transformation is given by,

$$\begin{pmatrix}H\\ V\end{pmatrix} = \begin{pmatrix}\cos\theta & -\sin\theta\\ \sin\theta & \cos\theta\end{pmatrix}\begin{pmatrix}a\\ a'\end{pmatrix}. \tag{1.9}$$

Written in the new basis,

$$\begin{aligned}\left|\phi^{+}\right\rangle &= \frac{1}{\sqrt{2}}\big((\cos\theta\left|a\right\rangle_A - \sin\theta\left|a'\right\rangle_A)(\cos\theta\left|a\right\rangle_B - \sin\theta\left|a'\right\rangle_B) \\ &+ (\sin\theta\left|a\right\rangle_A + \cos\theta\left|a'\right\rangle_A)(\sin\theta\left|a\right\rangle_B + \cos\theta\left|a'\right\rangle_B)\big) \\ &= \frac{1}{\sqrt{2}}((\left|a\right\rangle_A\left|a\right\rangle_B + \left|a'\right\rangle_A\left|a'\right\rangle_B), \end{aligned} \tag{1.10}$$

which is of the same form as Eqn.(1.8). The Bell state $|\psi^{-}\rangle$ is also a rotationally invariant state.

1.5 Projective measurements

Projective measurements are measurements performed along a certain measurement vector, say $\mathbf{n}$, that project a quantum state either along the vector $\mathbf{n}$ or in its orthogonal subspace. The probability of a successful projection is dictated by the Born rule, i.e.,

$$P(\mathbf{n}) = Tr[\Pi_{\mathbf{n}}\rho], \tag{1.11}$$

where ρ is the density matrix of the system, and $\Pi_{\mathbf{n}} = |\mathbf{n}\rangle\langle\mathbf{n}|$, is the projection operator along $\mathbf{n}$. After the projective measurement the state "collapses" to either a state $|\mathbf{n}\rangle$ (if successful), or to an orthogonal state. Now say we wish to measure the polarisation along the state given by, $|\theta,\phi\rangle = \cos\theta\,|H\rangle + e^{i\phi}\sin\theta\,|V\rangle$. Then, the corresponding projection operator is given by,

$$\begin{aligned}\Pi_{\theta,\phi} &= |\theta,\phi\rangle\langle\theta,\phi| \\ &= \begin{pmatrix}\cos^2\theta & e^{-i\phi}\sin\theta\cos\theta \\ e^{+i\phi}\sin\theta\cos\theta & \sin^2\theta\end{pmatrix}. \end{aligned} \tag{1.12}$$

If we are confined to the HV plane, then $\phi = 0$, and

$$\Pi_{\theta,\phi=0} = \begin{pmatrix}\cos^2\theta & \sin\theta\cos\theta \\ \sin\theta\cos\theta & \sin^2\theta.\end{pmatrix} \tag{1.13}$$

The joint projection operator for polarisation measurements for Alice along θ_A and Bob along θ_B is given by the tensor product of individual operators,

$$\Pi_{\theta_A,\theta_B} = \Pi_{\theta_A,\phi=0} \otimes \Pi_{\theta_B,\phi=0}. \tag{1.14}$$

The joint probability of detecting two photons along θ_A, and θ_B respectively for a state ψ^{-} is given by,

$$\begin{aligned}\mathcal{P}_{AB} &= Tr[\rho_{\psi^-}\Pi_{\theta_A,\theta_B}] \\ &= \frac{1}{4}\big(1 - \cos 2(\theta_A - \theta_B)\big). \end{aligned} \tag{1.15}$$

1.6 Expectation values

The expectation value of an operator $\hat{O}$ is the average of the the experimental outcomes of measurement of $\hat{O}$ performed on a system. The polarisation operator along θ, $\hat{O}_{\theta,\phi=0}$ is given by,

$$\begin{aligned}
\hat{O}_{\theta,\phi=0} &= |\theta,0\rangle\langle\theta,0| - \left|\theta+\frac{\pi}{2},0\right\rangle\left\langle\theta+\frac{\pi}{2},0\right| \\
&= \begin{pmatrix} \cos^2\theta & \sin\theta\cos\theta \\ \sin\theta\cos\theta & \sin^2\theta \end{pmatrix} - \begin{pmatrix} \sin^2\theta & -\sin\theta\cos\theta \\ -\sin\theta\cos\theta & \cos^2\theta \end{pmatrix} \\
&= \begin{pmatrix} \cos 2\theta & \sin 2\theta \\ \sin 2\theta & \cos 2\theta \end{pmatrix} \qquad (1.16)
\end{aligned}$$

The joint polarisation operator for Alice and Bob along θ_A, and θ_B is given by the tensor product of the individual operators,

$$\hat{O}_{\theta_A,\theta_B} = \hat{O}_{\theta_A,0} \otimes \hat{O}_{\theta_B,0} \qquad (1.17)$$

Now the expectation value of the operator $\hat{O}_{\theta_A,\theta_B}$ is given by,

$$\begin{aligned}
E[\hat{O}_{\theta_A,\theta_B}] &= Tr[\rho_{\psi^-}\hat{O}_{\theta_A,\theta_B}] \\
&= -\cos 2(\theta_A - \theta_B). \qquad (1.18)
\end{aligned}$$

Chapter 2

Quantum Entanglement

This chapter is based on the following paper:

- D. Paneru *et al.*, Entanglement: quantum or classical?, *Reports on Progress in Physics* **83**, 064001 (2020).

2.1 Entanglement

Quantum entanglement is an uniquely quantum phenomenon that defies a classical intuition. In the simplest terms, two particles are said to be entangled if their joint state cannot be expressed as a tensor product of separable states in their individual Hilbert spaces.

$$|\psi\rangle_{AB} \neq |\psi\rangle_A \otimes |\psi\rangle_B \,. \tag{2.1}$$

The most common examples of the entangled states are the four Bell states we encountered before. Alternatively it can also be explained in terms of the Schmidt decomposition, which also serves as a quantifer of entanglement. In general the state of any bipartite system can be written in the following form,

$$|\psi\rangle_{AB} = \sum_i \sum_j c_{ij} \, |a\rangle_i \otimes |b\rangle_j \,, \tag{2.2}$$

where $|a\rangle_i$ and $|b\rangle_j$, $i, j \in \{1, \ldots, n\}$ are the complete sets of vectors in the Hilbert spaces $\mathcal{H}_A$, and $\mathcal{H}_B$ respectively.

If we decompose the state in the following particular form (the Schmidt decomposition) ,

$$|\psi\rangle_{AB} = \sum_i c_i \, |u\rangle_i \otimes |v\rangle_i \,, \tag{2.3}$$

where $|u\rangle_i$ and $|v\rangle_i$, $i \in \{1, \ldots, n\}$ are complete sets of orthonormal vectors in the Hilbert spaces $\mathcal{H}_A$, and $\mathcal{H}_B$ respectively. The number of nonzero coefficients c_j in Equation (2.3), is defined as the Schmidt rank of the system. In mathematical terms a bipartite system is said to be entangled if its Schmidt rank is strictly greater than one.

2.2 Local realism

Einstein, Podolsky and Rosen (EPR) in their 1935 paper [20], argued for the incompleteness of quantum mechanics. According to EPR, a physical theory is complete if to every physical element of reality, there exists a physical quantity in the theory. A real physical quantity needs to have a pre-existing deterministic value irrespective of measurement. Heisenberg's uncertainty principle forbids the simultaneous "reality"of any two non-commuting observables in quantum mechanics. Thus, quantum mechanics is incompatible with the idea of realism. Another aspect of local realism, is the idea of locality, the notion that space-like separated measurements do not influence each other. This again is contradicted by the existence of quantum entanglement, where the measurement outcomes are instantaneously correlated between two entangled particles. Local realism also gave rise to the local hidden variable theories, whose existence is falsified by Bell inequalities.

2.3 Hidden variables

Hidden variables are extra parameters, usually denoted by λ, that are added to quantum theory in order to restore determinism. In a local hidden variables theory, the hidden variables for a particular quantum system are local and unaffected by experiments performed at any other space like separated locations. Consider the usual Alice and Bob scenario, where each of them have access to one of the photons in an EPR pair. Let $\mathbf{A}$ and $\mathbf{B}$ be the polarisation outcomes along $\mathbf{a}$ and $\mathbf{b}$, respectively. Then in a local hidden variable theory, the experimental outcomes $\mathbf{A}$ depends only upon the measurement setting $\mathbf{a}$ and the hidden variable λ. It is independent of B's measurement setting $\mathbf{b}$, and similarly for B, i.e.,

$$\begin{aligned} \mathbf{A} &= \mathbf{A}(\lambda, \mathbf{a}), \\ \mathbf{B} &= \mathbf{B}(\lambda, \mathbf{b}). \end{aligned} \tag{2.4}$$

We also assume that the hidden variable has probability distribution $\rho(\lambda)$. In this formalism, the expectation value of the product of the two outcomes of $\mathbf{A}$ and $\mathbf{B}$, is then given by,

$$P(\mathbf{a}, \mathbf{b}) = \sum_{\lambda} \rho(\lambda)\, \mathbf{A}(\mathbf{a}, \lambda)\, \mathbf{B}(\mathbf{b}, \lambda). \tag{2.5}$$

Simpler proofs for incompatibility of local hidden variables with quantum mechanics is provided in the subsequent paper attached at the end of the chapter. It also discusses several other hidden variables in more detail including the non-local and crypto-nonlocal hidden variable models.

2.4 CHSH inequality

In 1969, John Clauser, Michael Horne, Abner Shimony, and Richard Holt (CHSH) [21] came up with an inequality based on the local hidden variable model. Experimentally, it is easier

to use the Bell-CHSH parameter [21], to verify the entanglement between two photons. The usual two parties, Alice and Bob can each choose from a set of two measurements $\mathbf{a_1}/\mathbf{a_2}$ and $\mathbf{b_1}/\mathbf{b_2}$. If we treat $\mathbf{a_1}$, $\mathbf{a_2}$, $\mathbf{b_1}$, and $\mathbf{b_2}$, as binary classical variables, we have:

$$\mathbf{a_1}, \mathbf{a_2}, \mathbf{b_1}, \mathbf{b_2} = \pm 1.$$

Consider the expression,

$$b_1(a_1 + a_2) + b_2(a_1 - a_2).$$

In every possible combination of a_1 and a_2, either they take the same or different values, either one of the $(a_1 - a_2)$, and $(a_1 + a_2)$ would be zero, and the other one would be ± 2. Hence,

$$|b_1(a_1 + a_2) + b_2(a_1 - a_2)| = 2.$$

Since,

$$|\langle b_1 a_1 + b_1 a_2 + b_2 a_1 - b_2 a_2 \rangle| \leq \langle |b_1 a_1 + b_1 a_2 + b_2 a_1 - b_2 a_2| \rangle ,$$

$$\text{CHSH} = |\langle b_1 a_1 \rangle + \langle b_1 a_2 \rangle + \langle b_2 a_1 \rangle - \langle b_2 a_2 \rangle| \leq 2. \tag{2.6}$$

This inequality is the famous CHSH inequality. To see how we can violate the inequality in quantum mechanics, suppose that Alice and Bob share a pair of photons in the state Eq.(1.8). We know that the expectation value of joint polarisation measurement along $\mathbf{a}$,$\mathbf{b}$ is given by $\cos 2(\theta_a - \theta_b)$.

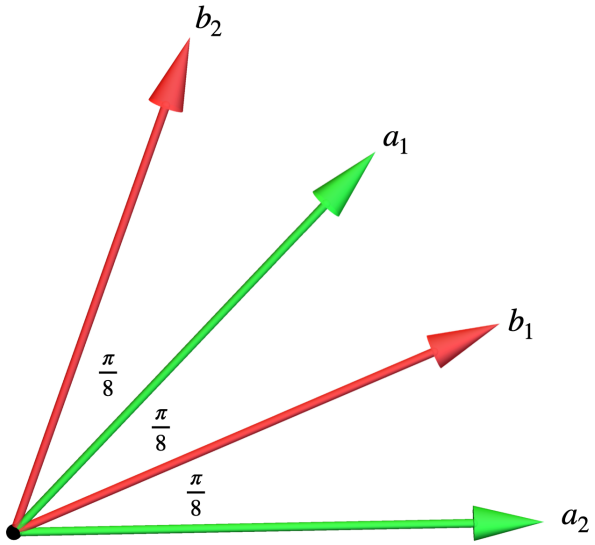

Figure 2.1: The vectors for maximal violation of CHSH inequality.

Now if we choose the vectors $\mathbf{b_2}$,$\mathbf{a_1}$,$\mathbf{b_1}$, and $\mathbf{a_2}$, such that they are separated successively by $\frac{\pi}{8}$, Figure 2.1, then,

$$\begin{aligned} \langle b_1 a_1 \rangle &= \langle b_1 a_2 \rangle = \langle b_2 a_1 \rangle = \cos\left(\frac{\pi}{4}\right) = \frac{1}{\sqrt{2}}, \\ \langle b_2 a_2 \rangle &= \cos\left(\frac{3\pi}{4}\right) = -\frac{1}{\sqrt{2}}. \end{aligned}$$

Then the inequality Eq. (2.6) is violated,

$$2\sqrt{2} > 2.$$

In fact $2\sqrt{2}$ is also the upper limit that can be achieved by quantum mechanics. Hence,

$$\text{CHSH}_{LHV} \leq 2, \;\; \text{CHSH}_{QM} \leq 2\sqrt{2}, \tag{2.7}$$

where CHSH_{LHV}, and CHSH_{QM} are the values of parameter CHSH parameter, Eq. (2.6), as predicted by Local Hidden Variables (LHVs), and Quantum mechanics respectively.

2.5 Single Particle "Entanglement"

States exhibiting non-separability between two different degrees of freedom of a single particle also exhibit interesting correlations [22]. For example, states like,

$$|\psi\rangle = \frac{1}{\sqrt{2}} \left(|\text{Left,H}\rangle + |\text{Right,V}\rangle \right), \tag{2.8}$$

where Left/Right represent the path degree of freedom, and H/V represent the polarisation degree of freedom, cannot be separated into a product of individual states in either of the two Hilbert spaces. As we shall later discuss, these states help to test the classical notion of contextuality, i.e, experimental outcomes are independent of the "context" of a measurement. Using Bell-like inequalities for such states, we can rule out the "local non-contextual hidden variable" description for such states.

Another interesting case of a single particle non-seperable states is the multimode entangled state for a single photon,

$$|\psi\rangle = \frac{1}{\sqrt{2}} \left(|0\rangle_A |1\rangle_B + |1\rangle_A |0\rangle_B \right), \tag{2.9}$$

where A and B are two different optical modes the photon could occupy. These states cannot be prepared by any Local Operations and Classical Communication (LOOC), which satisfies one notion of entanglement. In quantum theory, superselection rules forbid coherence between two eigenstates of certain observables. In quantum optics, if two frames of reference, lack a phase reference, then there is a corresponding superselection rule for photon number [23] which dictates that, any state one prepares in one frame will be block diagonal in the eigenstates of the total number operator in the other. Hence one cannot use just this state to violate Bell's inequality, or perform information processing tasks with it, as that will violate the local photon number superselection rule. Going by this notion, this state would not appear to be entangled. Non-locality of such single photon states have been discussed in many works [24–28], and we will discuss them later as well.

REPORT ON PROGRESS

Entanglement: quantum or classical?

To cite this article: Dilip Paneru *et al* 2020 *Rep. Prog. Phys.* **83** 064001

IOP Publishing Reports on Progress in Physics
Rep. Prog. Phys. **83** (2020) 064001 (19pp) https://doi.org/10.1088/1361-6633/ab85b9

Entanglement: quantum or classical?

Dilip Paneru[1], Eliahu Cohen[1,2], Robert Fickler[1,3], Robert W Boyd[1] and Ebrahim Karimi[1,4]

[1] Department of Physics, University of Ottawa, 25 Templeton Street, Ottawa, Ontario, K1N 6N5 Canada
[2] Faculty of Engineering and the Institute of Nanotechnology and Advanced Materials, Bar Ilan University, Ramat Gan 5290002, Israel
[3] Photonics Laboratory, Physics Unit, Tampere University, Tampere, FI-33720, Finland

E-mail: ekarimi@uottawa.ca

Received 5 November 2019, revised 24 February 2020
Accepted for publication 1 April 2020
Published 26 May 2020

Abstract

From its seemingly non-intuitive and puzzling nature, most evident in numerous EPR-like gedanken experiments to its almost ubiquitous presence in quantum technologies, entanglement is at the heart of modern quantum physics. First introduced by Erwin Schrödinger nearly a century ago, entanglement has remained one of the most fascinating ideas that came out of quantum mechanics. Here, we attempt to explain what makes entanglement fundamentally different from any classical phenomenon. To this end, we start with a historical overview of entanglement and discuss several hidden variables models that were conceived to provide a classical explanation and demystify quantum entanglement. We discuss some inequalities and bounds that are violated by quantum states thereby falsifying the existence of some of the classical hidden variables theories. We also discuss some exciting manifestations of entanglement, such as N00N states and the non-separable single particle states. We conclude by discussing some contemporary results regarding quantum correlations and present a future outlook for the research of quantum entanglement.

Keywords: quantum entanglement, hidden variables, foundations of quantum mechanics, contextuality

(Some figures may appear in colour only in the online journal)

1. Introduction

Until the beginning of the twentieth century, classical mechanics, e.g. Newtonian or Lagrangian, together with Maxwell's electrodynamics were successful in describing and prognosticating nearly all physical phenomena. Eventually, classical physics failed to describe several effects such as black-body radiation, Compton scattering, and the photoelectric effect [1]. Starting with the introduction of the apparently smallest energy quantum by Max Planck [2], the formalism of quantum mechanics was developed in the 1920s to describe the atomic and subatomic world. Since its inception, quantum theory has found numerous theoretical and practical applications in physics, and has even branched out to areas such as biology [3–5], chemistry [6–8], and computer science [9–13]. Countless experiments have validated its predictions, and quantum theory remains today one of the most successful scientific theories developed by mankind. Although very few people disagree or question the correctness of quantum formalism as a mathematical model, its foundational aspects still confound physicists even after more than 90 years since its initial formulation. Issues such as the nature of the wave function and its collapse (in the Copenhagen interpretation) and the state superposition, as well as entanglement, still inspire debates among physicists [14–16]. Apart from the 'standard' Copenhagen interpretation, there are several other interpretations of the quantum formalism such as the pilot wave theories (e.g. Bohmian mechanics [17, 18]), many worlds theories [19], QBism [20], the retro causal interpretations [21, 22], and many more. The 'apparent incompleteness of the wave function description was one of the main reasons that led to these different interpretations. Therefore, physicists suggested to augment

[4] Author to whom any correspondence should be addressed.
Corresponding Editors: Professor Masud Mansuripur.

the wave function with different entities, nowadays referred to as hidden variables [23]. Among the different classes of hidden variables, local [24] and crypto-nonlocal hidden variable theories [25] have been tested and ruled out experimentally, thus showing quantum mechanics to be incompatible with local realistic and even some non-local realistic theories. Alternatively, as the formalism perfectly describes the application of quantum theory to physical problems, many scientists choose to not dwell on the meaning behind the formalism, i.e. on the foundations of quantum mechanics, but rather adopt the famous 'Shut up and calculate' proverb [26]. However, some relatively new developments in closing various experimental loopholes, e.g. freedom-of-choice, fair-sampling, communication (or locality), coincidence and memory loopholes [27–32], have led to a resurgence of interest in quantum foundations, especially in quantum entanglement, even including a global test of entanglement involving many countries, institutes and layman participants [33].

Researchers have also been striving to reach a clear understanding of what really differentiates a quantum theory from a classical theory. For instance, the concept of superposition also appears in classical wave mechanics. In Young's double-slit experiment, coherent light waves, diffracted from two slits, superpose and interfere constructively or destructively at different positions in space, resulting in bright and dark fringes at the far-field region of the slits. This experiment, easily explained by Maxwell's equations, is conceptually different when repeated with a single photon source, or any single quantum objects. Though the probability of detecting photons in the far-field region follows the same fringes pattern, one may ask 'which slit does the photon choose to traverse through?' One can assign some sort of unknown local physical parameters (hidden variables) which determine the path of the single photon. However, these 'hidden variables' are incapable of describing the experimental outcome at the single-photon regime. Even in principle, if we have some way of obtaining the which-path information, then the interference pattern is different. It is impossible to assign local hidden variables to describe the photon's whereabouts before it is actually detected on the screen. These kinds of experiments, analyzing particles at the atomic or molecular level [34–41], touch the very heart of quantum foundations and, in fact, according to Feynman the two-slit experiment contains 'the only mystery' of quantum mechanics [42, 43]. This renders quantum mechanics completely different from any classical theory, and classical electrodynamics in particular, for the above example, and also illustrates many of the questions that have been puzzling scientists since the last century. Very recently, wave super positions among different degrees of freedom of a physical system, e.g. polarization and spatial modes of an optical beam, have been referred to as 'classical entanglement' [44, 45]. We believe that the term 'classical entanglement' is a misnomer as it can easily lead to confusion among non-experts and, sometimes, even experts in the field. First, classical electrodynamics can perfectly describe the physics, as well as correlations, among these different degrees of freedom of optical waves. Thus, there is no need to invoke quantum mechanics for super positions of different degrees of freedom of light. Moreover, entanglement is the fundamental feature of quantum physics between two (or more) systems and the consequences drawn from the obtained correlations do not apply to any classical system, i.e. classical correlations cannot lead to the same conclusions as quantum entanglement. While analogies might be seen in the mathematical formulation, the possibility of spatial separation, which is the key aspect of entanglement, does not hold for the classical counterpart. However, it is important to point out that superposition among different degrees of freedom of a quantum object, e.g. single photon [46, 47] or neutron [48], can be used to test the contextuality of quantum mechanics, which is a *rich* subject of research in itself [47]. Historically, the term entanglement ('verschr' 'ankt' in German) was introduced by Schrödinger to describe nonlocal correlations among different quantum systems. Numerous experiments performed on multi particle entangled states, such as the Hong–Ou–Mandel effect [49], the Franson interferometer [50], etc. have exhibited correlations that do not have any classical counterparts, thus showing entanglement to be purely a quantum effect. Here, we try to provide a comprehensive perspective on entanglement, local and crypto-nonlocal hidden variables, as well as contextual hidden variable theories. We further discuss the relatively new terminology of 'classical entanglement' and hope to clarify its limitations. In addition to these concepts, some recent developments in understanding entanglement, e.g. improvements of nonlocal bounds and their relation to generalized uncertainty principles. We conclude with a future outlook in these areas.

2. Popper's diffraction experiment

In 1934, Karl Popper proposed a thought experiment [51] with entangled particles aimed at analyzing the correctness of the Copenhagen interpretation of quantum mechanics. In his experiment (figure 1), he considered a pair of particles entangled in position and transverse momentum that are traveling in opposite directions towards the two slits. When one of the particles passes through a slit, then by virtue of entanglement we also acquire position information of the second particle. Popper then analyzed the two possible ways the measurement result of the momentum of the second particle could unfold. The first one, which he argued, is according to his understanding of the Heisenberg uncertainty principle, is that position measurement of first particle should cause a large spread in the momentum of the second particle. Heisenberg uncertainty principle for position and momentum of a single particle states,

$$\Delta x \Delta p \geqslant \frac{\hbar}{2}, \tag{1}$$

where Δx and Δp are the uncertainties in the position and momentum, respectively. We see that, according to the Heisenberg uncertainty relation, when the position is known precisely there is a large spread in the momentum. However, this violates the principle of causality as, due to the narrowing or widening of the slit for the first particle, we would instantaneously affect the momentum spread of the second particle. Therefore, according to Popper, we are presented with the choice between relativistic causality and the Copenhagen interpretation.

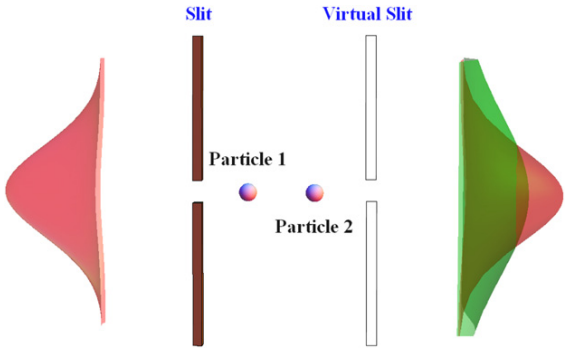

Figure 1. Popper's ghost diffraction setup. Two entangled particles which we label as 1 and 2 travel in opposite directions from a source S. One of the particles, say particle 1, passes through a slit. We then look at the effect of it, i.e. changing the uncertainties in the position of particle 1, on the momentum spread of particle 2. The green curve is the original particle wave function, and the red curve is the second particle's wave function after particle 1 passes through the slit. While particle 2 is more localized, the momentum spread remains constant, thereby saturating the uncertainty relation, but not violating it.

Popper suggested that the momentum spread would not change in an experiment and came to the conclusion that the Copenhagen interpretation must be inadequate [52].

Looking at this experiment more closely, when considering the uncertainty relation for the second particle, we should use the uncertainties in position and momentum that are conditioned upon the measurement result of the first particle. The uncertainty relation reads,

$$\Delta(x_2|x_1)\Delta(p_2|x_1) \geqslant \frac{\hbar}{2}, \tag{2}$$

where $\Delta(x_2|x_1)$ and $\Delta(p_2|x_1)$ are the uncertainties in the position and the momentum of the second particle, respectively conditioned upon the outcome of the position measurement of the first particle. A recent experiment performed using entangled photons generated by spontaneous parametric down conversion (SPDC) [53, 54], has shown that, while there is no spreading of the wave function, it is still consistent with the standard quantum formalism and the conditioned uncertainty principle. While there is less uncertainty in position, the momentum uncertainty remains the same and the product saturates the uncertainty relation but does not violate it. Several other experiments analyzing the different aspects of Popper's experiment have also vindicated the correctness of standard quantum formalism [53–59]. Popper's experiment first showed that entangled states raise profound questions about the nature of quantum mechanics, and indeed we will see in the subsequent sections how entanglement plays a fundamental role in quantum foundations.

2.1. EPR and local realism

In 1935, Einstein, Podolsky and Rosen (EPR) first considered the now well-known EPR pair of particles in their highly influential paper [60], although without using the term 'entanglement'. Analyzing these entangled states, they questioned the completeness of quantum mechanics. In line with the EPR argument, a theory is complete only if it has a physical quantity corresponding to each element of reality. As defined by EPR, a physical quantity is real if its value can be predicted with certainty irrespective of and before any measurement. For example, in classical mechanics, the set of position and momentum (or velocity) is sufficient to assign definite values to any other dynamical physical quantities such as kinetic energy, angular velocity, etc. In this sense, the description provided by classical mechanics can be considered a complete characterization of reality for the particle. EPR questioned whether the wave function (or the state vector) in quantum mechanics is a complete description of physical reality. In quantum mechanics, two physical quantities represented by non-commuting observables cannot be measured simultaneously with arbitrary precision. Whenever we measure one observable, we influence the state in such a way that the measurement outcomes for the other observable is disturbed. Therefore, simultaneous 'realities', at least as per the EPR criteria, do not exist for non-commuting observables. Thus, EPR argued that either (a) quantum theory is incomplete because it cannot simultaneously describe the reality of both of these observables, or (b) there is no simultaneous reality of two non-commuting observables. By using an example of an entangled system with two particles they claimed that there exist two different simultaneous realities for a physical system according to quantum theory. Thus, EPR concluded that quantum theory must be incomplete *in its current form*. Note that EPR excluded the possibility of measurements between spacelike separated events affecting each other instantaneously, or in Einstein's words 'spooky action at a distance' [61], as in their opinion this would contradict special relativity. We will come back to this important issue of non locality later in this section.

Although EPR phrased their argument in terms of position and momentum correlation (just like Popper), it is more useful in the context of this manuscript to use the simpler example of particles entangled in the spin degree of freedom introduced by Bohm [62, 63]. Consider an anti-correlated spin state of two particles A and B, e.g. generated via spontaneous decay,

$$|\psi\rangle = \frac{1}{\sqrt{2}}\left(|\uparrow\rangle_A|\downarrow\rangle_B - |\downarrow\rangle_A|\uparrow\rangle_B\right), \tag{3}$$

where $|\uparrow\rangle$ and $|\downarrow\rangle$ are *spin up* and *spin down* states in the z direction respectively. Note that this formalism can be extended to any other two-dimensional vector spaces, e.g. photonic polarisation or path.

Let us assume that the two particles A and B are spatially separated, such that any local *physical* interaction between them is circumvented. One can perform a measurement on the spin state of particle A in two different bases, say Eigen states of the $\hat{\sigma}_z$ and $\hat{\sigma}_x$ operators, similar to the position and momentum basis in the original EPR argument. Upon performing these measurements, two scenarios will arise for the spin state of particle B:

$\hat{\sigma}_z$: depending upon the outcome of the particle A spin-state measurement, the spin state of particle B is either $|\uparrow\rangle_B$ or $|\downarrow\rangle_B$—it is always opposite to the particle A

spin-state, since the two particles are anti-correlated in the spin degree of freedom. Upon finding the particle A in, say $|\uparrow\rangle_A$, according to EPR, since the first particle cannot affect the second, the state of the second particle should be $|\downarrow\rangle_B$ and the spin in z direction has a value of $-\hbar/2$.

$\hat{\sigma}_x$: now we perform the measurement in the Eigen basis of the $\hat{\sigma}_x$ operator, i.e. $|\pm\rangle = \frac{1}{\sqrt{2}}\left(|\uparrow\rangle \pm |\downarrow\rangle\right)$. The original state written in this basis is,

$$|\psi\rangle = \frac{1}{\sqrt{2}}\left(|+\rangle_A|-\rangle_B - |-\rangle_A|+\rangle_B\right). \tag{4}$$

Note that this state has the same form as in the $|\uparrow\rangle, |\downarrow\rangle$ basis. In fact, the original state has the same form in any orthogonal basis, and we call such states rotationally invariant. Let us assume that we observe particle A in the $|+\rangle$ state. Again we do not disturb the second particle and thus we conclude particle B to be in the state, $|-\rangle = \frac{1}{\sqrt{2}}\left(|\uparrow\rangle - |\downarrow\rangle\right)$. This is an Eigen state of $\hat{\sigma}_x$ with spin $-\hbar/2$.

Without in any way disturbing or interacting with the second particle, we have obtained two simultaneous spin values and states for $\hat{\sigma}_z$ and $\hat{\sigma}_x$, e.g. $|\psi\rangle_B = |\downarrow\rangle$ and $|\psi'\rangle_B = |-\rangle = \frac{1}{\sqrt{2}}\left(|\uparrow\rangle - |\downarrow\rangle\right) \neq |\psi\rangle_B$. Therefore, EPR claim that it is possible to assign the spin values for the two non-commuting operators. This means that the state vector description of quantum mechanics must be an incomplete description of reality.

Nowadays, we understand that there are several problems with the EPR reasoning. One is that a single particle state vector is not an accurate description of the single particle when it is in an entangled state. Quantum mechanics resolves the ambiguity in spin values and the state representation of a particle in an entangled state by using density matrices, which provide a more complete way of representing mixed states. In the density matrix formalism, the joint state of the two particles is represented by the density matrix,

$$\begin{aligned}\hat{\rho}_{AB} &= |\psi\rangle\langle\psi| \\ &= \frac{1}{2}\left(|\uparrow\rangle_A|\downarrow\rangle_B - |\downarrow\rangle_A|\uparrow\rangle_B\right)\left(\langle\uparrow|_A\langle\downarrow|_B - \langle\downarrow|_A\langle\uparrow|_B\right).\end{aligned}$$

If we consider only particle B, its density matrix is,

$$\begin{aligned}\hat{\rho}_B &= \mathrm{Tr}_A\left(|\psi\rangle\langle\psi|\right) \\ &= \frac{1}{2}(|\uparrow\rangle_B\langle\uparrow| + |\downarrow\rangle_B\langle\downarrow|) = \frac{1}{2}\hat{\mathbb{I}},\end{aligned} \tag{5}$$

where $\hat{\mathbb{I}}$ is the identity operator.

Similarly if we decide to measure in the $|+\rangle, |-\rangle$ basis,

$$\begin{aligned}\hat{\rho}_{AB} &= |\psi\rangle\langle\psi| \\ &= \frac{1}{2}\left(|+\rangle_A|-\rangle_B - |-\rangle_A|+\rangle_B\right)\left(\langle+|_A\langle-|_B - \langle-|_A\langle+|_B\right). \\ \hat{\rho}'_B &= \mathrm{Tr}_A\left(|\psi\rangle\langle\psi|\right) \\ &= \frac{1}{2}(|+\rangle_B\langle+| + |-\rangle_B\langle-|), \\ &= \frac{1}{2}\hat{\mathbb{I}}.\end{aligned} \tag{6}$$

Hence, we observe that density matrices resolve the ambiguity in the state representation for photon B. Photon B possesses a unique density matrix, $\hat{\rho}'_B = \hat{\rho}_B = \hat{\mathbb{I}}/2$ what we refer to as maximally mixed state, independent of performing a measurement on photon A spin state.

The state of photon B if considered independently of A is a mixed state. On the contrary, as described before, a measurement conditioned on the outcome of photon A leads to a perfectly predictable outcome for photon B, i.e. perfect correlation in any bases.

There is another fundamental issue of non locality pertaining to entangled states: the idea that measurements performed in spatially separated locations can affect each other. EPR assumed that nature is local and believed that it would violate the principle of causality if experiments performed in one location could affect experiments in far away places. As we will discuss, Bell later showed that a local-realistic description of entangled states is inconsistent with quantum mechanics, effectively ruling out the local hidden variables description of entangled states [24].

2.2. Schrödinger's cat state and 'entanglement'

Erwin Schrödinger, inspired by the EPR paper, introduced the term 'entanglement' for the first time in his 1935 paper [64]. He used the phrase 'entanglement of our knowledge of the bodies' to refer to the joint states where the state of one system is intrinsically linked with the state of another system. Additionally, he also provided a thought experiment involving a macroscopic (classical) object, namely a cat, to illustrate the nature of quantum super positions in entangled states. In his experiment, a cat is placed inside a steel chamber with a small amount of radioactive material. The radioactive material is coupled with a Geiger counter and a vial of poisonous hydro cyanic acid. With a finite probability, one atom of the radioactive material may decay in the course of next few hours, which then registers a click in the Geiger counter. A mechanical apparatus is arranged such that once the counter clicks, it smashes the bottle of hydro cyanic acid releasing the poisonous gas, which kills the cat.

Initially, when no atom has decayed and the cat is alive, the states of the atom and the cat are:

$$|\psi\rangle_{\text{atom}} = |\text{no-decay}\rangle, \quad |\psi\rangle_{\text{cat}} = |\text{alive}\rangle. \tag{7}$$

After some time, it is now impossible to say whether any atom has decayed or not. Depending upon the state of the radioactive atom, it is impossible in turn to ascertain whether the cat is alive or dead. So, until an external observer checks whether the atom has decayed or not, the cat is in a *weird* state of being *dead* and *alive* at the same time. The joint state of the atom and the cat is,

$$\begin{aligned}|\psi\rangle &= |\text{atom and cat}\rangle \\ &= \frac{1}{\sqrt{2}}\left(|\text{decay}\rangle|\text{dead}\rangle + |\text{no-decay}\rangle|\text{alive}\rangle\right).\end{aligned} \tag{8}$$

In the words of Schrödinger, our knowledge of the two bodies becomes entangled. He further elaborated the definition

of entanglement by adding that, even if the two bodies are taken very far from each other, 'knowledge of the two systems cannot be separated into the logical sum of knowledge about two bodies'. It is not possible to express the state of the cat and the atom independently of each other. Until an external observer opens the door of the chamber, thereby performing the measurement, the state remains in the superposition.

Schrödinger initially proposed this thought experiment linking the microscopic world to the macroscopic, classical world to question the Copenhagen interpretation claiming such 'blurred' states where the cat is in some kind of superposition of being alive and dead can only be observed in the microscopic world. It raises the question when the macroscopic objects stop being in a superposition and transform into either one or the other of the alternatives, and if this transition needs to happen at all. This is still an ongoing debate, and there are numerous experiments pushing the limits of 'macroscopic' super positions [65–68]. More importantly, this experiment illustrates the nature of quantum superposition in the context of entangled states.

Wigner [69] proposed an extension of this experiment, with two observers. One observer, say Wigner, stays outside the chamber and another, say Wigner's friend, is positioned inside the chamber. Wigner's friend, by virtue of being inside the chamber can observe a definite outcome, i.e. whether the cat is dead or alive. On the other hand, Wigner has no way of knowing the outcome until his friend mentions it to him. For Wigner, the joint state of the whole system is,

$$|\psi\rangle = \frac{1}{\sqrt{2}}\left[|\text{no-decay}\rangle\,|\text{alive}\rangle\,|\text{friend sees alive cat}\rangle + |\text{decay}\rangle\,|\text{dead}\rangle\,|\text{friend sees dead cat}\rangle\right]. \quad (9)$$

The paradox occurs when we ask 'when did the cat stop being in a superposition state?' For Wigner's friend, it occurs whenever he decides to check if the cat is alive. Wigner, however, sees the state in superposition until his friend tells him the outcome. The two observers will not agree about the time when the cat will be in a definite state. Until today, similar arguments are discussed with novel twists [70–74], which show that the perplexing nature of the entanglement between a 'macroscopic' (or classical) and a 'microscopic' (or quantum) object is still worth a discussion.

3. Hidden variables

In the spirit of EPR, who argued that quantum mechanics is incomplete, hidden variable theories attempt to supplement quantum mechanics by adding some extra parameters. These parameters, or the so called 'hidden variables', are assumed to exist beyond the standard formalism of quantum mechanics and are supposed to resolve the probabilistic nature of quantum experiments. In other words, the hidden variables ensure that in principle there can be a deterministic description of all observables, which might just be unknown to us, thereby restoring the realistic (in the above mentioned sense) description of nature. To look at a simple example of how such hidden variables work, consider, for instance, a photon's polarization. We could represent the polarization of a photon by a three dimensional vector in a sphere called the Poincaré sphere, with each dimension representing the corresponding polarization component. Let us look at four such photons whose polarization vectors make the same angle, $\theta < \frac{\pi}{2}$ as shown in figure 2, with the z-axis, implying that they all have a positive z component. However, along the x-axis and y-axis they can have different polarization. In general, there can be infinitely many such vectors with the same z component that form a cone around the z-axis. Standard quantum mechanics postulates that for the particles measured to have positive polarization in the z-direction, the polarization measurement along say the y axis can give rise, probabilistically, to either the positive, (meaning diagonal polarization $|D\rangle$) or negative (meaning antidiagonal polarization $|A\rangle$). However, in the classical picture we considered, one can assign a hidden variable $\lambda := \lambda(\phi)$, such that,

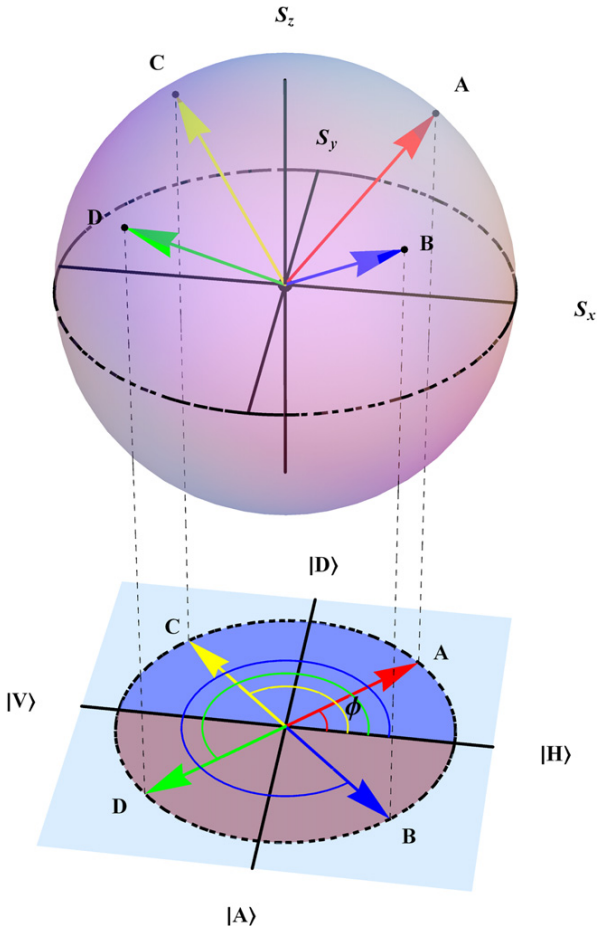

Figure 2. Four polarization-vectors A, B, C and D are represented in Poincaré sphere. The angles made by each vector with the y-axis, which determines which half of the x–y plane each vector lies, could the hidden variables for polarization components in the other two directions (x and y). Here the vectors A and C with projections in the region shaded by blue have positive polarization in the x direction, while vectors B and D with projections in the region shaded by red have negative polarization in x direction.

$$\lambda(\phi) = \begin{cases} +1 & \text{if } 0 \leqslant \phi \leqslant \pi \\ -1 & \text{if } \pi \leqslant \phi \leqslant 2\pi \end{cases} . \tag{10}$$

The variable λ would then accurately describe the polarization in the y direction. For the vectors with $\lambda = +1$, i.e. whose projection vector in the x–y plane lies on the positive half-plane (the region shaded blue in figure 2), the polarization in the y direction is positive. For the vectors with $\lambda = -1$, i.e. whose projection vector in the x–y plane lies on the negative half-plane (the region shaded red in figure 2) the polarization in the y direction is negative. Here, λ serves an example of a hidden variable for the polarization along y-direction.

Different variations of the hidden variables exist depending on their properties and the dependence of these variables on measurement settings in a quantum experiment. We present below some classes of hidden variables theories, a few of which have already been proven to be incompatible with the predictions of quantum theory.

Local hidden variables and Bell's proof. As the name implies, a local hidden variables theory assumes that the hidden variables for a particular quantum system are local and unaffected by experiments performed at any other spatially separated locations. To define it more formally, consider an EPR-like setup with two space-like separated and strongly correlated particles A and B. Again let λ be the hidden variable, and **A** and **B** the spin values of A and B measured along directions **a** and **b**, respectively. Then according to a local hidden variables theory, the measurement result **A** depends only upon the measurement setting **a** and the hidden variable λ. It is independent of B's measurement setting **b**, and similarly for B,

$$\begin{aligned} \mathbf{A} &= \mathbf{A}(\lambda, \mathbf{a}), \\ \mathbf{B} &= \mathbf{B}(\lambda, \mathbf{b}). \end{aligned} \tag{11}$$

We also assume that the hidden variable has probability distribution $\rho(\lambda)$. Apart from these, we do not make any assumptions about the nature of the hidden variable or its probability distribution. Note that by such local hidden variables, the only assumption made are locality and realism; hence, at this stage, no knowledge of quantum mechanics has to be known. Then, in this hidden variable formalism, the two particle correlation, or the expectation value of the product of the two observations of **A** and **B**, is then given by,

$$P(\mathbf{a}, \mathbf{b}) = \sum_{\lambda} \rho(\lambda)\, \mathbf{A}(\mathbf{a}, \lambda)\, \mathbf{B}(\mathbf{b}, \lambda). \tag{12}$$

In his seminal paper [24], Bell proved that any theoretical prediction for measurement outcomes fulfilling the ideas of locality and realism is upper bounded for a given set of measurements (the so-called Bell inequality). He also showed that quantum mechanics allows for the possibility to exceed this bound proving that quantum correlations cannot be obtained from any local realistic hidden variable theories with the form described by equation (12).

Bell's proof proceeds along the following lines [24]. Consider three variables a, b and c as well as the following algebraic quantity,

$$|ab - ac| - bc.$$

Now, if $a, b, c = \pm 1$, then the following inequality holds,

$$|ab - ac| - bc \leqslant 1. \tag{13}$$

This can be seen by further simplifying the expression on left as,

$$|a| \cdot |b - c| - bc \leqslant 1 \tag{14}$$

If both b and c have the same values, then the quantity on the left becomes zero and the whole expression takes a value of $-1 \leqslant 1$. In contrast, if b and c have different values, then the expression on the left becomes $2 - 1 = 1 \leqslant 1$.

The average values of the product terms in equation (13) will also satisfy the inequality,

$$|P(a, b) - P(a, c)| - P(b, c) \leqslant 1. \tag{15}$$

This is the inequality Bell derived in his original paper [24], which is satisfied by any classical hidden variable theories. It is easy to see how quantum mechanics would violate this inequality. Consider the same spin-anti-correlated EPR state we considered before. Assume that **a**, **b**, and **c** are three vectors along which we choose to measure the spin. Quantum mechanically,

$$P(a, b) = -\cos\, \theta_{a,b} \tag{16}$$

where $\theta_{a,b}$ is the angle between two vectors **a** and **b**. Now let us suppose **a**, **b**, and **c** lie in the same plane, with **a** and **c**, and **b** and **c** at 45° with each other, and **b** and **a**, at 90°. So,

$$\begin{aligned} P(a, b) &= 0, \\ P(a, c) = P(b, c) &= -0.707. \end{aligned}$$

Plugging it in equation (13), we obtain,

$$0.707 + 0.707 = 1.414 > 1,$$

clearly violating the bell inequality.

Experimentally the following form of Bell's inequality [75], called the Clauser–Horne–Shimony–Holt (CHSH) inequality, is commonly used,

$$|P(a, b) + P(a', b) + P(a, b') - P(a', b')| \leqslant 2. \tag{17}$$

where **a**, **b**, **a**′, and **b**′ again are the different vectors along which we can measure spin/polarization. If **a**′, **b**, **a**, and **b**′, are separated successively by 45°, then,

$$\begin{aligned} P(a, b) = P(a', b) = P(a, b') &= -\cos\, 45^\circ = -\frac{1}{\sqrt{2}}, \\ P(a'b') &= -\cos\, 45^\circ = \frac{1}{\sqrt{2}}. \end{aligned}$$

Then the inequality equation (17) is violated,

$$2\sqrt{2} > 2.$$

which clearly shows that quantum mechanics can violate the inequality. Now in an experiment, typically one would have

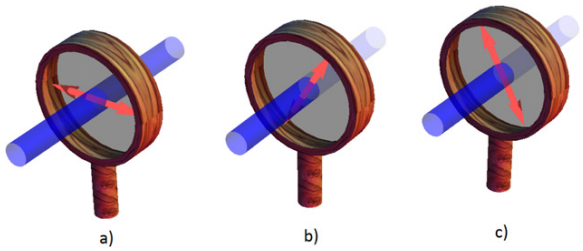

Figure 3. Three different directions for the polarization measurements: **(a)** 0, **(b)** $-2\pi/3$, and **(c)** $+2\pi/3$.

Table 1. Single photon polarization values in three different directions in local hidden variable theory. ✓ means the photon will pass through the polarizer set in that direction and ✗ means that it will be blocked by the polarizer.

Outcomes	$\boldsymbol{a_1/b_1}(0)$	$\boldsymbol{a_2/b_2}(+2\pi/3)$	$\boldsymbol{a_3/b_3}(-2\pi/3)$
1	✓	✓	✓
2	✓	✓	✗
3	✓	✗	✓
4	✓	✗	✗
5	✗	✓	✓
6	✗	✓	✗
7	✗	✗	✓
8	✗	✗	✗

two parties sharing a maximally entangled state, measuring the polarization/spin along the specified vectors, and then the expectation value of the product would be given in terms of the detector counts as,

$$P(a,b) = \frac{N_{++} - N_{+-} - N_{-+} + N_{--}}{N_{++} + N_{+-} + N_{-+} + N_{--}}, \qquad (18)$$

and so on. Here N_{+-} refers to the number of counts detected along positive a and negative b and so on.

Since the appearance of Bell's paper, numerous experiments have been performed that attested the correctness of quantum mechanics and falsified the assumption of local hidden variables [29–33, 76], most recently even loophole-free [28, 77, 78]. Contrary to the EPR assumption, nature does seem to allow the measurement of one particle to affect the 'reality' of the other, if such reality does exist.

We present here a simpler proof of incompatibility of local hidden variables with quantum mechanics. Consider a source that prepares a pair of photons with perfectly correlated polarization in any direction, i.e. if one is horizontally polarized then the other is also horizontally polarized and so on. In our experiment, we are able to measure the polarization of each of the two photons, at angles 0, $+2\pi/3$, and $-2\pi/3$ using three different polarizer settings (figure 3).

Assuming that the polarization results in these three directions are pre-defined by local hidden variables before the measurement, we tabulate all the eight possible combinations of the hidden variables for each photon (table 1).

We then look at the results of Alice's and Bob's measurements in two different directions (table 2) and note whether they get the same results or not (table 3). From the table, we can

Table 2. Two photon polarization measurement results. $\boldsymbol{a_1 b_2}$ refers to the polarizer for the first photon is set at 0 and that for second photon is set at $2\pi/3$, and so on. ✓ means that both photons have same outcomes for the directions specified, i.e. either both photons pass through the specified polarizers or both are blocked. ✗ means that they have different outcomes.

Outcomes	$\boldsymbol{a_1, b_2}$	$\boldsymbol{a_2, b_3}$	$\boldsymbol{a_3, b_1}$	$\mathcal{P}_{\text{same}}$
1	✓	✓	✓	1
2	✓	✗	✗	1/3
3	✗	✗	✓	1/3
4	✗	✓	✗	1/3
5	✗	✓	✗	1/3
6	✗	✗	✓	1/3
7	✓	✗	✗	1/3
8	✓	✓	✓	1

Table 3. Possible combinations of the values of the binary variables α, β, α', and β' as per the classical non-contextual theory. $\mathcal{P}_i$s are the corresponding probabilities for the particular combination of binary values of the variables.

Probability	α	β	α'	β'
$\mathcal{P}_1$	+1	+1	+1	+1
$\mathcal{P}_2$	+1	+1	+1	−1
$\mathcal{P}_3$	+1	+1	−1	+1
$\mathcal{P}_4$	+1	+1	−1	−1
$\mathcal{P}_5$	+1	−1	+1	+1
$\mathcal{P}_6$	+1	−1	+1	−1
$\mathcal{P}_7$	+1	−1	−1	+1
$\mathcal{P}_8$	+1	−1	−1	−1
$\mathcal{P}_9$	−1	+1	+1	+1
$\mathcal{P}_{10}$	−1	+1	+1	−1
$\mathcal{P}_{11}$	−1	+1	−1	+1
$\mathcal{P}_{12}$	−1	+1	−1	−1
$\mathcal{P}_{13}$	−1	−1	+1	+1
$\mathcal{P}_{14}$	−1	−1	+1	−1
$\mathcal{P}_{15}$	−1	−1	−1	+1
$\mathcal{P}_{16}$	−1	−1	−1	−1

deduce that the probability of seeing the same result is always at least 1/3. To see why this is true, let us assume we are dealing with the pair of photons represented by the second row of the table. Now if we randomly perform the measurement then, one third of the time we would be measuring in the $\boldsymbol{a_1 b_2}$ basis and we would see the states to be the same. In the remaining two-thirds, we would see the states to be different. Looking at rows 2–7 we see that each of them has the same probability, 1/3, for observing the same outcome. For the cases in rows 1 and 8, we get the same results every time. Hence if we assume the existence of local hidden variables, then we should see the same results at least one third of the time. One subtle point to note here is that we have not made any assumptions about how often each of the eight possible combinations occurs in nature. Each of the eight possible combinations of the hidden variables could occur with any probability and still the result would be the same. Therefore, according to a local hidden variable (LHV) theory, the probability for observing the same outcome is bounded as,

$$\mathcal{P}(\text{LHV, same}) \geqslant \frac{1}{3}. \qquad (19)$$

Now we turn to quantum mechanics and what it tells us about such states. For a source that produces photons with perfectly correlated polarizations in any direction, the initial two-photon state is an entangled state which is written as,

$$|\psi\rangle = \frac{1}{\sqrt{2}}\left(|H\rangle_A|H\rangle_B + |V\rangle_A|V\rangle_B\right), \tag{20}$$

where $|H\rangle$ and $|V\rangle$ refer to the horizontal and vertical polarization respectively.

Let us denote the three measurement directions (or polarization bases) for A by $\mathbf{a_i}$, and for B by $\mathbf{b_i}$. Written in terms of $|H\rangle$ and $|V\rangle$,

$$\begin{aligned} |\boldsymbol{a_1}\rangle &= |H\rangle, \\ |\boldsymbol{a_2}\rangle &= -\frac{1}{2}|H\rangle + \frac{\sqrt{3}}{2}|V\rangle, \\ |\boldsymbol{a_3}\rangle &= -\frac{\sqrt{3}}{2}|H\rangle - \frac{1}{2}|V\rangle, \end{aligned} \tag{21}$$

and similarly for B.

Then the probability of observing the same polarization in the same basis is given by the cosine of the angle between the two states, which is $2\pi/3$ in our case. Hence, according to quantum mechanics(QM),

$$\mathcal{P}(Q\mathrm{M}, \mathrm{same}) = \cos^2(2\pi/3) = 0.125. \tag{22}$$

Thus, we observe that the probability obtained from the assumption of local hidden variables contradicts the probability derived by quantum mechanics. Experimentally, the results have always vindicated the predictions of quantum mechanics, thus favoring quantum mechanics over local hidden variables theories. Alongside with many Bell inequalities [76] that were proposed to rule out local hidden variables models, it is worth mentioning the existence of proofs which do not invoke inequalities, most notably using GHZ states [79–81] which show that local hidden variable theories cannot account for the results even in an experiment with certain outcomes, and the non-locality of single photons [82].

3.1. Nonlocal hidden variables theories

Until now we restricted the hidden variable model to be local, which is an assumption well-justified by another major physical theory known today, i.e. general relativity. However, as we have seen above, local hidden variable models cannot explain the correlations in entangled states; thus, it might be a natural thing to ask if the locality assumption is too strong and can be lifted to find an agreement with quantum mechanics. Leggett laid out a more general nonlocal hidden variable theory [25], which assumes that:

(a) Each pair of photons in an EPR-like setup is characterized by a hidden variable λ.

(b) The distribution of the hidden variable λ, $\rho(\lambda)$, is independent of the measurement settings **a**, and **b** and the results of the measurements **A**, and **B** of either of the particles.

(c) The results of each measurements **A** and **B** depend upon the hidden variable λ, as well as both of the measurement settings **a** and **b**, and the results of the measurement performed on the other particle. i.e.,

$$\mathbf{A} = \mathbf{A}(\boldsymbol{a}, \boldsymbol{b}, \lambda, \mathbf{B}), \tag{23}$$

$$\mathbf{B} = \mathbf{B}(\boldsymbol{a}, \boldsymbol{b}, \lambda, \mathbf{A}). \tag{24}$$

Previously, in the local hidden variable theory, equation (11), we saw that the outcomes **A** and **B** depend only on the hidden variable λ and the respective measurement settings. In a local theory, the measurement settings of A and its results cannot affect the outcomes of B and vice versa, as it assumes that space-like separated events cannot influence each other. In contrast, a nonlocal hidden variable theory assumes nature is non-local, and, consequently, the outcomes for A and B are dependent not only upon their respective measurement settings, but also upon the setting of the other party and their outcomes. In such a theory, the expectation value of the product of the two outcomes is then given by,

$$P(\boldsymbol{a}, \boldsymbol{b}) = \sum_{\lambda} \rho(\lambda)\, \mathbf{A}(\boldsymbol{a}, \boldsymbol{b}, \lambda, \mathbf{B})\, \mathbf{B}(\boldsymbol{a}, \boldsymbol{b}, \lambda, \mathbf{A}), \tag{25}$$

or for the case of a continuous hidden variable λ,

$$P(\boldsymbol{a}, \boldsymbol{b}) = \int_{\lambda} \mathrm{d}\lambda\, \rho(\lambda)\, \mathbf{A}(\boldsymbol{a}, \boldsymbol{b}, \lambda, \mathbf{B})\, \mathbf{B}(\boldsymbol{a}, \boldsymbol{b}, \lambda, \mathbf{A}). \tag{26}$$

Such nonlocal hidden variable models can describe any correlations possible-they can both give rise to the quantum mechanical predictions, for e.g. Bohmian mechanics [17, 18], or in some cases even exceed the correlations given by quantum mechanics. Although some of them have to be considered non-physical, they are interesting lines of thought themselves [83, 84]. To enable a test of a subclass of such nonlocal hidden variables (NLHV) models called crypto-nonlocal theories, Leggett added another condition, namely:

(d) The outcomes **A** and **B** each depend upon the measurement setting of the other but are independent of the outcome,

$$\begin{aligned} \mathbf{A}(\boldsymbol{a}, \boldsymbol{b}, \lambda, \mathbf{B}) &= \mathbf{A}(\boldsymbol{a}, \boldsymbol{b}, \lambda), \\ \mathbf{B}(\boldsymbol{a}, \boldsymbol{b}, \lambda, \mathbf{A}) &= \mathbf{B}(\boldsymbol{a}, \boldsymbol{b}, \lambda). \end{aligned}$$

Let us look at a nonlocal hidden variable model [89] that satisfies this condition. We will see how this model successfully recreates quantum correlations for photons when the polarization measurement vectors are confined to a certain plane in the Poincaré sphere. As a consequence, for measurements performed in that plane, the model can even account for the violation of the CHSH inequality [75], an inequality which is satisfied by local hidden variable theories. However once we start performing measurements in a different plane, this model fails to recreate the quantum correlations. We will then look at

the Leggett inequality that bounds correlations obtained from this type of nonlocal hidden variable model, which nevertheless is violated by quantum correlations.

Our two parties, Alice and Bob each share a pair of photons A and B, with the initial polarization vectors **u** and **v**, respectively. We denote the polarization measurement vectors by **a** and **b**, respectively, for A and B. The measurement outcomes **A** and **B** both are binary valued (± 1) variables and as required for a crypto-nonlocal theory, do not depend upon each other. The hidden variable model predicts the measurement outcome for A as follows,

$$\mathbf{A} = \begin{cases} +1 & \text{if } 0 \leqslant \lambda \leqslant \lambda_A \\ -1 & \text{if } \lambda_A \leqslant \lambda \leqslant 1 \end{cases},$$

where λ_A depends upon A's initial polarization and the measurement setting as,

$$\lambda_A = \frac{1}{2}(1 + \boldsymbol{u}\cdot\boldsymbol{a}). \tag{27}$$

Similarly for B,

$$\mathbf{B} = \begin{cases} +1 & \text{if } x_1 \leqslant \lambda \leqslant x_2 \\ -1 & \text{if } 0 \leqslant \lambda \leqslant x_1 \ \&\ x_2 \leqslant \lambda \leqslant 1. \end{cases}$$

Now if we choose the parameters x_1 and x_2 such that,

$$x_1 = \frac{1}{4}(1 + \boldsymbol{u}\cdot\boldsymbol{a} - \boldsymbol{v}\cdot\boldsymbol{b} + \boldsymbol{a}\cdot\boldsymbol{b}), \tag{28}$$

$$x_2 = \frac{1}{4}(3 + \boldsymbol{u}\cdot\boldsymbol{a} + \boldsymbol{v}\cdot\boldsymbol{b} + \boldsymbol{a}\cdot\boldsymbol{b}) \tag{29}$$

then the model reproduces Malus' law,

$$\langle A\rangle = \int_0^{\lambda_A} \mathrm{d}\lambda - \int_{\lambda_A}^{1} \mathrm{d}\lambda = \boldsymbol{u}\cdot\boldsymbol{a},$$

$$\langle B\rangle = \int_{x_1}^{x_2} \mathrm{d}\lambda - \int_0^{x_1} \mathrm{d}\lambda - \int_{x_2}^{1} \mathrm{d}\lambda = \boldsymbol{u}\cdot\boldsymbol{b}.$$

Also, the expectation value of the product of **A** and **B** is given by,

$$\langle AB\rangle = -\int_0^{x_1} \mathrm{d}\lambda + \int_{x_1}^{\lambda_A} \mathrm{d}\lambda - \int_{\lambda_A}^{x_2} \mathrm{d}\lambda + \int_{x_2}^{1} \mathrm{d}\lambda = -\boldsymbol{a}\cdot\boldsymbol{b}, \tag{30}$$

which is the same expression as obtained from quantum mechanics. However, the problem with this model is that it is inconsistent for some measurement directions. To see how, we first note that the variables x_1 and x_2 also have to satisfy the condition,

$$0 \leqslant x_1,\, x_2 \leqslant 1. \tag{31}$$

Substituting the expressions for x_1 and x_2, equations (28) and (29), in the above equation, leads to the following inequality,

$$|\boldsymbol{a}\cdot\boldsymbol{b} \pm \boldsymbol{u}\cdot\boldsymbol{a}| \leqslant 1 \mp \boldsymbol{v}\cdot\boldsymbol{b}. \tag{32}$$

For this hidden variables model to successfully give rise to quantum correlations, inequality (32) needs to be satisfied.

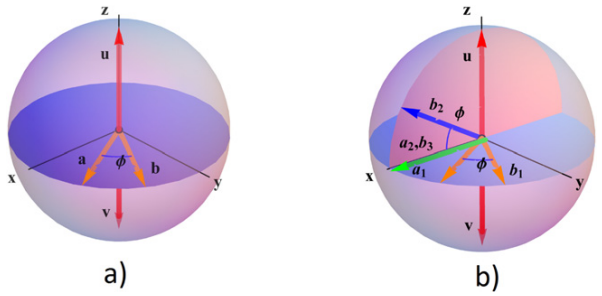

Figure 4. (**a**) The nonlocal hidden variable model reproduces quantum correlations and can even violate the CHSH inequality for measurements performed along vectors **a** and **b** lying in the plane (purple) perpendicular to the **u** and **v**. (**b**) Leggett's inequality is violated once the measurement vectors are not in the plane perpendicular to **u** and **v**.

We observe that in a plane perpendicular to the initial polarization vectors $\boldsymbol{u}$ and $\boldsymbol{v}$, no matter what $\boldsymbol{a}$ and $\boldsymbol{b}$ we choose, the inequality (32) is always satisfied. Hence for any measurement directions $\boldsymbol{a}$ and $\boldsymbol{b}$ lying in this plane (colored purple in figure 4), this model correctly predicts quantum correlations and hence we can also observe the violation of the CHSH inequality. However for some polarization vectors lying outside this plane, the inequality cannot be satisfied, and this is where the model fails.

For a nonlocal hidden variable model as described above, when A uses two different measurement settings $\boldsymbol{a_1}$, $\boldsymbol{a_2}$, and B uses three $\boldsymbol{b_1}$, $\boldsymbol{b_2}$ and $\boldsymbol{b_3} = \boldsymbol{a_2}$, a more general Leggett's inequality is given by,

$$S_{\mathrm{NLHV}} = |E_{11}(\phi) + E_{23}(0)| + |E_{22}(\phi) + E_{23}(0)| \leqslant 4 - \frac{4}{\pi}\left|\sin\frac{\phi}{2}\right|, \tag{33}$$

where, E_{kl} is the expectation value of the product $\mathbf{A_k}\mathbf{B_l}$ over all the initial polarization directions $\boldsymbol{u}$ and $\boldsymbol{v}$.

$$E_{kl} = \int_{\boldsymbol{u},\boldsymbol{v}} \mathrm{d}\boldsymbol{u}\,\mathrm{d}\boldsymbol{v}\, F(\boldsymbol{u},\boldsymbol{v})\, \mathbf{A}(\boldsymbol{a_k},\boldsymbol{b_l},\lambda)\, \mathbf{B}(\boldsymbol{a_k},\boldsymbol{b_l},\lambda), \tag{34}$$

where $F(\boldsymbol{u},\boldsymbol{v})$ is the distribution of the initial polarization of two photons. Quantum mechanically, this expectation value is given by,

$$E_{kl} = -\boldsymbol{a_k}\cdot\boldsymbol{b_l} = -\cos\,\phi_{\boldsymbol{a_k},\boldsymbol{b_l}}. \tag{35}$$

Substituting the expression in the left-hand side of inequality (34), the quantity S takes the value,

$$S_{QM} = |2(\cos\,\phi + 1)|\,. \tag{36}$$

For some values of ϕ, $S_{\mathrm{QM}} > S_{\mathrm{NLHV}}$ goes above the upper bound set by equation (34) (the maximal violation occurs when $\phi = 18.8^{\circ}$). Hence, we can conclude that the crypto-nonlocal hidden variable theories also fail to fully describe quantum correlations.

Experiments performed with photon pairs entangled in polarization and spatial modes have indicated the violation of Leggett's inequality [89, 90]. Apart from the concepts of local

and non-local realism, there is also the notion of macroscopic realism whose incompatibility with quantum mechanics is defined by the Leggett–Garg inequality [85, 86]. The incompatibility of macroscopic realism with quantum mechanics has also been observed experimentally [87, 88].

3.2. Non-contextuality

After looking into correlations between space-like separated quantum systems, we turn our focus to another feature of quantum mechanics, namely the context of the measurement. Two physical observables are non-commuting if they do not have a set of simultaneous Eigen states. Therefore, the order in which one measures the two non-commuting quantities affects their measurement outcomes. Mathematically, the two measurement results, say for observables $\hat{A}$ and $\hat{B}$, are related by the uncertainty relation,

$$\sigma_A \sigma_B \geqslant \left| \frac{[\hat{A}, \hat{B}]}{2i} \right|, \tag{37}$$

where σ_A and σ_B are the uncertainties in the two physical quantities $\hat{A}$ and $\hat{B}$. The commutator, $[\hat{A}, \hat{B}]$, is zero if $\hat{A}$ and $\hat{B}$ commute with each other, i.e. if their order of measurement does not matter, and is non-zero if they do not commute (i.e. if their order of measurement matters).

$$[\hat{A}, \hat{B}] \begin{cases} = 0 & \text{if } \hat{A} \text{ and } \hat{B} \text{ commute.} \\ \neq 0 & \text{if } \hat{A} \text{ and } \hat{B} \text{ do not commute.} \end{cases}$$

For the non-commuting physical quantities, we see that the uncertainty principle forbids simultaneous assignment of predetermined measurement results. Moreover, if we now include a third observable $\hat{C}$ that also commutes with $\hat{A}$, i.e. $[\hat{A}, \hat{C}] = 0$, which does not need to commute with $\hat{B}$, i.e. $[\hat{B}, \hat{C}] \neq 0$, the value assigned to $\hat{A}$ is considered to be non-contextual. In other words, the outcome of a measurement should not be different if the observable $\hat{A}$ is measured alone, together with $\hat{B}$ or together with $\hat{C}$. In the spirit of the EPR argument, one can now discuss non-contextual realism by assigning predefined values $v(\hat{A}_i)$ to all the observables $\hat{A}_i$.

Therefore, non-contextuality, i.e. the notion that the measurement of a physical quantity is independent of the measurement of any other commuting physical quantities, or the 'context' of the measurement, seemed like a valid assumption in quantum mechanics. However, Bell and Kochen–Specker (BKS) [91–93] separately proved that it is impossible for the commuting observables to have pre-existing values independent of the context of the measurement. Kochen and Specker considered special kinds of observables that have binary Eigenvalues (0 or 1), e.g. projection operators, and proved that it is impossible to assign values classically to the projection operators in a 3-dimensional Hilbert space. For the proof, they used projection operators along 117 different vectors. Cabello later provided a simpler proof [94] of quantum contextuality, involving only 18 projection directions in a four dimensional Hilbert space. Additionally, Klyachko, Can, Binicioğlu and Shumovsky (KCBS) simplified it even further and found a proof that only requires 5 measurements for spin-1 particles [95].

In the following, we focus on the latter, i.e. the KCBS version of the Bell–Kochen–Specker theorem, as it is the most simple BKS-proof regarding measurement settings and dimensionality of the quantum state [95, 96]. Mathematically, if we assume quantum theory to be non-contextual, then for a state ψ described by commuting observables say $\{\hat{A}, \hat{B}, \ldots\}$, it is possible to assign an underlying value for the outcomes of each observables as say $\{v(\hat{A}), v(\hat{B}), \ldots\}$ independent and before the actual measurement (non-contextual realism). Since we know that the result of projective measurement of an observable can return only one of its Eigenvalues, the value of the observable also must be one of the Eigenvalues.

Now classically if these observables satisfy the equation,

$$f(A, B, \ldots) = 0, \tag{38}$$

then the pre-assigned values should also satisfy the equation,

$$f(v(A), v(B), \ldots) = 0. \tag{39}$$

Note that a special case of this logical step, i.e. equation (38) $\Rightarrow$ equation (39), is the so-called sum rule

$$A = B + C \Rightarrow v(A) = v(B) + v(C). \tag{40}$$

Let us now consider five numbers a, b, c, d, e that can either take the value $+1$ or -1. For all possible combinations, the following algebraic inequality has a minimal value of -3:

$$ab + bc + cd + de + ea \geqslant -3. \tag{41}$$

This can be easily seen because at least one term always needs to be $+1$. As we already discussed above, according to a non-contextual hidden variable model each measurement has a predefined value, which is independent of the context, i.e. $v(A)_B = v(A)_C$. As this holds for all members of the ensemble, we can rewrite the inequality in terms of ensemble averages:

$$\langle AB \rangle + \langle BC \rangle + \langle CD \rangle + \langle DE \rangle + \langle EA \rangle \geqslant -3. \tag{42}$$

We note that this inequality holds not only for non-contextual hidden variable models but also for any joint probability distribution describing the measurements.

However, KCBS realized that this inequality can be violated by quantum mechanics using five measurements of a spin-1 particle [95]. The measurements required are expressed by the spin operator $\hat{A}_i = 2\hat{S}_i^2 - I$, where the operator $\hat{S}_i^2$ has the Eigenvalues 0 and 1 and, thus, needs to be rescaled and shifted to realize the required ± 1 values. The five observables $\hat{A}_i$ are defined by the projection directions $\vec{l}_i$ according to:

$$\hat{A}_i = 2\hat{S}_i^2 - I = I - 2\left|\vec{l}_i\right\rangle \left\langle \vec{l}_i\right|. \tag{43}$$

Two measurements $\hat{A}_i$ and $\hat{A}_j$ (for $i \neq j$) are commuting, i.e. are compatible, if and only if the projections $\vec{l}_i$ and $\vec{l}_j$ are orthogonal, which means that we need to find five pairwise orthogonal measurement directions. As the directions $\vec{l}_i$ can be directly depicted in a real three-dimensional space, we find

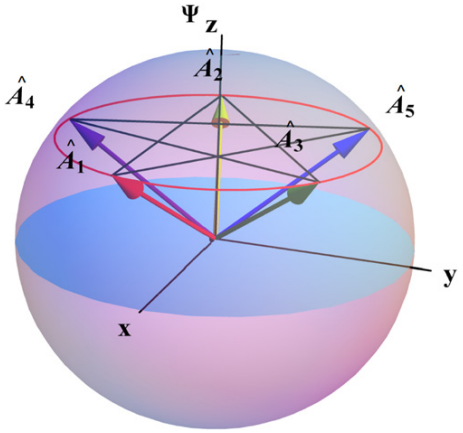

Figure 5. Three-dimensional representation of the measurement directions $\hat{A}_j$. We see that each measurement is orthogonal to two other directions and as such is compatible with it, i.e. commuting with these two other measurements. However, when using a quantum state Ψ along the symmetry axis, the inequality for non-contextual hidden variable models given in formula (42) can be violated.

that they form a pentagram. The maximal violation of the above described minimal value for non-contextual hidden variable can then be found for a quantum state Ψ that lies on the symmetry axis of the pentagram (see figure 5). If we now use these five pairwise orthogonal projections as our measurements on the quantum state Ψ_0, the quantum mechanical prediction is $5-4\sqrt{5}\approx -3.944$; thus, we can surpass the lowest limit given above. This simple proof demonstrates that quantum mechanics cannot be modeled by a non-contextual hidden variable model. Although there have been some discussions about the general validity of an experimental test of quantum contextuality [97], nowadays it has been generally accepted to be a valid task and many of experiments have been conducted [98], including one verifying the quantum mechanical prediction for the above given KCBS proof [99].

Interestingly, Bell searched for a more physical assumption than non-contextuality, and thus he studied locality instead. The important connection between the two arguments is that, simply phrased, in nonlocal hidden variable models, measurements cannot depend on measurements done in a space-like separated place. On the other hand, in non-contextual hidden variable models, measurements can 'only' question the dependence of the measurement on the context if local or nonlocal. In other words, showing the mismatch between quantum mechanics and local realistic theories according to the Bell theorem is a stronger statement and as such includes (as a special case) non-contextual realistic theories. Thus, the possibility of space-like separation is an essential assumption in the Bell argument and requires two entangled particles that can be separated.

3.3. Single particle 'entanglement'

So far we have only taken one degree of freedom of the quantum system into account. However, there are other quantum properties of single-particle systems that are similar in form to those of multipartite entangled states, i.e. non-separable correlations between two different degrees of freedom of a single particle. For instance, if we pass a diagonally polarized light through a polarizing beam splitter, it gets transformed to the state:

$$|\psi\rangle = \frac{1}{\sqrt{2}}\left(|\mathrm{I,H}\rangle + |\mathrm{II,V}\rangle\right), \tag{44}$$

where the $|\mathrm{I,H}\rangle$ indicates that the photon is in path I and is horizontally polarized, and similarly for $|\mathrm{II,V}\rangle$. The mathematical expression for such states cannot be separated into a product of individual states in each of the two Hilbert spaces, quite similar to the entangled states. Although lacking non locality, these states have been shown to violate the CHSH inequality [47]. Such 'entanglement' tests can be used to probe the non-separability of such states. However, by using Bell-like inequalities, these experiments are challenging classical concepts that are closer to non-contextuality rather than non locality. Consequently, the violation of these inequalities rules out the 'local non-contextual hidden variable' description for such states.

We will discuss the details about such tests below [100], following an idea that was originally proposed for non locality by Hardy [82]. Let us look at three statements regarding probabilities, which, when simultaneously satisfied, would also imply a fourth statement in classical probability theory. We will then show that for certain quantum states and measurements in which the first three statements are true, the fourth statement turns out to be false, resulting in a contradiction with the classical picture. We assume that:

$$\begin{aligned}\mathcal{P}(\alpha=+1,\beta=+1)&=0,\\ \mathcal{P}(\alpha=-1,\beta'=-1)&=0,\\ \mathcal{P}(\alpha'=-1,\beta=-1)&=0,\end{aligned} \tag{45}$$

where, α, α', β, and β' are all binary variables which can take values ± 1. $P(\alpha=+1,\beta=+1)$ refers to the probability that $\alpha=+1$ and $\beta=+1$, and so on. Now if all three statements are true, then logically a fourth statement should follow:

$$\mathcal{P}(\alpha'=-1,\beta'=-1)=0. \tag{46}$$

Let us first see why this is true for a classical non-contextual theory. We tabulate all the possibilities for these binary variables in table 3.

Looking at table 3, the first statement, i.e. $P(\alpha=+1,\beta=+1)=0$ implies,

$$\mathcal{P}_1+\mathcal{P}_2+\mathcal{P}_3+\mathcal{P}_4=0. \tag{47}$$

Similarly, from the second and third statements,

$$\mathcal{P}_{10}+\mathcal{P}_{12}+\mathcal{P}_{14}+\mathcal{P}_{16}=0 \tag{48}$$

$$\mathcal{P}_7+\mathcal{P}_8+\mathcal{P}_{15}+\mathcal{P}_{16}=0. \tag{49}$$

Since probabilities cannot be negative, these statements imply that the individual probabilities

$P_1, P_2, P_3, P_4, P_7, P_8, P_{10}, P_{12}, P_{14}, P_{15}, P_{16}$ are all zero. Now, for the fourth statement to be true, the following expression must be satisfied,

$$\mathcal{P}_4 + \mathcal{P}_8 + \mathcal{P}_{12} + \mathcal{P}_{16} = 0. \tag{50}$$

We observe that all the individual terms on the left-hand side are already zero from the first three statements. Hence, it follows that the fourth statement must be true.

Now in the quantum version, we assume that our usual two parties, namely Alice and Bob, each have access to one of the two different degrees of freedom of the single particle quantum state:

$$|\psi\rangle = \cos\gamma|0\rangle_A|1\rangle_B - \sin\gamma|1\rangle_A|0\rangle_B. \tag{51}$$

The two kets can represent any two degrees of freedom of a single particle (for e.g. path and polarization) in the two dimensional Hilbert space. Alice can perform a measurement of two projection operators α and α', and Bob can perform his measurement of projection operators β and β'.

The projection operators α, β and α', β' are defined as,

$$\alpha, \beta = |+\rangle\langle -| - |-\rangle\langle +| \tag{52}$$

$$\alpha', \beta' = |+\rangle'\langle -| - |-\rangle'\langle +|. \tag{53}$$

where,

$$|+\rangle = N\left(\sqrt{\sin\gamma}|0\rangle + \sqrt{\cos\gamma}\,|1\rangle\right) \tag{54}$$

$$|-\rangle = N\left(-\sqrt{\cos\gamma}|0\rangle + \sqrt{\sin\gamma}\,|1\rangle\right) \tag{55}$$

$$|+\rangle' = N'\left(\sqrt{\cos^3\gamma}|0\rangle + \sqrt{\sin^3\gamma}\,|1\rangle\right) \tag{56}$$

$$|-\rangle' = N'\left(-\sqrt{\sin^3\gamma}|0\rangle + \sqrt{\cos^3\gamma}\,|1\rangle\right) \tag{57}$$

and $N = \frac{1}{\sqrt{\sin\gamma + \cos\gamma}}$ and $N' = \frac{1}{\sqrt{\sin^3\gamma + \cos^3\gamma}}$ are the normalization constants. For these states we find that the probabilities are as defined in equation (45). However the expression for the fourth probability is,

$$P(\alpha' = -1, \beta' = -1) = \left(\frac{\sin 4\gamma}{4(\cos^3\gamma + \sin^3\gamma)}\right)^2 \tag{58}$$

For certain angles γ, this expression is not zero which is in conflict with the assumption that the values of the four operators can pre-exist before we conduct the measurement. Thus, it disproves the non-contextual hidden variable description for non-maximally separable states.

Spin-energy entangled states in massive single particles such as neutrons have also been used [101] to demonstrate the violation of Leggett type inequalities for the contextual realistic hidden variables theories.

4. N00N states

After having discussed various scenarios where quantum systems involving one or two particles, show features that cannot be explained with classical theories, we now turn to many-body quantum systems that resemble bipartite systems and exhibit interesting correlations. One such state is a N00N state [102–104], which is an equal superposition of N indistinguishable particles in one mode and none in the other, and vice versa. Mathematically, such states have the form,

$$|\psi\rangle = \frac{1}{\sqrt{2}}\left(|N\rangle_a|0\rangle_b + |0\rangle_a|N\rangle_b\right), \tag{59}$$

where the subscripts 'a' and 'b' now refer to the modes a and b which photons can occupy, in contrast to our previous notation where the subscripts represented the photons themselves. These states are sometimes also referred to as Schrödinger cat states [105] as they represent a superposition of N particles (in theory N could be arbitrarily large) in two distinct states, comparable to the 'dead' or 'alive' states. These N00N states have interesting applications in quantum metrology [105–107] and can provide sensitivity even up to the Heisenberg limit.

For our purposes, N00N states present an interesting case of 'entanglement'. For instance, let us consider the simplest N00N state with just a single particle,

$$|\psi\rangle = \frac{1}{\sqrt{2}}\left(|1\rangle_a|0\rangle_b + |0\rangle_a|1\rangle_b\right). \tag{60}$$

Expressed in the number basis, here it looks like we have a single particle 'entangled' with the vacuum. It gets even more intriguing when we have a particle in this state interacting with other atoms or particles. Let us look at a photon in such a state, which is generated by passing a photon through a 50 : 50 beam splitter, and creating a superposition between the two different paths (modes). In each of the two paths, we place an atom in a ground state such that it jumps into an excited state when it comes in contact with the photon. Unless we perform a measurement, we do not know which path the photon has taken and which one of the atoms is in the excited state. At this instant, the joint state of the two atoms is,

$$|\psi\rangle = \frac{1}{\sqrt{2}}\left(|e\rangle_a|g\rangle_b + |g\rangle_a|e\rangle_b\right), \tag{61}$$

where $|e\rangle_a|g\rangle_b$ denotes that the atom in mode a is in the excited state and the atom in mode b is in the ground state, and so on. Now this is unequivocally an entangled state. As any local operations cannot increase or decrease entanglement, this also strengthens the claim that the single photon state possess some characteristics similar to an entangled state. Similar arguments on the 'nonlocality' of a single particle have been much debated in the literature [108–112].

N00N states with two indistinguishable particles also offer an interesting case. For instance, let us look at two such photons in a 2002 state, with equal superposition of either both being diagonally polarized or anti-diagonally polarized,

$$|\psi\rangle = \frac{1}{\sqrt{2}}\left(|2\rangle_A|0\rangle_D - |0\rangle_A|2\rangle_D\right). \tag{62}$$

When written in a terms of individual kets of each photons,

$$|\psi\rangle = \frac{1}{\sqrt{2}}\left(|A\rangle_1|A\rangle_2 - |D\rangle_1|D\rangle_2\right). \tag{63}$$

This two photon state can be obtained by passing two indistinguishable photons in a state,

$$|\psi\rangle = |1\rangle_H|1\rangle_V \tag{64}$$

through a polarizing beam splitter (PBS) set at an angle of 45°,

$$\begin{aligned}|\psi\rangle &= \hat{a}_H^\dagger \hat{a}_V^\dagger |0\rangle \\ &= \frac{1}{2}(\hat{a}_A^\dagger + \hat{a}_D^\dagger)(\hat{a}_A^\dagger - \hat{a}_D^\dagger)|0\rangle \\ &= \frac{1}{2}(\hat{a}_A^\dagger\hat{a}_A^\dagger + \hat{a}_A^\dagger\hat{a}_D^\dagger - \hat{a}_D^\dagger\hat{a}_A^\dagger - \hat{a}_D^\dagger\hat{a}_D^\dagger)|0\rangle \\ &= \frac{1}{2}(\hat{a}_A^\dagger\hat{a}_A^\dagger - \hat{a}_D^\dagger\hat{a}_D^\dagger)|0\rangle \\ &= \frac{1}{\sqrt{2}}\left(|2\rangle_A|0\rangle_D - |0\rangle_A|2\rangle_D\right).\end{aligned}$$

The two photons are clearly entangled with each other after passing through the beam splitter. Note that this is the famous Hong–Ou–Mandel (HOM) interference for two identical photons passing through a beam splitter [49]. One crucial point to be made here is that the entangled state is created by the physical action of the beam splitter on both of these photons. It may seem that the entangled state could be obtained simply by just changing the basis of polarization as,

$$\begin{aligned}|\psi\rangle &= |H\rangle\,|V\rangle \\ &= \frac{1}{2}(|A\rangle + |D\rangle)(|A\rangle - |D\rangle) \\ &= \frac{1}{2}(|A\rangle\,|A\rangle - |A\rangle\,|D\rangle + |D\rangle\,|A\rangle - |D\rangle\,|D\rangle).\end{aligned} \tag{65}$$

and then one could say that the kets $|A\rangle\,|D\rangle$ and $|D\rangle\,|A\rangle$ refer to the same state, i.e., a two photon state with one photon diagonally polarized and the other anti-diagonally polarized. Since their amplitudes are of the same magnitude, but with opposite sign, the terms cancel each other and we seem to have an entangled state. However, there are two things that have to be considered. First, since we are dealing with two indistinguishable photons, it is essential to symmetrize the initial state and hence equation (65) does not characterize the state of two indistinguishable photons. The second state, written in the number basis (in fock space), i.e. equation (64), is the correct approach for writing such states. It captures all the possible combination of the two photons in such a state. Another fundamental reason is that the physics, or the phenomenon of entanglement in this case, should not change just by altering the basis. In contrast to the discussion before, where we had a beam splitter performing a joint physical action on the two photons, here only a rotation of the coordinate system has been performed. Such a rotation cannot lead to a change or creation of entanglement.

5. Bounds on quantum correlations

In the preceding sections, we saw how local, crypto-nonlocal or non-contextual hidden variable theories are bounded by Bell-like inequalities and how quantum correlations can violate these and reach beyond the classical bounds. We now shift our focus to the other side of this picture, i.e. *to what extent quantum mechanics departs from classical physics and what promise such maximal violations hold for unique quantum technologies?* Mathematically, the maximal violation of a Bell inequality is given by the Tsirelson bound, following the seminal work in this respect [116]. It was shown that,

$$S = \langle A_0\,B_0\rangle + \langle A_0\,B_1\rangle + \langle A_1\,B_0\rangle - \langle A_1\,B_1\rangle \leqslant 2\sqrt{2}, \tag{66}$$

where $\langle A_iB_j\rangle$ are the expectation values of the product of Alice's and Bob's ±1-valued observables A_i and B_j, respectively. Quantum correlations can therefore violate the CHSH inequality [75], $S \leqslant 2$ mentioned above by at most a multiplicative factor of $\sqrt{2}$.

Despite its importance, the Tsirelson bound provides only the point of maximal violation; hence, a much more detailed characterization of quantum mechanics would consist of all nonlocal correlations achievable by quantum operators acting on quantum states, i.e. the quantum set of correlations. In between these two descriptions, there are partial characterizations of quantum correlations such as the Uffink inequality [117], some of which have already been tested experimentally with a high-fidelity source of polarization-entangled photons [118]. However, a general, finite characterization of the quantum set is still missing. In the simplest bipartite case with binary inputs and outputs, the TLM (Tsirelson–Landau–Masanes) inequality is known to be necessary and sufficient for the correlators to be realizable in quantum mechanics [119–121]

$$|c_{00}\,c_{10} - c_{01}\,c_{11}| \leqslant \sum_{j=0,1}\sqrt{(1-c_{0j}^2)\,(1-c_{1j}^2)}, \tag{67}$$

where we have used $c_{ij} = \langle A_iB_j\rangle$. In recent years, there has been a growing interest in further exploring this set of quantum correlations from within and from outside the quantum formalism [122–127] in order to derive the strength of quantum correlations based on first principles [128–133].

According to a recent approach [134], some well-known bounds on quantum correlations (such as the Tsirelson and TLM bounds), as well as some new ones, originate from a principle called 'relativistic independence', encapsulating relativistic causality and indeterminism. This means that even a very general probabilistic structure can give rise to quantum-like correlations (but not stronger-than-quantum correlations) if it obeys a generalized uncertainty principle (i.e. an uncertainty principle which is applicable even beyond quantum mechanics, but when assuming an Hilbert space structure reduces to the well-known Schrödinger–Robertson uncertainty relation), which is moreover local. Locality in this context means that choices made by remote parties do not affect

the uncertainty relations of other parties. This result quantitatively supports a famous conjecture [135–137] arguing that quantum mechanics can be as nonlocal as it is without violating relativistic causality only due to its inherent indeterminism. Moreover, it shows that entanglement-assisted nonlocal correlations and uncertainty are two aspects of the same phenomenon, imprinted in the algebra of quantum mechanics (which can be accessed from outside the quantum formalism using local uncertainty relations). This result therefore attributes the differences between classical and quantum correlations to the existence of fundamental uncertainty within quantum mechanics. Several applications of this approach can be found in [138–140]. For related analyses see [141, 142]. Many applications of the quantum formalism rely on highly entangled states. We have already mentioned one such application, namely, quantum metrology with N00N states. Additional applications are super dense coding [113] and quantum teleportation [114]. Among the many other entanglement-based or entanglement-enhanced protocols, there are cryptographic schemes using entangled states whose security relies on entanglement monogamy, with the first being the E91 protocol [115].

5.1. 'Classical entanglement'

Having discussed different aspects of quantum physics, such as realism, locality and non-contextuality for single and multiple particles, we can now study how concepts such as 'classical entanglement' relate to these fundamental concepts. Some works [44, 45, 143–147] have compared the true quantum phenomenon of entanglement with classical waves of light and called the analogies 'classical entanglement'. For instance, instead of single photons if we send a classical electromagnetic wave through the polarizing beam splitter, then the electric field is now written as a superposition of the two components,

$$\boldsymbol{E}(\boldsymbol{r}) = E_{\mathrm{H}}(\boldsymbol{r})\,\boldsymbol{e}_H + E_{\mathrm{V}}(\boldsymbol{r})\,\boldsymbol{e}_V,$$

where $\boldsymbol{e}_H$ and $\boldsymbol{e}_V$ are unit vectors along horizontal and vertical directions, and $E_H(\boldsymbol{r})$ and $E_V(\boldsymbol{r})$ are the corresponding electric field components, respectively. The electric field and the polarization are correlated and the intensities also violate inequalities that resemble Bell inequalities [47, 148, 149]. However, in this case, classical fields are used instead of single particles, such as photons, and, therefore, we are not performing tests of the assumptions such as realism, locality, non-contextuality or any class of hidden variables. As all these considerations using classical states of light, i.e. coherent states, are fully described by Maxwell's equations, i.e. only require a wave picture without invoking the field quantization, they cannot challenge any of the above mentioned fundamental concepts. All contradictions to classical concepts and mind-boggling questions arose upon considering the *particle* nature of light, i.e. when using single photons. Hence, it is misleading to challenge fundamental concepts using states of light that are fully described by the electromagnetic wave picture and Maxwell's equations. Therefore, we suggest that the term entanglement should only be used in connection to quantum experiments with single or multiple particles, and in particular for the cases involving nonlocality as it was originally suggested by Schrödinger. Using the equally valid term of 'non-separability', which is not as closely related to fundamental ideas as entanglement, might be more appropriate and simplify the distinction between classical and quantum correlations, for experts as well as the interested layman. Moreover, although analogies might be correct, the beauty as well as deep implications due to quantum entanglement might otherwise be misinterpreted, oversimplified or even entirely misunderstood. This type of classical states, i.e. non-separable states, nevertheless have important applications [45] for example in polarization metrology [147], kinematic sensing [150], computation [151], communication [152, 153], and many more [154, 155]. It could be of interest to compare the above treatment of 'classical entanglement' with the Koopman–von Neumann description [156, 157], introducing a non commutative algebra of observables for addressing classical mechanics and classical field theories [158, 159].

6. Conclusion

Stemming directly from the principles of quantum mechanics, the presence of entanglement in any multipartite system marks a distinct departure from classical physics. Defying any classical explanation, entanglement raises some intriguing fundamental questions about the physical universe such as realism, non-locality, etc. Some exciting manifestations of entanglement, such as Schrödinger cat states and N00N states, serve to question the boundary between the quantum and classical world, highlighting some stark differences between the two regimes. Non-separable single-particle states, similar to entangled states in their mathematical form, yet lacking non-locality, present some intriguing instances of correlations allowing one to investigate the meaning of contextuality. Classical electromagnetic phenomena analogous in their form to entangled states, although useful in a variety of applications [147, 150–155], cannot act as tests of the fundamental concepts of non-locality, realism or contextuality as entangled states can. As such, we suggest 'non-seperability' as a more appropriate term for these states to clearly distinguish them from the quantum phenomenon of entanglement.

In addition to being an integral concept of quantum foundations, entanglement is also a key resource in modern technological advances in quantum computing, quantum communication and quantum metrology. To a large extent, the second quantum revolution we are witnessing these days strongly relies on generation and manipulation of entangled quantum states. Bell inequalities [24] and Tsirelson bounds [116] quantify the lower and upper limits, respectively, on the correlations obtainable from entangled states to be non-classical and still considered quantum. Striking forms of quantum correlations, different from entanglement, have also been studied, most notably, quantum discord [160–163], which poses some avenues for future research. Moreover, non locality itself is believed to be a broader phenomenon than presented here, often including dynamical non locality [164, 165], such as

the one commonly attributed to the Aharonov–Bohm effect [166, 167], which is also closely connected to entanglement [168–171]. This type of non locality still merits further quantitative study [164].

Acknowledgments

We thank Leon Bello and Avishy Carmi and the members of the SQO group for helpful comments. This work was supported by Canada Research Chairs (CRC), Canada First Excellence Research Fund (CFREF), and Ontario's Early Researcher Award. RF acknowledge the support of the Academy of Finland through the Competitive Funding to Strengthen University Research Profiles (301820) and the Photonics Research and Innovation Flagship (PREIN-320165).

ORCID iDs

Robert Fickler https://orcid.org/0000-0001-6251-753X
Ebrahim Karimi https://orcid.org/0000-0002-8168-7304

References

[1] Actually, the photoelectric effect can also be described, to some extent, by classical electrodynamics but quantum mechanics offers far more clear and intuitive explanation
[2] Planck M 1899 Über irreversible Strahlungsvorgänge, Sitzungsberichte der Königlich Preußischen Akademie der Wissenschaften zu Berlin **5** pp 440–80
[3] Lambert N, Chen Y-N, Chen Y-C, Li C-M, Chen G Y and Nori F 2013 Quantum biology *Nat. Phys.* **9** 10–8
[4] Gray H B and Winkler J R 2003 Electron tunneling through proteins *Q. Rev. Biophys.* **36** 341–72
[5] Engel G S *et al* 2007 Evidence for wavelike energy transfer through quantum coherence in photosynthetic systems *Nature* **446** 782
[6] Levine I N, Busch D H and Shull H 2000 *Quantum Chemistry* (Upper Saddle River, NJ: Prentice Hall)
[7] Szabo A and Ostlund N S 2012 Introduction to advanced electronic structure theory courier corporation *Modern Quantum Chemistry*
[8] Halpin A *et al* 2014 Two-dimensional spectroscopy of a molecular dimer unveils the effects of vibronic coupling on exciton coherences *Nat. Chem.* **6** 196
[9] Nielsen M A and Chuang I 2000 *Quantum Computation and Quantum Information* (Cambridge: Cambridge University Press)
[10] Benioff P 1980 The computer as a physical system: a microscopic quantum mechanical Hamiltonian model of computers as represented by Turing machines *J. Stat. Phys.* **22** 563–91
[11] Feynman R P 1982 Simulating physics with computers *Int. J. Theor. Phys.* **21** 467–88
[12] DiVincenzo D P 1995 Quantum computation *Science* **270** 255–61
[13] Deutsch D 1985 Quantum theory, the Church–Turing principle and the universal quantum computer *Proc. R. Soc. London* A **400.1818** 97–117
[14] Saunders S, Barrett J, Kent A and Wallace D 2010 Many worlds? *Everett, Quantum Theory, and Reality* (Oxford: Oxford University Press)
[15] Bacciagaluppi G and Valentini A 2009 *Quantum Theory at the Crossroads: Reconsidering the 1927 Solvay Conference* (Cambridge: Cambridge University Press)
[16] Bell J S 2004 *Speakable and Unspeakable in Quantum Mechanics: Collected Papers on Quantum Philosophy* (Cambridge: Cambridge University Press)
[17] Bohm D 1952 A suggested interpretation of the quantum theory in terms of hidden variables I *Phys. Rev.* **85** 166
[18] Bohm D 1952 A suggested interpretation of the quantum theory in terms of hidden variables II *Phys. Rev.* **85** 180
[19] Everett H 1957 Relative state formulation of quantum mechanics *Rev. Mod. Phys.* **29** 454–62
[20] Fuchs C A 2010 QBism, the perimeter of quantum Bayesianism (arXiv:1003.5209)
[21] Cramer J G 1986 The transactional interpretation of quantum mechanics *Rev. Mod. Phys.* **58** 647–87
[22] Aharonov Y and Vaidman L 2008 The two-state vector formalism: an updated review *Time in Quantum Mechanics* (Berlin, Heidelberg: Springer) 399–447
[23] Genovese M 2005 Research on hidden variable theories: A review of recent progresses *Phys. Rep.* **413** 319–96
[24] Bell J S 1964 On Einstein–Podolsky–Rosen paradox *Physics* **1** 195
[25] Leggett A J 2003 Nonlocal hidden-variable theories and quantum mechanics: an incompatibility theorem *Found. Phys.* **33** 1469–93
[26] Mermin N D 2004 Could Feynman have said this *Phys. Today* **57** 10
[27] Scheidl T *et al* 2010 Violation of local realism with freedom of choice *Proc. Natl Acad. Sci. USA* **107** 19708–13
[28] Hensen B *et al* 2015 Loophole-free Bell inequality violation using electron spins separated by 1.3 kilometers *Nature* **526** 682
[29] Giustina M *et al* 2013 Bell violation using entangled photons without the fair-sampling assumption *Nature* **497** 227
[30] Rauch D *et al* 2018 Cosmic Bell test using random measurement settings from high-redshift quasars *Phys. Rev. Lett.* **121** 080403
[31] Ansmann M *et al* 2009 Violation of Bell's inequality in Josephson phase qubits *Nature* **461** 504
[32] Rowe M A *et al* 2001 Experimental violation of a Bell's inequality with efficient detection *Nature* **409** 791
[33] The BIG Bell Test Collaboration 2018 Challenging local realism with human choices *Nature* **557** 212–6
[34] Jönsson C 1961 Elektronen interferenzen an mehreren künstlich hergestellten Feinspalten *Z. Phys.* **161** 454–74
[35] Zeilinger A, Gahler R, Shull C G, Treimer W and Mampe W 1988 Single-and double-slit diffraction of neutrons *Rev. Mod. Phys.* **60** 1067–73
[36] Carnal O and Mlynek J 1991 Young's double-slit experiment with atoms: a simple atom interferometer *Phys. Rev. Lett.* **66** 2689
[37] Arndt M *et al* 1999 Wave-particle duality of C60 molecules *Nature* **401** 680–2
[38] Andrews M R *et al* 1997 Observation of interference between two bose condensates *Science* **275** 637–41
[39] Hackermuller L *et al* 2003 Wave nature of biomolecules and fluoro fullerenes *Phys. Rev. Lett.* **91** 090408
[40] Nairz O, Arndt M and Zeilinger A 2003 Quantum interference experiments with large molecules *Am. J. Phys.* **71** 319–25
[41] Gerlich S *et al* 2011 Quantum interference of large organic molecules *Nat. Commun.* **2** 263
[42] Feynman R P, Leighton R B and Sands M 1965 *The Feynman Lectures on Physics* vol 3 (Reading, MA: Addison-Wesley)
[43] Feynman R P 1965 *The Character of Physical Law* (New York: Modern Library)

[44] Spreeuw R J C 1998 A Classical Analogy of Entanglement *Found. Phys.* **28** 361–74
[45] Aiello A, Töppel F, Marquardt C, Giacobino E and Leuchs G 2015 Quantum-like non separable structures in optical beams *New J. Phys.* **17** 043024
[46] Lee H-W and Kim J 2000 Quantum teleportation and Bell's inequality using single-particle entanglement *Phys. Rev.* A **63** 012305
[47] Karimi E, Leach J, Slussarenko S, Piccirillo B, Marrucci L, Chen L, She W, Franke-Arnold S, Padgett M J and Santamato E 2010 Spin-orbit hybrid entanglement of photons and quantum contextuality *Phys. Rev.* A **82** 022115
[48] Hasegawa Y, Loidl R, Badurek G, Baron M and Rauch H 2003 Violation of a Bell-like inequality in single-neutron interferometry *Nature* **425** 45–58
[49] Hong C K, Ou Z Y and Mandel L 1987 Measurement of sub pico second time intervals between two photons by interference *Phys. Rev. Lett.* **59** 2044
[50] Franson J D 1989 Bell inequality for position and time *Phys. Rev. Lett.* **62** 2205–8
[51] Popper K R 1934 *Quantum Theory and the Schism in Physics Die Naturwissenshaften* **22** 807
[52] Popper K R 2013 *Quantum Theory and the Schism in Physics: From the Postscript to the Logic of Scientific Discovery* (New York: Routledge)
[53] Bolduc E, Karimi E, Piche K, Leach J and Boyd R W 2017 Experimental investigation of Popper's proposed ghost-diffraction experiment *J. Opt.* **19** 104002
[54] Moreau P-A, Morris P A, Toninelli E, Gregory T, Aspden R S, Spalding G, Boyd R W and Padgett M J 2018 Experimental limits of ghost diffraction: Popper's thought experiment *Sci. Rep.* **8** 13183
[55] Qureshi T 2012 Analysis of Popper's experiment and its realization *Prog. Theor. Phys.* **127** 645–56
[56] Qureshi T 2005 Understanding Popper's experiment *Am. J. Phys.* **73** 541–4
[57] Qureshi T 2012 Popper's experiment: a modern perspective (arXiv:1206.1432)
[58] Kim Y-H and Shih Y 1999 Experimental realization of Popper's experiment: violation of the uncertainty principle? *Found. Phys.* **29** 1849
[59] Moreau P-A *et al* 2018 Experimental limits of ghost diffraction: Popper's thought experiment *Sci. Rep.* **8** 13183
[60] Einstein A, Podolsky B and Rosen N 1935 Can quantum-mechanical description of physical reality be considered complete? *Phys. Rev.* **47** 777
[61] M Born (ed) 1971 *The Born Einstein Letters* 221 (London: Macmillan)
[62] Bohm D 1951 *Quantum Theory* (New York: Prentice Hall)
[63] Bohm D and Aharonov Y 1957 Discussion of experimental proof for the paradox of Einstein, Rosen, and Podolsky *Phys. Rev.* **108** 1070
[64] Schrödinger E 1935 Die gegenwärtige Situation in der Quantenmechanik (The present situation in quantum mechanics) *Naturwissenschaften* **23** 807–12
[65] Dur̈ W and Briegel H J 2004 Stability of macroscopic entanglement under decoherence *Phys. Rev. Lett.* **92** 180403
[66] Kovachy T, Asenbaum P, Overstreet C, Donnelly C C A, Dickerson S M, Sugarbaker A and Kasevich M A 2015 Quantum superposition at the half-metre scale *Nature* **528** 530
[67] Vedral V 2008 Quantifying entanglement in macroscopic systems *Nature* **453** 1004
[68] Paternostro M, Vitali D, Gigan S, Kim M S, Brukner C, Eisert J and Aspelmeyer M 2007 Creating and probing multipartite macroscopic entanglement with light *Phys. Rev. Lett.* **99** 250401
[69] Wigner E P 1995 Remarks on the mind-body question *Philosophical Reflections and Syntheses* (Berlin, Heidelberg: Springer) 247–60
[70] Vedral V 2016 Observing the observer (arXiv:1603.04583)
[71] Vedral V 2018 Observing the observer II: can I know I am in a superposition and still be in a superposition? (arXiv:1803.03523)
[72] Proietti M, Pickston A, Graffitti F, Barrow P, Kundys D, Branciard C, Ringbauer M and Fedrizzi A 2019 Experimental test of local observer independence *Sci. Adv.* **5** eaaw9832
[73] Brukner C 2018 A no-go theorem for observer-independent facts *Entropy* **20** 350
[74] Frauchiger D and Renner R 2018 Quantum theory cannot consistently describe the use of itself *Nat. Commun.* **9** 3711
[75] Clauser J F, Horne M A, Shimony A and Holt R A 1969 *Phys. Rev. Lett.* **23** 880
[76] Brunner N *et al* 2014 Bell non locality *Rev. Mod. Phys.* **86** 419
[77] Giustina M *et al* 2015 Significant-Loophole-free test of Bell's theorem with entangled photons *Phys. Rev. Lett.* **115** 250401
[78] Shalm L K *et al* 2015 Strong Loophole-free test of local realism *Phys. Rev. Lett.* **115** 250402
[79] Greenberger D M, Horne M, Shimony A and Zeilinger A 1990 Bell's theorem without inequalities *Am. J. Phys.* **58** 1131
[80] Greenberger D M, Horne M and Zeilinger A 1989 *Bell's Theorem, Quantum Theory, and Conceptions of the Universe* (Dordrecht: Kluwer Academic)
[81] Pan J W, Bouwmeester D, Daniell M, Weinfurter H and Zeilinger A 2000 Experimental test of quantum non locality in three-photon Greenberger-Horne-Zeilinger entanglement *Nature* **403** 515–9
[82] Hardy L 1993 Non locality for two particles without inequalities for almost all entangled states *Phys. Rev. Lett.* **71** 1665
[83] Horodecki M, Horodecki P and Horodecki R 2006 Properties of quantum non signaling boxes *Phys. Rev.* A **74** 012305
[84] Broadbent A and Methot A A 2006 On the power of non-local boxes *Theor. Comput. Sci.* **358** 3–14
[85] Leggett A J and Garg A 1985 Quantum mechanics versus macroscopic realism: is the flux there when nobody looks? *Phys. Rev. Lett.* **54** 857
[86] Kofler J and Brukner C 2013 Condition for macroscopic realism beyond the Leggett–Garg inequalities *Phys. Rev.* A **87** 052115
[87] Goggin M E, Almeida M P, Barbieri M, Lanyon B P, O'brien J L, White A G and Pryde G J 2011 Violation of the Leggett–Garg inequality with weak measurements of photons *Proc. Natl Acad. Sci.* **108** 1256–61
[88] Williams N S and Jordan A N 2008 Weak values and the Leggett–Garg inequality in solid-state qubits *Phys. Rev. Lett.* **100** 026804
[89] Groblacher S, Paterek T, Kaltenbaek R, Brukner C, Zukowski M, Aspelmeyer M and Zeilinger A 2007 An experimental test of non-local realism *Nature* **446** 871–5
[90] Paterek T, Fedrizzi A, Gröblacher S, Jennewein T, ?ukowski M, Aspelmeyer M and Zeilinger A 2007 Experimental test of nonlocal realistic theories without the rotational symmetry assumption *Phys. Rev. Lett.* **99** 210406
[91] Bell J S 1966 On the problem of hidden variables in quantum mechanics *Rev. Mod. Phys.* **38** 447–52
[92] Kochen S and Specker E P 1967 The problem of hidden variables in quantum mechanics *J. Math. Mech.* **17** 59–87

[93] Mermin N D 1993 Hidden variables and the two theorems of John Bell *Rev. Mod. Phys.* **65** 803

[94] Cabello A 1997 A Proof with 18 vectors of the Bell–Kochen–Specker theorem *New Developments on Fundamental Problems in Quantum Physics. Fundamental Theories of Physics* (An International Book Series on the Fundamental Theories of Physics: Their Clarification, Development and Application vol 81) ed M Ferrero and A van der Merwe (Dordrecht: Springer)

[95] Klyachko A A, Ali Can M, Binicioğlu S and Shumovsky A S 2008 Simple test for hidden variables in spin-1 systems *Phys. Rev. Lett.* **101** 020403

[96] Cabello A, Severini S and Winter A 2014 Graph-theoretic approach to quantum correlations *Phys. Rev. Lett.* **112** 040401

[97] Meyer D A 1999 Finite precision measurement nullifies the Kochen–Specker theorem *Phys. Rev. Lett.* **83** 3751

[98] Ambrosio V D, Herbauts I, Amselem E, Nagali E, Bourennane M, Sciarrino F and Cabello A 2013 Experimental implementation of a Kochen-Specker set of quantum tests *Phys. Rev.* X **3** 011012

[99] Lapkiewicz R, Li P, Schaeff C, Langford N K, Ramelow S, Wieśniak M and Zeilinger A 2011 Experimental non-classicality of an indivisible quantum system *Nature* **474** 490

[100] Karimi E, Cardano F, Maffei M, de Lisio C, Marrucci L, Boyd R W and Santamato E 2014 Hardy's paradox tested in the spin-orbit Hilbert space of single photons *Phys. Rev.* A **89** 032122

[101] Hasegawa Y, Schmitzer C, Bartosik H, Klepp J, Sponar S, Durstberger-Rennhofer K and Badurek G 2012 Falsification of Leggett's model using neutron matter waves *New J. Phys.* **14** 023039

[102] Sanders B C 1989 Quantum dynamics of the nonlinear rotator and the effects of continual spin measurement *Phys. Rev.* A **40** 2417

[103] Boto N A *et al* 2000 Quantum inter ferometric optical lithography: exploiting entanglement to beat the diffraction limit *Phys. Rev. Lett.* **85** 2733

[104] Lee H, Kok P and Dowling J P 2002 A quantum Rosetta stone for interferometry *J. Mod. Opt.* **49** 2325–38

[105] Dowling J P 2008 Quantum optical metrology–the lowdown on high-N00N states *Contemp. Phys.* **49** 125–43

[106] Jones J A *et al* 2009 Magnetic field sensing beyond the standard quantum limit using 10-spin N00N states *Science* **324** 1166–8

[107] Israel Y, Shamir R and Silberberg Y 2014 Polarization microscopy using NOON states of light *Phys. Rev. Lett.* **112** 103604

[108] Tan S M, Walls D F and Collett M J 1991 Nonlocality of a single photon *Phys. Rev. Lett.* **66** 252

[109] Hardy L 1994 Non locality of a single photon revisited *Phys. Rev. Lett.* **73** 2279

[110] Greenberger D M, Horne M A and Zeilinger A 1995 Nonlocality of a single photon? *Phys. Rev. Lett.* **75** 2064

[111] Vaidman L 1995 Non locality of a single photon revisited again *Phys. Rev. Lett.* **75** 2063

[112] Aharonov Y and Vaidman L 2000 Nonlocal aspects of a quantum wave *Phys. Rev.* A **61** 052108

[113] Bennett C H and Wiesner S J 1992 Communication via one-and two-particle operators on Einstein–Podolsky–Rosen states *Phys. Rev. Lett.* **69** 2881

[114] Bennett C H, Brassard G, Crépeau C, Jozsa R, Peres A and Wootters W K 1993 Teleporting an unknown quantum state via dual classical and Einstein–Podolsky–Rosen channels *Phys. Rev. Lett.* **70** 1895

[115] Ekert A K 1991 Quantum Cryptography based on Bell's theorem *Phys. Rev. Lett.* **67** 661

[116] Cirelson B S 1980 Quantum generalizations of Bell's inequality *Lett. Math. Phys.* **4** 93–100

[117] Uffink J 2002 Quadratic Bell inequalities as tests for multipartite entanglement *Phys. Rev. Lett.* **88** 230406

[118] Christensen B G, Liang Y C, Brunner N, Gisin N and Kwiat P G 2015 Exploring the limits of quantum non locality with entangled photons *Phys. Rev.* X **5** 041052

[119] Tsirelson B S 1987 Quantum analogues of the Bell inequalities. The case of two spatially separated domains *J. Sov. Math.* **36** 557–70

[120] Landau L L 1988 Empirical two-point correlation functions *Found. Phys.* **18** 449–60

[121] Masanes L 2003 Necessary and sufficient condition for quantum-generated correlations (arXiv:quant-ph/0309137)

[122] Popescu S and Rohrlich D 1994 Quantum nonlocality as an axiom *Found. Phys.* **24** 379–85

[123] Navascués M, Pironio S and Acín A 2008 A convergent hierarchy of semi definite programs characterizing the set of quantum correlations *New J. Phys.* **10** 073013

[124] Goh K T, Kaniewski J, Wolfe E, Vertesi T, Wu X, Cai Y, Liang Y-C and Scarani V 2018 Geometry of the set of quantum correlations *Phys. Rev.* A **97** 022104

[125] Popescu S 2014 Nonlocality beyond quantum mechanics *Nat. Phys.* **10** 264

[126] Rai A, Duarte C, Brito S and Chaves R 2019 Geometry of the quantum set on no-signaling faces *Phys. Rev.* A **99** 032106

[127] Pozas-Kerstjens A, Rabelo R, Rudnicki L, Chaves R, Cavalcanti D, Navascues M and Acin A 2019 Bounding the sets of classical and quantum correlations in networks (arXiv:1904.08943)

[128] Pawlowski M *et al* 2009 Information causality as a physical principle *Nature* **461** 1101–4

[129] Oppenheim J and Wehner S 2010 The uncertainty principle determines the nonlocality of quantum mechanics *Science* **330** 1072–4

[130] Navascués M and Wunderlich H 2010 A glance beyond the quantum model *Proc. Roy. Soc.* A **466** 881–90

[131] Fritz T *et al* 2013 Local orthogonality as a multipartite principle for quantum correlations *Nat. Commun.* **4** 2263

[132] Brassard G *et al* 2006 Limit on non locality in any world in which communication complexity is not trivial *Phys. Rev. Lett.* **96** 250401

[133] Linden N, Popescu S, Short A J and Winter A 2007 Quantum nonlocality and beyond: limits from nonlocal computation *Phys. Rev. Lett.* **99** 180502

[134] Carmi A and Cohen E 2019 Relativistic independence bounds nonlocality *Sci. Adv.* **5** eaav8370

[135] Shimony A 1984 Controllable and uncontrollable non-locality *Proceedings of the International Symposium: Foundations of Quantum Mechanics in the Light of New Technology* ed S Kamefuchi *et al* (Tokyo: Physical Society of Japan) 225–30

[136] Shimony A 1986 Events and processes in the quantum world *Quantum Concepts of Space and Time* ed R Penrose and C Isham (Oxford: Oxford University Press)

[137] Aharonov Y *Unpublished Lecture Notes* (Tel-Aviv University Tel Aviv)

[138] Carmi A and Cohen E 2018 On the significance of the quantum mechanical covariance matrix *Entropy* **20** 500

[139] Carmi A, Herasymenko Y, Cohen E and Snizhko K 2019 Bounds on nonlocal correlations in the presence of signaling and their application to topological zero modes *New J. Phys.* **21** 073032

[140] Te'eni A, Peled B Y, Cohen E and Carmi A 2019 Multiplicative Bell inequalities *Phys. Rev.* A **99** 040102

[141] Hofmann H F 2019 Local measurement uncertainties impose a limit on nonlocal quantum correlations *Phys. Rev.* A **100** 012123

[142] Zhou X and Yu S 2019 No disturbance without uncertainty as a physical principle (arXiv:1906.11807)
[143] Goldin M A *et al* 2010 Simulating Bell inequality violations with classical optics encoded qubits *J. Opt. Soc. Am.* B **27** 779
[144] Qian X F *et al* 2015 Shifting the quantum-classical boundary: theory and experiment for statistically classical optical fields *Optica* **2** 611
[145] Song X, Sun Y, Li P, Qin H and Zhang X 2015 *Sci. Rep.* **5** 14113
[146] Qian X-F, Little B, Howell J C and Eberly J H 2015 Shifting the quantum-classical boundary: theory and experiment for statistically classical optical fields *Optica* **2** 611–5
[147] Töppel F, Aiello F A, Marquardt C, Giacobino E and Leuchs G 2014 Classical entanglement in polarization metrology *New J. Phys.* **16** 073019
[148] Borges C V S *et al* 2010 Bell-like inequality for the spin-orbit separability of a laser beam *Phys. Rev.* A **82** 033833
[149] Kagalwala K H, Di Giuseppe G, Abouraddy A F and Saleh B E A 2013 Bell's measure in classical optical coherence *Nat. Photon.* **7** 72–8
[150] Berg-Johansen S, Töppel F, Stiller B, Banzer P, Ornigotti M, Giacobino E and Marquardt C 2015 Classically entangled optical beams for high-speed kinematic sensing *Optica* **2** 864–8
[151] Perez-Garcia B, Francis J, McLaren M, Hernandez-Aranda R I, Forbes A and Konrad T 2015 Quantum computation with classical light: the Deutsch algorithm *Phys. Lett.* A **379** 1675–80
[152] Li P, Wang B and Zhang X 2016 High-dimensional encoding based on classical non separability *Opt. Express* **24** 15143–59
[153] Ndagano B, Perez-Garcia B, Roux F S, McLaren M, Rosales-Guzman C, Zhang Y, Mouane O, Hernandez-Aranda R I, Konrad T and Forbes A 2017 Characterizing quantum channels with non-separable states of classical light *Nat. Phys.* **13** 397–402
[154] Guzman-Silva D *et al* 2016 Demonstration of local teleportation using classical entanglement *Laser Photon. Rev.* **10** 317–21
[155] Korolkova N and Leuchs G 2019 Quantum correlations in separable multi-mode states and in classically entangled light *Rep. Prog. Phys.* **82** 056001
[156] Koopman B O 1931 Hamiltonian systems and transformation in Hilbert space *Proc. Natl Acad. Sci. USA* **17** 315
[157] Neumann J 1932 Zur Operatorenmethode In Der Klassischen Mechanik *Ann. Math.* **33** 587–642
[158] Morgan P 2019 Classical states, quantum field measurement *Phys. Scr.* **94** 075003
[159] Morgan P 2020 An algebraic approach to Koopman classical mechanics *Ann. Phys.* 168090
[160] Zurek W H 2000 Einselection and de coherence from an information theory perspective *Ann. Phys.* **9** 855–64
[161] Ollivier H and Zurek W H 2001 Quantum discord: a measure of the quantumness of correlations *Phys. Rev. Lett.* **88** 017901
[162] Henderson L and Vedral V 2001 Classical, quantum and total correlations *J. Phys.* A **34** 6899
[163] Modi K, Brodutch A, Cable H, Paterek T and Vedral V 2012 The classical-quantum boundary for correlations: discord and related measures *Rev. Mod. Phys.* **84** 1655
[164] Popescu S 2010 Dynamical quantum non-locality *Nat. Phys.* **6** 151
[165] Aharonov Y *et al* 2017 Finally making sense of the double-slit experiment *Proc. Natl Acad. Sci. USA* **114** 6480–5
[166] Bohm Y A D 1959 Significance of electromagnetic potentials in the quantum theory *Phys. Rev.* **115** 485
[167] Aharonov Y, Cohen E and Rohrlich D 2016 Non locality of the Aharonov–Bohm effect *Phys. Rev.* A **93** 042110
[168] Vaidman L 2012 Role of potentials in the Aharonov-Bohm effect *Phys. Rev.* A **86** 040101
[169] Elitzur A C and Cohen E 2015 Quantum oblivion: a master key for many quantum riddles *Int. J. Quant. Inf.* **12** 1560024
[170] Aharonov Y, Cohen E and Rohrlich D 2016 Non locality of the Aharonov–Bohm effect *Phys. Rev.* A **93** 042110
[171] Marletto C and Vedral V 2019 The Aharonov–Bohm phase is locally generated (like all other quantum phases) (arXiv:1906.03440)

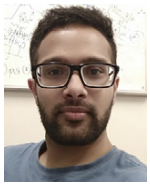

Dilip Paneru is currently a Masters student in Physics at University of Ottawa supervised by Prof. Ebrahim Karimi. He received his undergraduate degree in Electronics and Communication Engineering from the Institute of Engineering (IOE), Nepal. His general research interests lie at the intersection of Foundations of Quantum Mechanics and Quantum Optics. In the past, he worked in the area of weak values and weak measurements. At present, he is working on experimental tests of Quantum correlations and Quantum Imaging. Outside of physics he is also interested in and has worked on projects in Artificial Intelligence and Robotics. He is also a cofounder of Newrun Technology Pvt. Ltd., an artificial intelligence company based in Nepal.

Eliahu Cohen is an assistant professor in the Faculty of Engineering, Bar-Ilan University. He is a member of the Bar-Ilan Institute of Nanotechnology and Advanced Materials and the Center for Quantum Entanglement Science and Technology. He is also the head of the Quantum Engineering program at Bar-Ilan University. Eliahu Cohen has been exploring, theoretically and experimentally, various types of advanced quantum measurement techniques including: weak, sequential, partial, interaction-free, nonlocal, protective, and robust. He has also contributed to the study of entanglement and nonlocality, both kinematic and dynamic. He is interested in various photonic applications of the above, mainly for metrology, sensing, imaging and computation.

Robert Fickler received his masters degree in physics from Ulm University, Germany, in 2009. He also holds a bachelor's degree in philosophy and is a trained electronics engineer. He obtained his PhD degree in 2014 from the University of Vienna, Austria, and worked as a postdoctoral fellow at the University of Ottawa, Canada, and the Institute for Quantum Optics and Quantum Information - Vienna, Austria. Since 2019, he is an Assistant Professor at Tampere University, Finland, where is continuing to work on quantum photonics, quantum information, and light-matter interactions in the quantum regime. He has published more than 50 research papers. His research was named as one of the Top 10 breakthroughs of the year 2012 by IOPs Physics World, he received the Young Scientist Award 2015 of the IUPAP as well as the Banting Postdoctoral Fellowship of the Natural Sciences and Engineering Research Council of Canada 2016.

Robert W. Boyd was born in Buffalo, New York. He received the B.S. degree in physics from MIT and the Ph.D. degree in physics from the University of California at Berkeley. His Ph.D. thesis was supervised by Charles Townes and involves the use of nonlinear optical techniques in infrared detection for astronomy. He joined the faculty of University of Rochester in 1977 and in 2010 became Professor of Physics and Canada Excellence Research Chair in Quantum Nonlinear Optics at the University of Ottawa. His research involves studies of optical physics and of nonlinear optics. Professor Boyd has written two books, co-edited two anthologies, published over 400 research papers, and been awarded ten patents. He is a member of the Heidelberg Academy and of the Royal Society of Canada. He is a past winner of the Townes Award, Schawlow Prize and a Humboldt Research Award. He is a fellow of IEEE, OSA, APS and SPIE.

Ebrahim Karimi was born in Saghez, Kurdistan-Iran. He received the B.Sc. degree in Physics with an emphasis in mathematics from Kerman University in 2001, and M.Sc. from IASBS in 2003, and Ph.D. degree from the University of Naples "Federico II" in 2009. He holds Canada Research Chair in Structured Light at the University of Ottawa. His research focuses on structured quantum waves and their applications in quantum communication, quantum computation, and materials science. He has published over 120 scientific articles in peer-reviewed journals and is co-inventor on three patents. His contributions notably include studies pertaining to the relationship between the quantum spatial properties of photons and their internal properties. Professor Karimi is a Fellow of the OSA, member of the Global Young Academy, Visiting Fellow of the Max Planck Institute for the Science of Light, Fellow of the JCEP, and awarded the Ontario Early Researcher Award in 2018, and the University of Ottawa Early Career Researcher of the Year Award in 2019.

Chapter 3

Multiplicative Bell Inequalities

This chapter is based on the following work:

- D. Paneru, *et al.*, Experimental tests of Multiplicative Bell Inequalities, arXiv preprint arXiv:2009.03930 (2020).

3.1 Introduction to multiplicative Bell inequalities

As discussed in the previous chapters, Bell inequalities [13, 29] are expressions that demarcate the boundary between classical and quantum physics. Most of the Bell inequalities we looked at in Chapter 2 are in the form of the linear combination of bipartite correlations. Multiplicative Bell inequalities [19] are a new type of inequalities that involve the product of the two-point correlators. Corresponding to the number of measurement devices n Alice and Bob each have access to, there exists a multiplicative Bell parameter. In contrast to the linear Bell inequalities, finding quantum limits for any number n, is relatively easy for these parameters and is proven to be $n!$ [19].

3.1.1 Volume maximization game

Multiplicative Bell inequalities for general n, can be visualized as a two player coordinated game between Alice and Bob, where they try to maximize a certain parameter. For general n number of devices, it corresponds to maximizing the average volume of a hyperrectangle, traversed by a random walker. For the simplest case of two measurement devices, this corresponds to maximizing the area of a rectangle [19]. Say Alice and Bob have two distinct sets of orthogonal vectors $\mathbf{v}_1, \mathbf{v}_2$, and $\mathbf{u}_1, \mathbf{u}_2$. Additionally, they also have two binary variables $a, b \in \{+1, -1\}$. Alice and Bob can randomly choose a vector and values for the binary variables and pass it to a random walker. The random walker then takes a step forward or backward along Bob's chosen vector, depending on the conditions $a = b$, or $a \neq b$ respectively. After some rounds, the walker is at certain position, and a rectangle is formed by Bob's vectors, origin and the random walkers current position. The goal of

the game is to maximize the area of that rectangle.
On each round k, Alice and Bob choose their vectors $\mathbf{v}_i$, $\mathbf{u}_j$, and the variables a_i, b_j, randomly and independent of any other rounds. On each round the displacement vector for the walker can be written as,

$$\mathbf{s}_k = a_j b_j (\mathbf{v}_i \cdot \mathbf{u}_j) \cdot \mathbf{u}_j. \tag{3.1}$$

After certain rounds say N, the normalized area of the rectangle is given by,

$$A = \frac{1}{N^2} \left(\mathbf{u}_1 \cdot \sum_k^N \mathbf{s}_k \right) \left(\mathbf{u}_2 \cdot \sum_k^N \mathbf{s}_k \right) \tag{3.2}$$

$$= \frac{1}{N^2} \left(\mathbf{u_1} \cdot \sum_{k=1}^N a_i \mathbf{b}_j (\mathbf{v}_i \cdot \mathbf{u}_j) \cdot \mathbf{u}_j \right) \left(\mathbf{u_2} \cdot \sum_{k=1}^N a_i b_j (\mathbf{v}_i \cdot \mathbf{u}_j) \cdot \mathbf{u}_j \right), \tag{3.3}$$

Here k is the general index that represents a particular set of i, j for each step.

The average normalized area is given by,

$$\begin{aligned} E[A] &= \frac{1}{N^2} E \left[\mathbf{u_1} \cdot \sum_{k=1}^N a_i b_j (\mathbf{v}_i \cdot \mathbf{u}_j) \mathbf{u}_j \right] E \left[\mathbf{u_2} \cdot \sum_{k=1}^N a_i b_j (\mathbf{v}_i \cdot \mathbf{u}_j) \mathbf{u}_j \right], \\ &= \frac{1}{N^2} N.E \left[a_i b_j (\mathbf{v}_i \cdot \mathbf{u}_j)(\mathbf{u}_1 \cdot \mathbf{u}_j) \right] N.E \left[a_i b_j (\mathbf{v}_i \cdot \mathbf{u}_j)(\mathbf{u}_2 \cdot \mathbf{u}_j) \right] \\ &= E \left[a_i b_j (\mathbf{v}_i \cdot \mathbf{u}_1) \right] E \left[a_i b_j (\mathbf{v}_i \cdot \mathbf{u}_2) \right] \\ &= \frac{1}{4} \left(E[a, b | i = 1, j = 1] - E[a, b | i = 2, j = 1] \right) \\ &\quad \frac{1}{4} \left(E[a, b | i = 1, j = 2] + E[a, b | i = 2, j = 2] \right) \\ &= \frac{1}{16} (c_{11} - c_{21})(c_{12} + c_{22}), \end{aligned} \tag{3.4}$$

where $c_{ij} = E[ab|i, j]]$, is the correlation of Alice's and Bob's binary outcomes a, and b. Eq.(3.4), is proportional to the Bell parameter $\mathcal{B}_2$,

$$\mathcal{B}_2 = (c_{11} - c_{21})(c_{12} + c_{22}). \tag{3.5}$$

Similar generalizations can be made for the n device multiplicative Bell parameter, in which the game corresponds to maximizing a volume of a hyper rectangle in n- dimensional space. For each number of local measurements (n), Alice and Bob each can perform, there exists a multiplicative Bell parameter $\mathcal{B}_n$ associated with it, i.e,

$$\mathcal{B}_n \quad = \quad (c_{1n} + \cdots + c_{nn}) \prod_{j=1}^{n-1} \left(c_{1j} + \ldots + c_{jj} - j c_{j+1,j} \right). \tag{3.6}$$

3.1.2 Construction of the multiplicative Bell parameter

The general multiplicative Bell parameters for n measurement devices are constructed in the following way. Let A_i, and B_j be Alice's and Bob's operators with eigenvalues ± 1. Let us define a vector X of these operators,

$$X = \begin{pmatrix} B_j \\ A_1 \\ \vdots \\ A_n \end{pmatrix}. \tag{3.7}$$

The second moment matrix of X is defined as,

$$\Sigma_{ij} = \langle X_i X_j \rangle = \begin{pmatrix} \langle B_j B_j \rangle & \langle A_1 B_j \rangle & \langle A_2 B_j \rangle & \dots & \langle A_n B_j \rangle \\ \langle A_1 B_j \rangle & \langle A_1 A_1 \rangle & \langle A_1 A_2 \rangle & \dots & \langle A_1 A_n \rangle \\ \langle A_2 B_j \rangle & \langle A_2 A_1 \rangle & \langle A_2 A_2 \rangle & \dots & \vdots \\ \vdots & \vdots & \vdots & \vdots & \langle A_{n-1} A_n \rangle \\ \langle A_n B_j \rangle & \langle A_n A_1 \rangle & \dots & \langle A_n A_{n-1} \rangle & \langle A_n A_n \rangle \end{pmatrix} \tag{3.8}$$

To simplify our notations let us define,

$$c_{ij} = \langle A_i B_j \rangle, \tag{3.9}$$

as the two point correlation between Alice's and Bob's measurement outcomes. Similarly,

$$r_{ij} = \langle A_i A_j \rangle = \langle A_j A_i \rangle^*. \tag{3.10}$$

Also, $\langle B_i B_i \rangle = \langle A_i A_i \rangle = 1$. Using these relations, in Eq. (3.8),

$$\Sigma_{ij} = \begin{pmatrix} 1 & c_{1j} & c_{2j} & \dots & c_{1j} \\ c_{1j} & 1 & r_{12} & \dots & r_{1n} \\ c_{2j} & r_{21} & 1 & \dots & \vdots \\ \vdots & \vdots & \vdots & \vdots & r_{n-1,n} \\ c_{nj} & r_{n1} & \dots & r_{n,n-1} & 1 \end{pmatrix}. \tag{3.11}$$

From the positive semi-definiteness of Eq. (3.11), and using Schur's complement,

$$\mathcal{R} = \begin{pmatrix} 1 & \dots r_{ij} & \\ \vdots & \ddots & \vdots \\ r_{ji} & \vdots & 1 \end{pmatrix} \succcurlyeq \begin{pmatrix} c_{1j} \\ \vdots \\ c_{nj}. \end{pmatrix} \begin{pmatrix} c_{1j} & \dots & c_{nj} \end{pmatrix}. \tag{3.12}$$

Let us construct a symmetric $n \times n$ matrix,

$$\tau = \begin{pmatrix} 1 & r & \dots r & \\ r & 1 & r & \vdots \\ \vdots & r & \ddots & r \\ r & \dots & r & 1 \end{pmatrix}, \tag{3.13}$$

with following orthogonal eigenvectors,

$$\mathbf{u}_j(l) = \begin{cases} 1 & l \leq j \\ -j & l = j+1 \\ 0 & l > j+1 \end{cases},$$

for $1 \leq j < n$, and

$$\mathbf{u}_n = \begin{pmatrix} 1 \\ \vdots \\ 1 \end{pmatrix}.$$

Arranged as a column of a matrix, the vectors $\mathbf{u}_j$, can be written as,

$$V = \begin{pmatrix} 1 & 1 & \dots & 1 & 1 \\ -1 & 1 & \dots & 1 & 1 \\ 0 & -2 & \ddots & 1 & 1 \\ \vdots & \vdots & \ddots & \vdots & \vdots \\ 0 & 0 & 0 & -(n-1) & 1 \end{pmatrix}.$$

Using these eigenvectors,the construction of the Bell parameters can be done as,

$$\mathcal{B}_n = \prod_{j=1}^{n} c_j \cdot \mathbf{u}_j. \tag{3.14}$$

where c_j is the vector of correlation of Alice's measurements with B_j.

$$c_j = \begin{pmatrix} c_{1j} \\ c_{2j} \\ \vdots \\ c_{nj} \end{pmatrix} \tag{3.15}$$

As an example, for $n = 3$, the vectors are,

$$\mathbf{u}_1 = \begin{pmatrix} 1 \\ -1 \\ 0. \end{pmatrix} \quad \mathbf{u}_2 = \begin{pmatrix} 1 \\ +1 \\ -2. \end{pmatrix} \quad \mathbf{u}_3 = \begin{pmatrix} 1 \\ 1 \\ 1. \end{pmatrix} \tag{3.16}$$

$$\mathbf{c_1} = \begin{pmatrix} c_{11} \\ c_{21} \\ c_{31}. \end{pmatrix} \quad \mathbf{c}_2 = \begin{pmatrix} c_{12} \\ c_{22} \\ c_{32}. \end{pmatrix} \quad \mathbf{c}_3 = \begin{pmatrix} c_{13} \\ c_{23} \\ c_{33} \end{pmatrix}. \tag{3.17}$$

And the corresponding Bell parameter is,

$$\mathcal{B}_3 = (c_{13} + c_{23} + c_{33})(c_{11} - c_{21})(c_{12} + c_{22} - 2c_{32}).$$

3.2 Classical and Tsirelson bounds for multiplicative Bell Inequalities:

3.2.1 Tsirelson Bound:

The Tsirelson (quantum) bound for the n-device multiplicative Bell parameters (3.6), was proven to be,

$$|\mathcal{B}_n| \leq n! \tag{3.18}$$

We briefly discuss the outline of the proof [19] below: It can be proven that [19], (the proof is beyond the scope of this thesis),

$$\sum_{j=1}^{n} \hat{u}_j^T \mathcal{R}^T \hat{u}_j = n. \tag{3.19}$$

From Eq (3.12), we also have,

$$\hat{u}_j^T c_j c_j^T \hat{u}_j \leq \hat{u}_j^T \mathcal{R}^T \hat{u}_j. \tag{3.20}$$

From the inequality of Arithmetic and geometric means,

$$\prod_{j=1}^{n} \hat{u}_j^T \mathcal{R}^T \hat{u}_j \leq \left(\frac{\sum_{j=1}^{n} \hat{u}_j^T \mathcal{R}^T \hat{u}_j}{n} \right). \tag{3.21}$$

From equations (3.19), (3.20), and (3.21), we have,

$$\prod_{j=1}^{n} |c_j.\hat{u}_j|^2 \leq 1 \tag{3.22}$$

$$= \prod_{j=1}^{n} \frac{1}{\|\mathbf{u}_j\|^2} \prod_{j=1}^{n} |c_j.\mathbf{u}_j| \leq 1. \tag{3.23}$$

Now since,

$$\prod_{j=1}^{n} \|\mathbf{u}_j\|^2 = \|\mathbf{u}_n\|^2 \prod_{j=1}^{n-1} \|\mathbf{u}_j\|^2 = n \prod_{j=1}^{n-1} (j + j^2) = (n!)^2. \tag{3.24}$$

and,

$$\prod_{j=1}^{n} \|\mathbf{u}_j\| = n!. \tag{3.25}$$

From equations (3.22), and (3.25), we have,

$$|\mathcal{B}_n| = \left| \prod_{j=1}^{n} c_j \cdot \mathbf{u}_j \right| \leq n!. \tag{3.26}$$

3.2.2 Classical and Tsirelson Bound for n =2:

As outlined in [19], the classical and quantum bounds can be derived as follows: We have the multiplicative Bell parameter $\mathcal{B}_2$, and the CHSH parameter defined as,

$$\mathcal{B}_2 = |(c_{12} + c_{22})(c_{12} - c_{21})| \tag{3.27}$$

$$\text{CHSH} = |c_{12} + c_{22} + c_{12} - c_{21}|\,. \tag{3.28}$$

From the inequality of arithmetic and geometric means,

$$\mathcal{B}_2 = |(c_{12} + c_{22})(c_{12} - c_{21})| \leq \left(\frac{c_{12} + c_{22} + c_{12} - c_{21}}{2}\right)^2 = \left(\frac{\text{CHSH}}{2}\right)^2. \tag{3.29}$$

Now using the respective classical and quantum bounds (2.7),

$$\mathcal{B}_2^{\text{Classical}} \leq 1, \;\; \mathcal{B}_2^{\text{Quantum}} \leq 2. \tag{3.30}$$

3.2.3 Fully deterministic strategy and classical bounds for n =2, 3 and 4

Finding the classical Bell limits for the multiplicative Bell parameters is in general a difficult task. We just looked at the classical bound for $n = 2$. An independent and deterministic strategy was proposed for both Alice and Bob in [19], and the corresponding classical limit was calculated. In this strategy, Bob always chooses his random variable to be $+1$, while Alice alternates between $+1$ and -1 for all of her variables A_i, until $i < i_c$, where i_c is some cutoff number; and for $i > i_c$, she chooses A_i to be $+1$. The correlations take the following values,

$$c_{ij} = \begin{cases} (-1)^i & i \leq i_c \\ 1 & i > i_c \end{cases}. \tag{3.31}$$

The value for the cutoff i_c is taken so as to maximize the value for the Bell parameter. The value for $\mathcal{B}_n$ obtained from this fully deterministic strategy, FD_n, can be analytically expressed as,

$$\text{FD}_n = 2^{i_c} \left[\left(\frac{i_c}{2}\right)!\right]^2 (n - i_c)\; i_c^{(n-i_c-1)}. \tag{3.32}$$

An intriguing aspect of this strategy is that, the ratio of the fully deterministic strategy and Tsirelson bound, i.e. $\text{FD}_n/n!$, approaches $\sqrt{\pi/2e}$ as $n \to \infty$. Additive Bell parameters associated with the multiplicative Bell parameters, $\mathcal{B}_n' = \sum_{i=1}^n \mathbf{v}_i.\mathbf{c}_j$ are saturated by deterministic strategies. The tight classical bounds for these can be used to find classical bounds for multiplicative Bell parameters using the inequality of geometric and arithmetic means,

$$|\mathcal{B}_n| \leq \left(\frac{\mathcal{B}_n'}{n}\right)^n. \tag{3.33}$$

Using this one obtains $\mathcal{B}_2 \leq 1$, $\mathcal{B}_3 \leq 4.6$, and $\mathcal{B}_4 \leq 16$. The bounds for $\mathcal{B}_2$, and $\mathcal{B}_4$ coincide with the respective bounds obtained from the fully deterministic strategy FD_n.

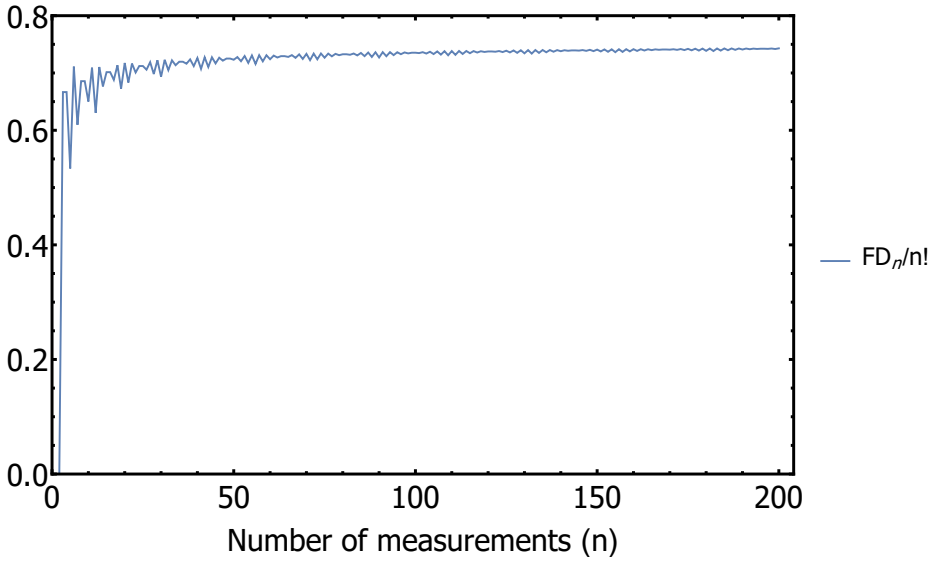

Figure 3.1: The ratio between the value of Bell parameters from a fully deterministic strategy (FD_n), and Tsirelson bound n!.

3.3 Strategy to saturate the Tsirelson limit

A strategy to select the vectors $\mathbf{a}_1 \ldots \mathbf{a}_n$, and $\mathbf{b}_1 \ldots \mathbf{b}_n$, so as to saturate the Tsirelson bounds ($|\mathcal{B}_n| \leq n!$) is outlined in [19]. We briefly summarize it here and do the explicit calculation for $\mathbf{a}_1 \ldots \mathbf{a}_n$, and $\mathbf{b}_1 \ldots \mathbf{b}_n$, upto $n = 4$.

1. Alice can choose $\mathbf{a}_1$ arbitrarily.

2. For each $i = 2 \ldots n$, Alice chooses $\mathbf{a}_i$ such that,

$$\mathbf{a}_i \cdot \sum_{j=1}^{i-1} \mathbf{a}_j = 0. \tag{3.34}$$

3. Bob's vectors, $\mathbf{b}_i$, are then given by the i$^{\text{th}}$ column of the matrix,

$$\mathbf{B} = F\mathbf{A}V. \tag{3.35}$$

where,

$$F = \begin{pmatrix} 1 & 0 & 0 \\ 0 & -1 & 0 \\ 0 & 0 & 1 \end{pmatrix}, \text{flips the sign of the y-component,} \tag{3.36}$$

$$\mathbf{A} = \begin{pmatrix} \vdots & \vdots & \vdots \\ \mathbf{a}_1 & \dots & \mathbf{a}_n \\ \vdots & \vdots & \vdots \end{pmatrix}, \text{and} \tag{3.37}$$

$$V = \begin{pmatrix} 1 & 1 & \dots & 1 & 1 \\ -1 & 1 & \dots & 1 & 1 \\ & -2 & \ddots & \vdots & 1 \\ & & \ddots & 1 & \vdots \\ & & & -(n-1) & 1 \end{pmatrix}. \tag{3.38}$$

4. Normalize each $\mathbf{a}_i$, and $\mathbf{b}_i$, i.e. $\hat{\mathbf{a}}_i = \frac{\mathbf{a}_i}{\|\mathbf{a}_i\|}, \hat{\mathbf{b}}_i = \frac{\mathbf{b}_i}{\|\mathbf{b}_i\|}$.

3.3.1 Explicit calculation for n=2, 3, and 4

Below we present the explicit calculation of the vectors $\mathbf{a}_i \dots \mathbf{a}_n$, and $\mathbf{b}_i \dots \mathbf{b}_n$ for $n = 2, 3,$ and 4.

1. **n = 2:**
   The Bell parameter for $n = 2$ is,

   $$\mathcal{B}_2 = |(c_{12} + c_{22})(c_{12} - c_{21})| \leq 2.$$

   (a) Let us choose $_1 = \begin{pmatrix} 1 \\ 0 \\ 0 \end{pmatrix}$

   (b) $\mathbf{a}_2 = \begin{pmatrix} 0 \\ 0 \\ 1 \end{pmatrix}$, satisfies the requirement $\mathbf{a}_1.\mathbf{a}_2 = 0$.

   (c) $V = \begin{pmatrix} 1 & 1 \\ -1 & 1. \end{pmatrix}$, and $A = \begin{pmatrix} \mathbf{a}_1 & \mathbf{a}_2 \end{pmatrix}$. Hence,

   $$B = \begin{pmatrix} \mathbf{a}_1 - \mathbf{a}_2 & \mathbf{a}_1 + \mathbf{a}_2 \end{pmatrix}.$$

   Since, all our vectors have zero Y-component, the flipping can be omitted.

(d) After normalization,

$$\mathbf{b}_1 = \begin{pmatrix} \frac{1}{\sqrt{2}} \\ 0 \\ -\frac{1}{\sqrt{2}}. \end{pmatrix}$$

$$\mathbf{b}_2 = \begin{pmatrix} -\frac{1}{\sqrt{2}} \\ 0 \\ \frac{1}{\sqrt{2}} \end{pmatrix}$$

The vectors are plotted in polarisation Poincaŕe sphere and the HV plane in Figure 3.2. Note that these vectors are the same as the vectors which maximize the CHSH parameter.

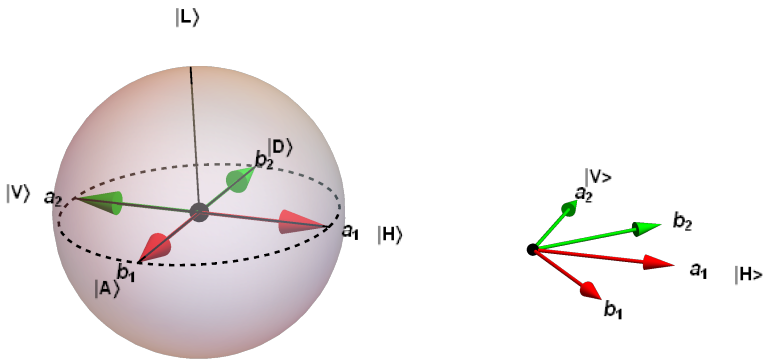

Figure 3.2: **Strategy for n = 2:** Alice's and Bob's vectors $\mathbf{a}_1, \mathbf{a}_2$, and $\mathbf{b}_1, \mathbf{b}_2$ in polarisation Poincaré sphere and 2D HV plane.

2. **n=3:** The Bell parameter for $n = 3$ is,

$$\mathcal{B}_3 = |(c_{13} + c_{23} + c_{33})(c_{11} - c_{21})(c_{12} + c_{22} - 2c_{32})| \leq 3!.$$

Alice and Bob can choose their vectors $\mathbf{a}_1, \mathbf{a}_2,$ and $\mathbf{a}_3$, $\mathbf{b}_1, \mathbf{b}_2,$ and $\mathbf{b}_3$, as follows,

(a) Let us choose $\mathbf{a}_1 = \begin{pmatrix} 1 \\ 0 \\ 0 \end{pmatrix}$

(b) $\mathbf{a}_2 = \begin{pmatrix} 0 \\ 0 \\ 1 \end{pmatrix}$, satisfies the requirement $\mathbf{a}_1.\mathbf{a}_2 = 0$.

(c) a_3 has to satisfy the requirement $\mathbf{a}_3.(\mathbf{a}_1 + \mathbf{a}_2) = 0$.
Since, $\mathbf{a}_1 + \mathbf{a}_2 = \begin{pmatrix} 1 \\ 0 \\ 1 \end{pmatrix}$ we can choose $\mathbf{a}_3 = \begin{pmatrix} 1 \\ 0 \\ -1 \end{pmatrix}$

(d) $V = \begin{pmatrix} 1 & 1 & 1 \\ -1 & 1 & 1 \\ 0 & -2 & 1. \end{pmatrix}$, and $\mathbf{A} = \begin{pmatrix} \mathbf{a}_1 & \mathbf{a}_2 & \mathbf{a}_3 \end{pmatrix}$. Hence,

$$\mathbf{B} = \begin{pmatrix} \mathbf{a}_1 - \mathbf{a}_2 & \mathbf{a}_1 + \mathbf{a}_2 - 2\mathbf{a}_3 & \mathbf{a}_1 + \mathbf{a}_2 + \mathbf{a}_3 \end{pmatrix}.$$

As before, all our vectors have zero Y-component, the flipping can be omitted.

(e) After normalization,

$$\mathbf{a}_1 = \begin{pmatrix} 1 \\ 0 \\ 0 \end{pmatrix}, \quad \mathbf{a}_2 = \begin{pmatrix} 0 \\ 0 \\ 1 \end{pmatrix}, \quad \mathbf{a}_3 = \begin{pmatrix} \frac{1}{\sqrt{2}} \\ 0 \\ -\frac{1}{\sqrt{2}} \end{pmatrix} \tag{3.39}$$

$$\mathbf{b}_1 = \begin{pmatrix} \frac{1}{\sqrt{2}} \\ 0 \\ -\frac{1}{\sqrt{2}} \end{pmatrix}, \mathbf{b}_2 = \begin{pmatrix} -0.1691 \\ 0.9856 \\ 0 \end{pmatrix}, \quad \mathbf{b}_3 = \begin{pmatrix} 0.9856 \\ 0 \\ 0.1691 \end{pmatrix} \tag{3.40}$$

(3.41)

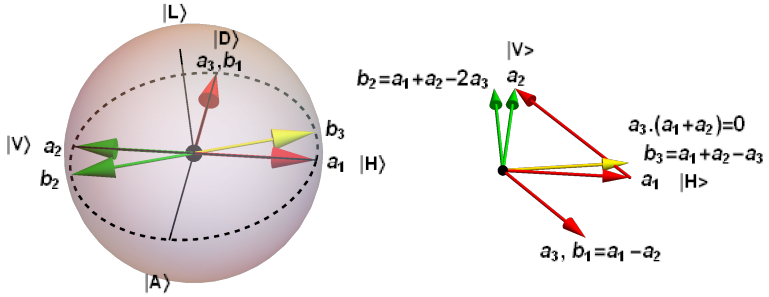

Figure 3.3: **Strategy for n= 3:** Alice's and Bob's vectors a_1, a_2, a_3, and b_1, b_2, b_3 in polarisation Poincaré sphere and 2D HV plane.

3. **n=4:** The Bell parameter for $n = 4$ is,

$$\mathcal{B}_4 = |(c_{14} + c_{24} + c_{34} + c_{44})(c_{11} - c_{21})(c_{12} + c_{22} - 2c_{32})(c_{13} + c_{23} + c_{33} - 3c_{43})| \leq 4!.$$

Alice and Bob can choose their vectors $\mathbf{a}_1, \ldots, \mathbf{a}_4$, and $\mathbf{b}_1, \ldots \mathbf{a}_4$, as follows,

(a) Since the vectors $\mathbf{a}_1, \mathbf{a}_2$, and $\mathbf{a}_3$ calculated for $n = 3$ satisfy the requirements $\mathbf{a}_1 \cdot \mathbf{a}_2 = 0$, and $\mathbf{a}_3 \cdot (\mathbf{a}_1 + \mathbf{a}_2) = 0$, our first three vectors can be the same.

$$\mathbf{a}_1 = \begin{pmatrix} 1 \\ 0 \\ 0 \end{pmatrix}, \quad \mathbf{a}_2 = \begin{pmatrix} 0 \\ 0 \\ 1 \end{pmatrix}, \quad \mathbf{a}_3 = \begin{pmatrix} \frac{1}{\sqrt{2}} \\ 0 \\ -\frac{1}{\sqrt{2}} \end{pmatrix}. \tag{3.42}$$

(b) $\mathbf{a}_4$ has to satisfy the requirement $\mathbf{a}_4 \cdot (\mathbf{a}_1 + \mathbf{a}_2 + \mathbf{a}_3) = 0$. So, we can choose a vector orthogonal to the sum.

Since, $\mathbf{a}_1 + \mathbf{a}_2 + \mathbf{a}_3 = \begin{pmatrix} 1 + \frac{1}{\sqrt{2}} \\ 0 \\ 1 - \frac{1}{\sqrt{2}} \end{pmatrix}$, $\mathbf{a}_4 = \begin{pmatrix} 1 - \frac{1}{\sqrt{2}} \\ 0 \\ -1 - \frac{1}{\sqrt{2}} \end{pmatrix}$.

Upon normalization, $\mathbf{a}_4 = \begin{pmatrix} 0.1691 \\ 0 \\ -0.9856 \end{pmatrix}$.

(c) $V = \begin{pmatrix} 1 & 1 & 1 & 1 \\ -1 & 1 & 1 & 1 \\ 0 & -2 & 1 & 1 \\ 0 & 0 & -3 & 1. \end{pmatrix}$, and $\mathbf{A} = \begin{pmatrix} \mathbf{a}_1 & \mathbf{a}_2 & \mathbf{a}_3 & \mathbf{a}_4 \end{pmatrix}$. Hence,

$$\mathbf{B} = \begin{pmatrix} \mathbf{a}_1 - \mathbf{a}_2 & \mathbf{a}_1 + \mathbf{a}_2 - 2\mathbf{a}_3 & \mathbf{a}_1 + \mathbf{a}_2 + \mathbf{a}_3 - 3\mathbf{a}_4 & \mathbf{a}_1 + \mathbf{a}_2 + \mathbf{a}_3 + \mathbf{a}_4 \end{pmatrix}.$$

As before, all our vectors have zero Y-component, the flipping can be omitted.

(d) After normalization,

$$\mathbf{a}_1 = \begin{pmatrix} 1 \\ 0 \\ 0 \end{pmatrix}, \quad \mathbf{a}_2 = \begin{pmatrix} 0 \\ 0 \\ 1 \end{pmatrix}, \quad \mathbf{a}_3 = \begin{pmatrix} \frac{1}{\sqrt{2}} \\ 0 \\ -\frac{1}{\sqrt{2}} \end{pmatrix}, \quad \mathbf{a}_4 = \begin{pmatrix} 0.1691 \\ 0 \\ -0.9856 \end{pmatrix}. \tag{3.43}$$

$$\mathbf{a}_1 = \begin{pmatrix} \frac{1}{\sqrt{2}} \\ 0 \\ -\frac{1}{\sqrt{2}} \end{pmatrix}, \quad \mathbf{a}_2 = \begin{pmatrix} -0.1691 \\ 0 \\ 0.9856 \end{pmatrix}, \quad \mathbf{a}_3 = \begin{pmatrix} 0.3463 \\ 0 \\ 0.9381 \end{pmatrix}, \quad \mathbf{a}_4 = \begin{pmatrix} -0.9381 \\ 0 \\ 0.3463 \end{pmatrix}. \tag{3.44}$$

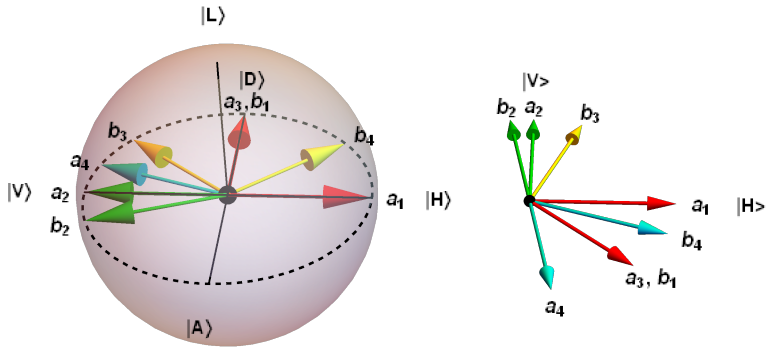

Figure 3.4: **Strategy for n= 4:** Alice's and Bob's vectors $\mathbf{a}_1, \mathbf{a}_2, \mathbf{a}_3, \mathbf{a}_4$, and $\mathbf{b}_1, \mathbf{b}_2, \mathbf{b}_3, \mathbf{b}_4$ in polarisation Poincaré sphere, and 2D HV plane.

3.4 Experimental Setup

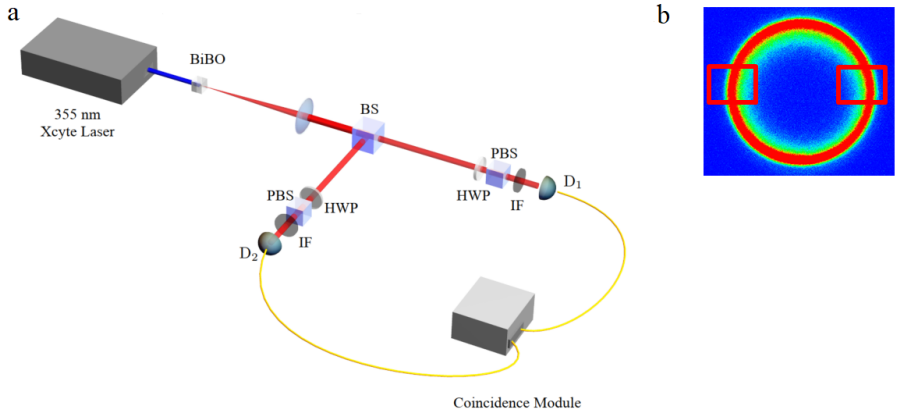

Figure 3.5: a) Experimental setup used for observing multiplicative Bell parameters. Entangled photon pairs are generated after pumping paired BiBO (Bismuth Triborate) crystals, and then separated by a 50:50 beamsplitter (BS) into two arms (Alice and Bob). On each side a half-wave plate (HWP) and polarising beamsplitter (PBS), constitute the polarisation measurement stage. The photons are filtered by a 710 nm interference bandpass filter (IF), and coupled into single mode fibres, and then detected using single photon avalanche diodes whose signals are sent to a coincidence module, Figure taken from D. Paneru,*et al.*, arXiv:2009.03930 (2020). b) Image of the SPDC ring taken from a CCD camera. Photons from diametrically opposite regions are entangled with each other.

The experimental setup for the test of the Multiplicative Bell Inequalities is shown in Fig. (3.5). Paired 0.5-mm-thick Type-I bismuth triborate crystal (BiBO) is pumped by a 100 mW, 355 nm beam to generate entangled photon pairs via SPDC at a degenerate wavelength of 710 nm. A half wave plate (HWP) placed before the paired crystals allows us to tailor the two photon entangled state. The 355 nm pump beam is filtered out afterwards with a band pass filter (IF). The photon pairs are separated by a 50:50 beamsplitter (BS), and the photons travel along two different arms. To select the diametrically opposite regions of the SPDC cone, we place a pair of irises on each arm such that they center on the required region. In each arm projective measurements in polarisation degree of freedom is performed by the combination of a quarter wave plate (QWP), a half wave plate (HWP), and a polarising beam splitter (PBS). The photons then are collected by a 20X objective and coupled into a single mode fiber of core diameter 5.4 micrometers. Then the photons are detected via a pair of Single Photon Avalanche Diode (SPAD) detectors (Excelitas SPCM-AQRH-14-FC), and are counted via a time correlated photon counting system.

3.4.1 Generation of Entangled photon pairs

3.4.2 Spontaneous parametric Down Conversion (SPDC)

Spontaneous Parametric Down Conversion (SPDC) is a nonlinear process in which an incident photon (also called pump photon) of higher energy is probabilistically converted into a pair of photons, called signal and idler photons, of lower energy via a non-linear crystal. The conservation of energy and momentum dictates that the energy and momentum of the down converted signal and idler photon add up to the total energy and momentum of the pump photon. The momentum conservation of the photons implies that the wave vectors obey $\hat{\mathbf{k_s}} + \hat{\mathbf{k_i}} = \hat{\mathbf{k_p}}$, where $\hat{\mathbf{k_s}}$, $\hat{\mathbf{k_i}}$, and $\hat{\mathbf{k_p}}$ are signal, idler and pump wave vectors respectively.

Energy conservation implies $\frac{1}{\lambda_p} = \frac{1}{\lambda_s} + \frac{1}{\lambda_i}$, where λ_p, λ_s, and λ_i, are pump, signal and idler wavelengths. Any pair of photons lying in diametrically opposite ends of the SPDC cone are entangled with each other (Figure 3.5).

SPDC has been widely used as a primary source of heralded single photon pairs in quantum cryptography, quantum metrology, quantum imaging, experimental Bell tests, quantum communication, to name a few. Depending upon the polarisation of the pump and the signal/idler photons obtained, the SPDC process can be classified into three different types:

1. Type 0: Signal, idler and the pump photons have the same polarisation.
2. Type I: The polarisation of signal and idler is orthogonal to that of the pump photon.
3. Type II: The polarisation of the signal and idler are orthogonal to each other.

In our experiment, we pump a pair of Type-I BiBO (Bismuth Triborate crystal) with a 355 nm 100 mW pump beam to generate entangled photon pairs. The polarisation of the pump photon can be adjusted by a HWP, placed before the non-linear crystal. Say we send pump photons in a state $|\psi\rangle = \alpha |H\rangle_p + \beta |V\rangle_p$, where α, and β are complex amplitudes. Then the process can be seen as,

$$|\psi\rangle \xrightarrow{\text{1st Crystal}} \alpha |H\rangle_p + \beta |H\rangle_s |H\rangle_i \tag{3.45}$$

$$\xrightarrow{\text{2nd Crystal}} \alpha |V\rangle_s |V\rangle_i + \beta e^{i\phi} |H\rangle_s |H\rangle_i . \tag{3.46}$$

For the purpose of generating maximally entangled photons we can send in a diagonally polarized pump beam, i.e. $\alpha = \frac{1}{\sqrt{2}}$, and $\beta = \frac{1}{\sqrt{2}}$. Due to the indistinguishably of source of the the two photons they are entangled in polarisation degree of freedom,

$$|\psi\rangle = \frac{1}{\sqrt{2}}\big(|H\rangle_s |H\rangle_i + e^{i\phi} |V\rangle_s |V\rangle_i \big). \tag{3.47}$$

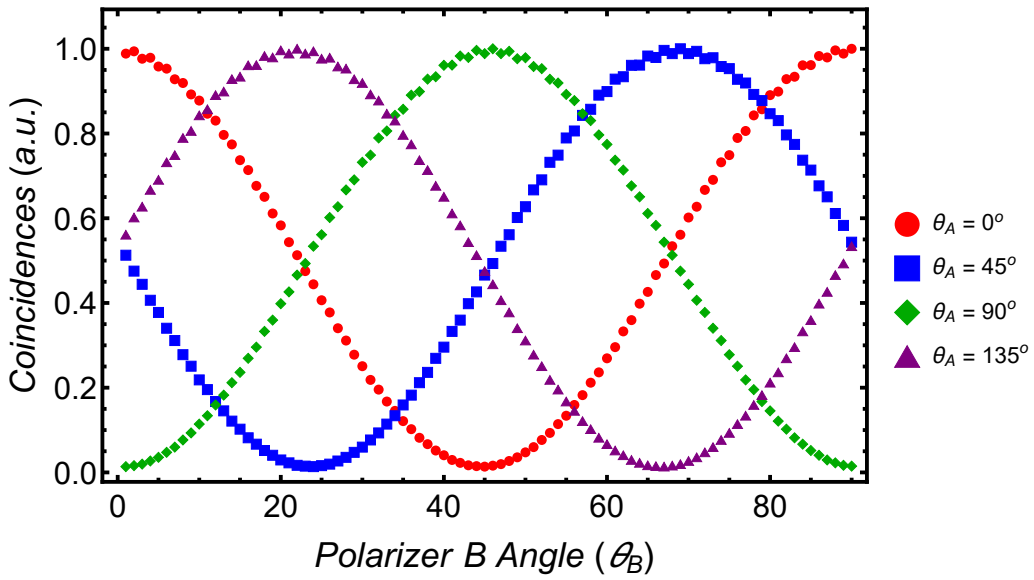

Figure 3.6: Normalized coincidence photon counts measured experimentally by fixing the Polarizer A (θ_A) at four different angles.

3.4.3 Experimental calculation of the expectation Values

Experimentally, typically the two parties, Alice and Bob, share a pair of photons in a maximally entangled state. Single photon counters and a coincidence module would then measure the number of photons detected for a particular combination of polarizer angles. The expectation value of the operator $\hat{\sigma}_a\hat{\sigma}_b$ is then calculated as,

$$\langle\hat{\sigma}_a\hat{\sigma}_b\rangle = \frac{N_{++} - N_{+-} - N_{-+} + N_{--}}{N_{++} + N_{+-} + N_{-+} + N_{--}}, \tag{3.48}$$

where N_{+-} refers to the number of counts detected along positive a and negative b and so on.

3.5 Tighter Bounds for CHSH and $\mathcal{B}_2$ parameters:

On the one side of the picture, quantum correlations cannot be explained by any classical theory [30], as we discussed in Chapter 2. On the other side the physical origin and the extent of quantum correlations have remained elusive [15,31,32]. Attempts have been made to explain why nature does not seem to allow stronger than quantum correlations [33–36] and provide physical principles which could naturally give rise to the quantum correlations. Recently, it was proposed that the principle of relativistic independence [37], the idea that local uncertainties are unaffected by the measurement choices of any spatially separated observers, can give rise to new bounds for nonlocal correlations. It was also shown that theories that allow stronger than quantum correlations violate either of the assumptions behind the theory, i.e, either they violate the underlying uncertainty relations or they

allow nonlocally effecting the uncertainty relations for spatially separated observers. In our work [38], we were able to obtain richer bounds for the CHSH parameter and the multiplicative Bell parameter $\mathcal{B}_2$ in terms of the local correlations on Alice and Bob's side. Let us first define the local Pearson correlations as,

$$\eta_A = \frac{\langle A_i A_j \rangle - \langle A_i \rangle \langle A_j \rangle}{\Delta_{A_i} \Delta_{A_j}}, \;\; \eta_B = \frac{\langle B_i B_j \rangle - \langle B_i \rangle \langle B_j \rangle}{\Delta_{B_i} \Delta_{B_j}}, \tag{3.49}$$

where $A_{i,j} = \mathbf{a}_{i,j} \cdot \hat{\sigma}$, and $B_{i,j} = \mathbf{b}_{i,j} \cdot \hat{\sigma}$, are two local observables for Alice, and Bob respectively, and $\Delta^2_{A_k} = \langle A_k^2 \rangle - \langle A_k \rangle^2$, and so on. Then new richer bounds for CHSH and $\mathcal{B}_2$, can be written as,

$$\text{CHSH} \leq \sqrt{2} \left(\sqrt{1 + \eta_{A,B}} + \sqrt{1 - \eta_{A,B}} \right) \tag{3.50}$$

$$\mathcal{B}_2 \leq 1 + \sqrt{1 - \eta^2_{A,B}} \tag{3.51}$$

For the special case of maximally entangled states, such as considered in the experiment, tighter bound for $\mathcal{B}_2$, was also obtained,

$$\mathcal{B}_2^{maximal} \leq 2\sqrt{1 - \eta^2_{A,B}} \tag{3.52}$$

The choice of η_A or η_B for the bounds depends upon whether we fix the local correlations on Alice's or Bob's side. If we fix η_A to a certain value, it means that on Alice's side the vectors, $\mathbf{a}_1$, and $\mathbf{a}_2$ are fixed. For a maximally entangled Bell state, $\langle A_{i,j} \rangle = 0$, and $\Delta_{A_{i,j}} = 1$. We also have $A_i A_j = (\mathbf{a_i} \cdot \mathbf{a_j}) \mathbb{I} + i.(\mathbf{a_i} \times \mathbf{a_j}) \cdot \hat{\sigma}$. Since the reduced density operator on Alice's side is a maximally mixed state in any basis, the expectation value of the second term is zero. Hence,

$$\eta_A = \mathbf{a}_i \cdot \mathbf{a}_j. \tag{3.53}$$

This also means that on Alice's side, the relative angle between the two vectors, $\mathbf{a}_1$, and $\mathbf{a}_2$ are fixed.

Then the Bell/CHSH parameters are obtained for any two randomly selected vectors $\mathbf{b}_1$, and $\mathbf{b}_2$, on Bob's side. These limits are plotted as a function of η in Figure 3.7, and also tabulated for some values in Table 3.1.

Table 3.1: **Quantum limits for CHSH and $\mathcal{B}_2$ parameters for different η.**

S.N	η	$\mathcal{B}_2$	$\mathcal{B}_2^{maximal}$	CHSH
1	0	2	2	$2\sqrt{2}$
2	0.3	1.953	1.908	2.796
3	0.5	1.866	1.732	2.732
4	0.7	1.714	1.428	2.618
5	0.8	1.6	1.2	2.530
6	0.9	1.436	0.872	2.397

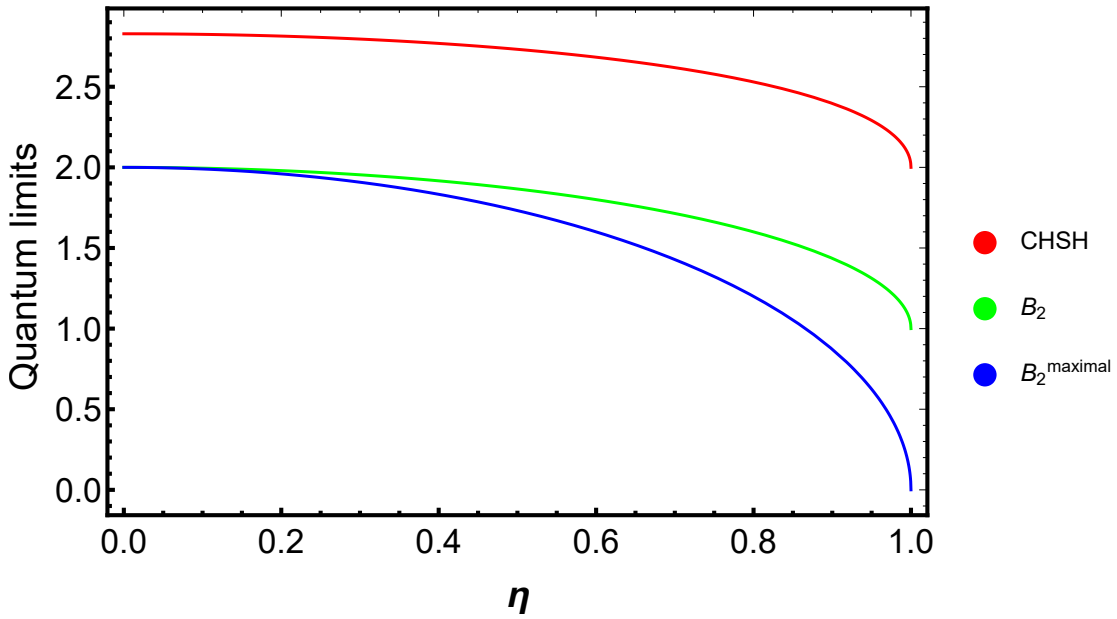

Figure 3.7: Theoretical limits for CHSH and $\mathcal{B}_2$ parameters plotted as a function of the local Pearson coefficient, η.

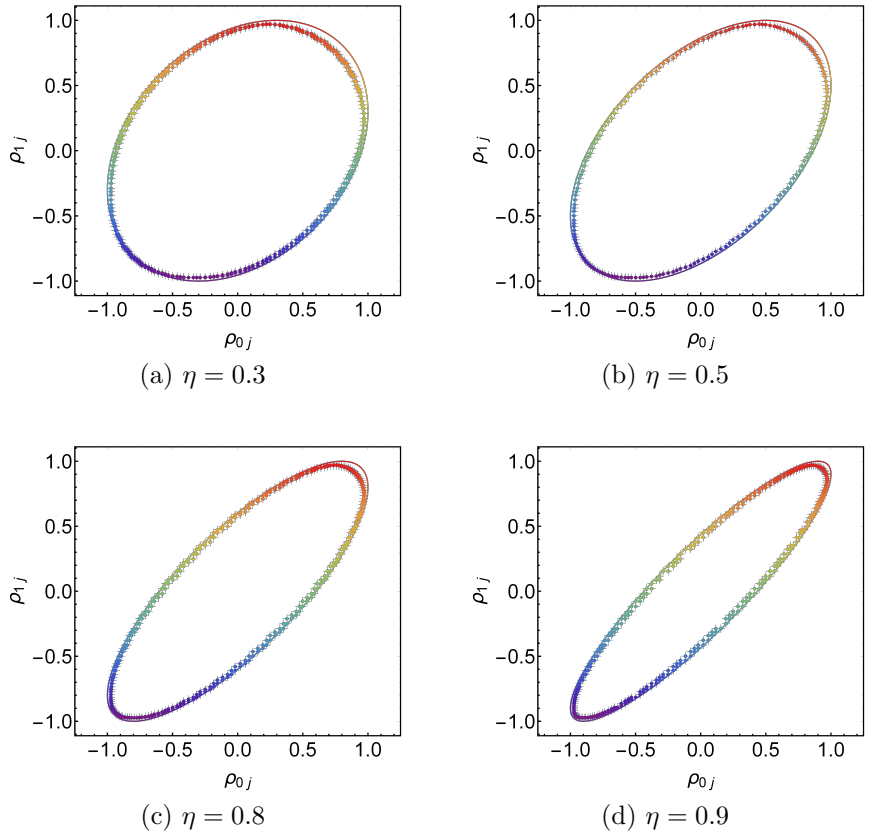

(a) $\eta = 0.3$ (b) $\eta = 0.5$

(c) $\eta = 0.8$ (d) $\eta = 0.9$

Figure 3.8: Distribution of the correlation vectors for four different values of η. The solid line indicates the region within which the correlation vectors should fall, and the points are experimentally measured vectors.

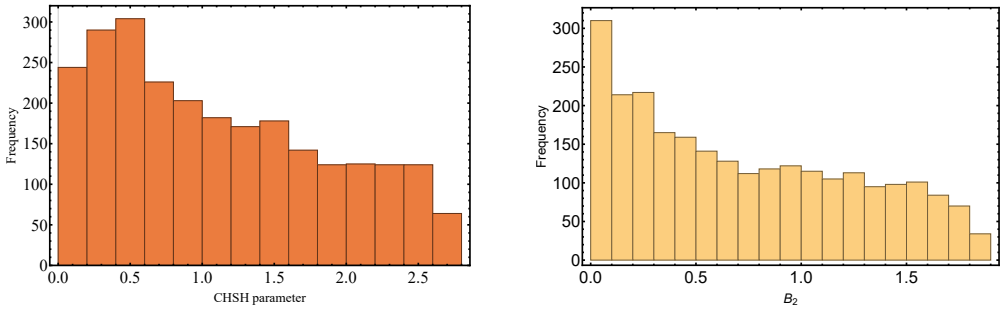

(a) $\eta = 0.3$

(b) $\eta = 0.3$

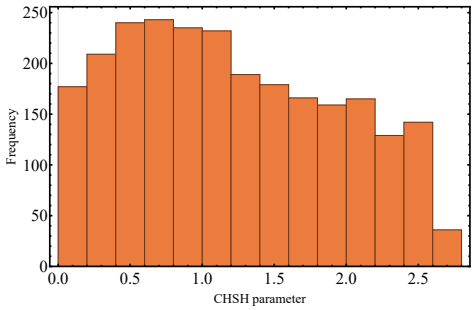

(c) $\eta = 0.5$

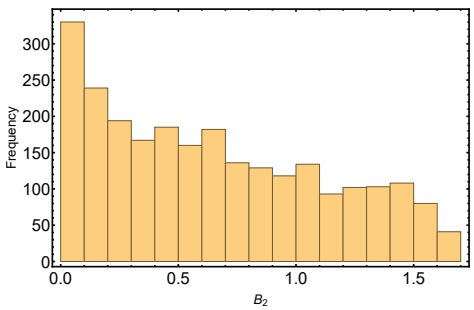

(d) $\eta = 0.5$

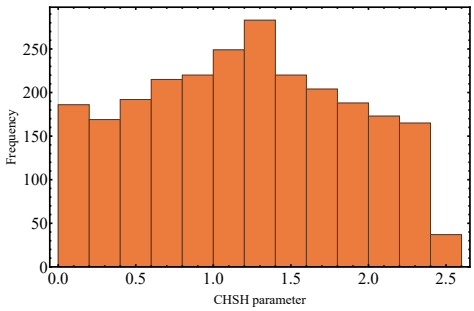

(e) $\eta = 0.8$

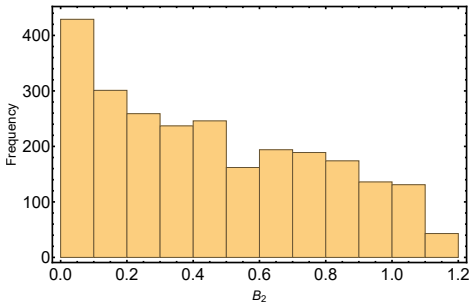

(f) $\eta = 0.8$

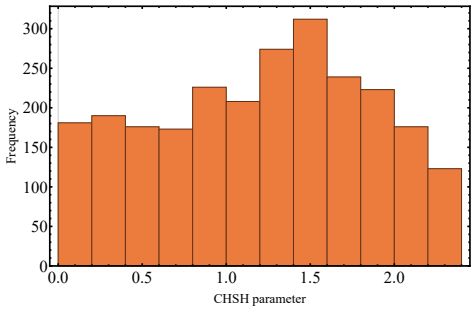

(g) $\eta = 0.9$

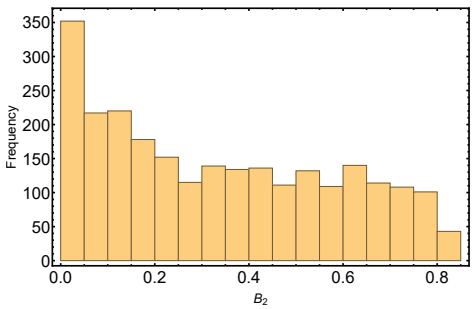

(h) $\eta = 0.9$

Figure 3.9: Distribution of the CHSH parameter (on left), and $\mathcal{B}_2$ (on right), for different values of η.

From our experimental data, we were also able to experimentally calculate the distri-

bution of the Bell parameters for different η_A. For a particular η_A, we randomly choose the two vectors $\mathbf{v}_1$, and $\mathbf{u}_2$ corresponding to it. Then we calculate the Bell parameters for different set of vectors on Bob's side. The distribution is also plotted in Figure 3.9, where we observe that all the values lie within the bound predicted by Equations (3.50) and (3.52). The local correlations also affect the distribution of the non-local correlation vectors, ρ_{ij}.

$$\rho_{ij} = \frac{\langle A_i B_j \rangle - \langle A_i \rangle \langle B_j \rangle}{\Delta_{A_i} \Delta_{B_j}}. \tag{3.54}$$

For instance, the correlation vectors (ρ_{0j}, ρ_{1j}), lie on an ellipse whose major and minor axes are determined by η_A, and similarly (ρ_{i0}, ρ_{i1}) η_B [37, 38]. This behaviour is observed in Figure 3.8 for different values of η.

Experimental Tests of Multiplicative Bell Inequalities

Dilip Paneru,[1] Amit Te'eni,[2] Bar Y. Peled,[3] James Hubble,[1] Yingwen Zhang,[4] Avishy Carmi,[3] Eliahu Cohen,[2,*] and Ebrahim Karimi[1,4]

[1]*Department of Physics, University of Ottawa, 25 Templeton Street, Ottawa, Ontario, K1N 6N5 Canada*
[2]*Faculty of Engineering and the Institute of Nanotechnology and Advanced Materials, Bar Ilan University, Ramat Gan 5290002, Israel*
[3]*Center for Quantum Information Science and Technology & Faculty of Engineering Sciences, Ben-Gurion University of the Negev, Beersheba 8410501, Israel*
[4]*National Research Council of Canada, 100 Sussex Drive, Ottawa, ON K1A0R6, Canada*

Bell inequalities are mathematical constructs that demarcate the boundary between quantum and classical physics. A new class of multiplicative Bell inequalities originating from a volume maximization game (based on products of correlators within bipartite systems) has been recently proposed. For these new Bell parameters, it is relatively easy to find the classical and quantum, i.e. Tsirelson, limits. Here, we experimentally test the Tsirelson bounds of these inequalities using polarisation-entangled photons for different number of measurements (n), each party can perform. For $n = 2, 3, 4$, we report the experimental violation of local hidden variable theories. In addition, we experimentally compare the results with the parameters obtained from a fully deterministic strategy, and observe the conjectured nature of the ratio. Finally, utilizing the principle of "relativistic independence" encapsulating the locality of uncertainty relations, we theoretically derive and experimentally test new richer bounds for both the multiplicative and the additive Bell parameters for $n = 2$. Our findings strengthen the correspondence between local and nonlocal correlations, and may pave the way for empirical tests of quantum mechanical bounds with inefficient detection systems.

Introduction.— Ever since quantum mechanics was introduced to describe the subatomic world, the foundational aspects, most notably the non-deterministic nature of experimental outcomes, have always been a topic of discussion among physicists and philosophers [1]. In their seminal work [2], Einstein, Podolsky and Rosen (EPR) argued for the incompatibility of quantum theory with the idea of local realism. Since then, attempts were made to incorporate extra parameters within the theory, the so called hidden variables, to "complete" the quantum formalism [3]. However, In 1964 John Bell showed that there exist experiments for which any local hidden variable theory must disagree with quantum mechanics about the predicted outcome [4]. This discrepancy is most conveniently illustrated by Bell parameters, i.e., measurable quantities whose values must be bounded to a certain extent in any local hidden variable theory, but can exceed these bounds according to quantum mechanics [5]. Experiments carried out to test these inequalities [6–9] have always vindicated quantum mechanics, thereby showing that local realistic theories do not present an adequate representation of the physical world. Recent new experiments have also significantly progressed towards closing loopholes in a typical Bell experiment, such as freedom-of-choice, fair-sampling, communication (or locality), coincidence and memory loopholes [10–16]. Several works have attempted to find the extent of Bell parameters involving quantum correlations [17–19]. However, finding the classical and quantum (Tsirelson) bounds of these expressions in general remains a challenging task. [18, 19]. Recently, Bell parameters with products of correlators between random variables shared between two parties, namely Alice and Bob, were introduced [20]. Corresponding to the number of random variables, n, measurable by each of the parties, the multiplicative Bell parameter would be proportional to a certain volume in the n-dimensional space (this was shown to result from a specific coordination game Alice plays with Bob). For the simplest case where Alice and Bob measure two random variables each, it was also proven that the bound for classical correlations is strictly less than that for quantum correlations. Moreover, these multiplicative Bell inequalities were shown to be more robust to detector inefficiency than the linear ones [20]. In general, the Tsirelson bound for the multiplicative Bell parameters $\mathcal{B}_n$, corresponding to measurement n, was shown to be $|\mathcal{B}_n| \leq n!$. The Tsirelson bounds were derived from the structure of the quantum covariance matrix [2], under the assumption of "relativistic independence" [1], mathematically expressing the requirement for locality of uncertainty relations. It was hoped that the nonlinear nature of these inequalities could shed light on the non-polytopic structure of the set of quantum correlations.

Here, we present the results of experiments testing the Tsirelson bounds for these multiplicative inequalities for different n values, and observe their non-intuitive behaviour for large n values. Moreover, we propose and put to test new Tsirelson bounds that are richer than those derived in [20].

Theory.— Let us consider, a photon pair entangled in the polarisation degree of freedom,

$$|\psi\rangle = \frac{1}{\sqrt{2}} \left(|H\rangle_A |V\rangle_B - |V\rangle_V |H\rangle_B \right), \tag{1}$$

where $|H\rangle$ and $|V\rangle$ stand for horizontal and vertical linear polarisation states, and the subscripts A and B represent photon states for Alice and Bob, two spatially separated observers. In the multiplicative Bell scenario, the observers have a different Bell parameter depending upon the number n of different measurements that each can perform. For a general n the Bell

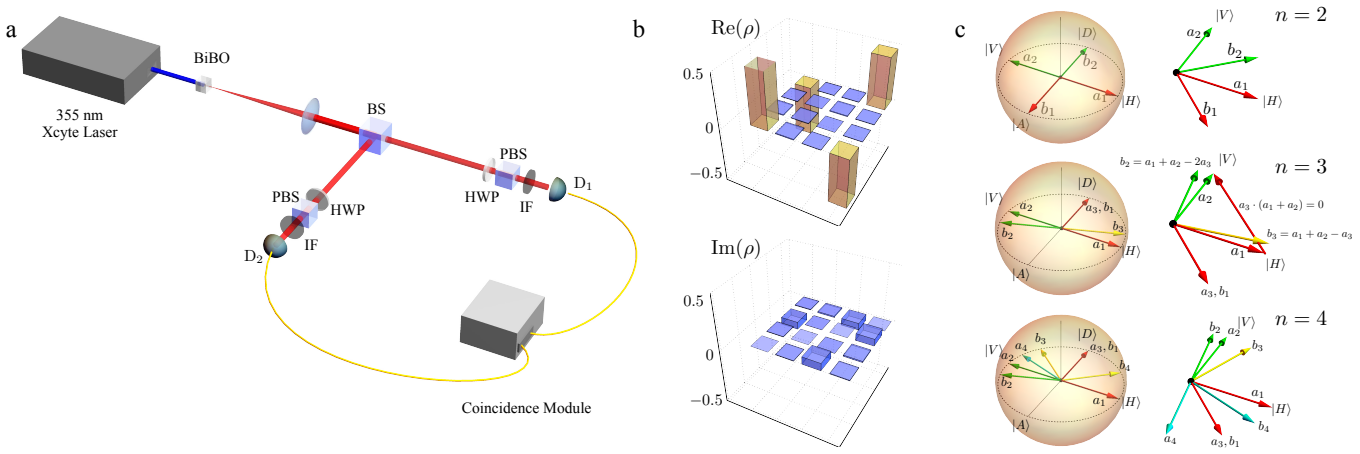

FIG. 1. Experimental scheme and the chosen strategy to perform measurement of multiplicative Bell parameters. (a) Sketch of the setup used for generating polarisation entangled photons and projecting them onto the states chosen by Alice and Bob's strategies. Entangled photon pairs are generated after pumping paired BiBO (Bismuth Triborate) crystals, and then separated by a 50:50 beamsplitter (BS) into two arms (Alice and Bob). The polarisation measurement stage on each side consists of a half-wave plate (HWP) and polarising beamsplitter (PBS). The photons are filtered by a 710 nm interference bandpass filter (IF), and coupled into single mode fibres, and then detected using single photon avalanche diodes whose signals are sent to a coincidence module from which coincidence events can be observed. (b) Real and imaginary parts of the experimentally reconstructed density matrix of the generated entangled state are shown in $|H\rangle_A|H\rangle_B$, $|H\rangle_A|V\rangle_B$, $|V\rangle_A|H\rangle_B$, and $|V\rangle_A|V\rangle_B$ basis. The generated state fidelity is $\simeq 0.977$. (c) The projective measurement strategy, i.e. $\{a_1, a_2, \ldots\}$ and $\{b_1, b_2, \ldots\}$, chosen by Alice and Bob are shown for $n = 2$, $n = 3$ and $n = 4$ on the polarisation Poincaré sphere.

parameter is defined as,

$$\mathcal{B}_n = \prod_{j=1}^{n} v_j \cdot c_j$$
$$= (c_{1n} + \cdots + c_{nn}) \prod_{j=1}^{n-1} \left(c_{1j} + \ldots + c_{jj} - j c_{j+1,j}\right), \quad (2)$$

where $c_{ij} = c_{a_i b_j}$ is the expectation value of the polarisation measurements along a_i and b_j. c_j is the vector comprised of all c_{ij} for a fixed value of j, and v_j is the jth column of the matrix:

$$V = \begin{bmatrix} 1 & 1 & \ldots & 1 & 1 \\ -1 & 1 & \ldots & 1 & 1 \\ & -2 & \ddots & \vdots & 1 \\ & & \ddots & 1 & \vdots \\ & & & -(n-1) & 1 \end{bmatrix}.$$

A strategy to select the vectors $a_1 \ldots a_n$, and $b_1 \ldots b_n$, so as to saturate the Tsirelson bounds ($|\mathcal{B}_n| \leq n!$) is outlined in [20]. The multiplicative Bell parameters, $\mathcal{B}_n \triangleq \prod_{j=1}^{n} v_j \cdot c_j$, can be associated with the additive Bell parameters, $B'_n \triangleq \sum_{j=1}^{n} v_j \cdot c_j$, using the following relation:

$$|\mathcal{B}_n| \leq \left(\frac{\mathcal{B}'_n}{n}\right)^n, \quad (3)$$

which is a result of the inequality of geometric and arithmetic means, i.e., $\sqrt[n]{\mathcal{B}_n} = \sqrt[n]{\prod_{j=1}^{n} v_j \cdot c_j} \leq \frac{\sum_{j=1}^{n} v_j \cdot c_j}{n}$. The latter expression can be used to find classical upper bounds (not necessarily tight) over $\mathcal{B}_n$, given the classical bounds over $\mathcal{B}'_n$. Using the known fact that additive Bell inequalities are saturated by deterministic strategies [23], one may go over all such strategies and find the tight classical bounds for $\mathcal{B}'_n$. The results are as follows:

$$\mathcal{B}'_2 \leq 2 \Rightarrow \mathcal{B}_2 \leq 1;$$
$$\mathcal{B}'_3 \leq 5 \Rightarrow \mathcal{B}_3 \leq \left(\frac{5}{3}\right)^3 \approx 4.6;$$
$$\mathcal{B}'_4 \leq 8 \Rightarrow \mathcal{B}_4 \leq 16. \quad (4)$$

$\mathcal{B}'_2$ is the well-known Bell-CHSH parameter [24]. For $n = 2$ and 4, this method yields $\mathcal{B}_2 = 1$ and $\mathcal{B}_4 = 16$, which set the tight classical bounds for these particular values of n. This scheme does not yield a useful classical bound for $n > 4$.

Since finding the classical limit for the Bell parameter, Eq. (2), is suspected to be difficult in general, an independent and deterministic strategy was proposed for both Alice and Bob [20], and the corresponding limit was calculated. In this strategy, Bob always chooses his random variable to be +1, while Alice's choice alternates between +1 and −1 for all of her variables A_i, until $i < i_c$, where i_c is some cutoff number; and for $i > i_c$, she chooses A_i to be +1. The correlations take the following values,

$$c_{ij} = \begin{cases} (-1)^i & i \leq i_c \\ 1 & i > i_c \end{cases}. \quad (5)$$

The value for the cutoff i_c is taken such that it maximizes the value for the Bell parameter. Analytically, the value $\mathcal{B}_n$ obtains for this fully deterministic strategy, FD_n, can be explic-

itly calculated, and its value is,

$$\mathrm{FD}_n = 2^{i_c}\left[\left(\frac{i_c}{2}\right)!\right]^2 (n-i_c)\, i_c^{(n-i_c-1)}. \quad (6)$$

The maximal values obtained from the fully deterministic strategy for $n = 2$ and 4, coincide with the classical bounds obtained in Eq. (4). The ratio of fully deterministic strategy and Tsirelson bound, i.e. $\mathrm{FD}_n/n!$, approaches $\sqrt{\pi/2e}$ as $n \to \infty$.

Experiment.— Paired 0.5-mm-thick type-I bismuth triborate crystals (BiBO), one rotated by 90-degrees with respect to the other, are pumped by a quasi-continuous wave 100 mW, 355 nm beam to generate photon pairs (signal and idler) via spontaneous parametric downconversion (SPDC) at a degenerate wavelength of 710 nm [25] – see Figure 1(a). A half-wave plate, placed before the paired crystals, is used to tailor the photon pair state by controlling the pump beam polarisation state. Due to indistinguishably, the generated photon pairs are entangled in the polarisation degree of freedom. The polarisation of the pump beam and the orientation of the crystal was tuned so as to obtain the state, $|\psi\rangle_{\mathrm{SPDC}} = \frac{1}{\sqrt{2}}(|H\rangle_A|H\rangle_B - |V\rangle_A|V\rangle_B)$. A half-wave plate was placed in one of the arms, say Bob, so that the horizontal and vertical polarisation states are exchanged and state in Eq. (1) was obtained. The 355 nm pump beam is afterwards filtered out with a long pass filter. The photon pairs are separated by a 50:50 beamsplitter (BS), and the photons travel along two different arms. To select two diametrically opposite regions of the SPDC cone, we place a pair of irises on each arm such that they center on the required region. In each arm projective measurement of the polarisation state is performed by a combination of a quarter-wave plate, a half-wave plate, and a polarizing beam splitter (PBS). Bandpass filters of (710 ± 5) nm are placed before 20× objectives so that only degenerate photon pairs are coupled into single mode fibers of core diameter 5 μm. Then, the photons are detected via a pair of single photon avalanche diode (SPAD) detectors (Excelitas SPCM-AQRH-14-FC), and are finally counted via a time-correlated single photon counting system. To achieve a maximally entangled state of Eq. (1), the angle of the waveplate before the crystal and the orientation of the crystal was appropriately adjusted. The coincidence rates depending upon the difference in the two half-wave plate orientations, ranged from 5220 s^{-1} to 34 s^{-1}. The visibility in H/V basis and ±45° linear polarisation states were (98.2 ± 0.5)%, and (97.3 ± 0.5)%, respectively. Real and imaginary parts of the generated photons' density matrix are shown in Figure 1(b). The fidelity of the generated state from the reconstructed density matrix was measured to be $\simeq 0.977$, confirming the high quality of the entangled source. Figure 1(c) illustrates the set of vectors used in projecting Alice and Bob's quantum states, i.e. $\{a_1, a_2, a_3, \ldots\}$ and $\{b_1, b_2, b_3, \ldots\}$, on the polarisation Poincaré sphere. The number of photon counts N detected in coincidence along a and b by Alice and Bob's detectors was recorded, from which one can obtain the expectation value of the measurement via $c_{ab} = (N_{++} - N_{+-} - N_{-+} + N_{--})/(N_{++} + N_{+-} + N_{-+} + N_{--})$,

TABLE I. **Classical ($\mathcal{B}_n^{\mathrm{Classical}}$), Fully deterministic FD_n, and Tsirelson ($\mathcal{B}_n^{\mathrm{Quantum}}$) bounds for the multiplicative Bell parameters, and the experimentally ($\mathcal{B}_n^{\mathrm{Experiment}}$) measured values.**

n	$\mathcal{B}_n^{\mathrm{Classical}}$	FD_n	$\mathcal{B}_n^{\mathrm{Experiment}}$	$\mathcal{B}_n^{\mathrm{Quantum}}$ $(n!)$
2	1	1	1.88 ± 0.05	2
3	4 – 4.6	4	5.85 ± 0.31	6
4	16	16	23.3 ± 1.4	24
5	N.A.	64	115 ± 9	120
6	N.A.	512	687 ± 59	720
7	N.A.	3072	4655 ± 374	5040

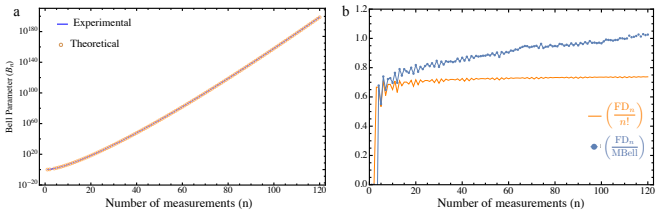

FIG. 2. Experimentally calculated multiplicative Bell parameters (MBell). (a) Logarithmic plot of the experimentally calculated Bell parameters (blue), and theoretical quantum limit of the Bell parameter, i.e. n!, (red). (b) Ratio of the parameters generated from the fully deterministic strategy FD_n taken with the Tsirelson bound, $n!$ (red), and with the experimentally observed Bell parameter MBell (blue).

such that N_{+-}, for instance, refers to the joint measurement where Alice and Bob set their apparatus to measure the state along the positive and negative direction of a and b, respectively. Using this approach, as a verification, the CHSH parameter for our single photon source is measured and found to be $2.748 \pm 0.026 \leq 2\sqrt{2}$, which lies beyond the classical limit of 2. The Bell parameter for $n = 2$ is $\mathcal{B}_2 = |(c_{12} + c_{22})(c_{12} - c_{21})|$. The classical and quantum limits of $\mathcal{B}_2$ are, respectively, $\mathcal{B}_2^{\mathrm{Classical}} \leq 1$ and $\mathcal{B}_2^{\mathrm{Quantum}} \leq 2!$. The value for $\mathcal{B}_2$ as calculated from our experiment was $\mathcal{B}_2 = 1.88 \pm 0.05$, which is beyond the classical limit 1. For $n = 3$ the Bell parameter is given by, $\mathcal{B}_3 = |(c_{13} + c_{23} + c_{33})(c_{11} - c_{21})(c_{12} + c_{22} - 2c_{32})|$. The classical limit for $\mathcal{B}_3$ lies somewhere between 4 and 4.6. Experimentally the observed value for $\mathcal{B}_3$ is 5.85 ± 0.31. Experimentally measured values for the Bell parameters up to $n = 7$ with the Tsirelson bounds and the classical limits (where applicable) are shown in Table I.

The experimentally measured Bell parameters for higher values of n are plotted in Figure 2(a). The primary contribution to the uncertainties in the Bell parameter is associated with the rotation of the half-wave plates in the detection state. Since the coincidence counts were taken by rotating motor controlled waveplates at intervals of 1°, the corresponding maximum and the average uncertainties in the expectation values are 0.0698 and 0.044, respectively. The uncertainty associated with photon counting from Poissonian statistics contributes to maximum uncertainty of 0.003. Thus the uncertainties, are dominated by the rotation of the waveplates, which is ex-

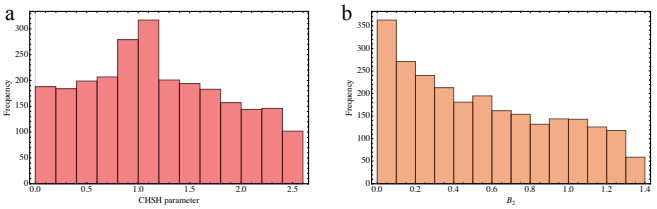

FIG. 3. Distribution of both (a) CHSH parameters (upper limit = 2.618) as well as (b) Bell parameters $\mathcal{B}_2$ (upper limit =1.428), for $\eta_A = 0.7$.

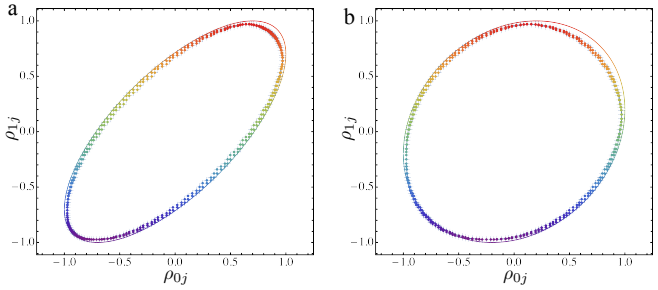

FIG. 4. Distribution of the correlation vectors for (a) $\eta_A = 0.7$ and (b) $\eta_A = 0.2$. The solid line indicates the region within which the correlation vectors should fall, and the points are experimentally measured vectors.

tremely small, and not visible in Figure 2(a). The obtained results are close to the corresponding Tsirelson bounds. In order to quantify the results, we plot the ratio between the maximal quantum bound and the observed parameters, see Figure 2(b). Most of the obtained results are within eighty percent of the maximal value. As a comparison with the fully deterministic strategy (6), the theoretical ($\mathrm{FD}_n/n!$) and the obtained experimental (FD_n/MBell) ratios are shown in Figure 2(b) for values of n up to 255. As the experimentally observed Bell parameters are less than the actual ones the experimentally calculated values for the ratio are slightly larger than the theoretical ones.

Locality of uncertainty and richer quantum bounds.— Recently it was proposed [1] that the locality of uncertainty, i.e. the requirement that local uncertainties are independent of the measurement choices of any other parties, can give rise to both known and hitherto unnoticed bounds on nonlocal correlations in any statistically meaningful theory. For two parties sharing a Bell state, richer bounds for the CHSH parameter and the multiplicative Bell parameter can be obtained in terms of the local correlations. Let us define the local correlation, say on Alice's side,

$$\eta_A = \frac{\langle A_i A_j\rangle - \langle A_i\rangle\langle A_j\rangle}{\Delta_{A_i}\Delta_{A_j}}, \tag{7}$$

where A_i, and A_j are two local observables for Alice, and $\Delta^2_{A_k} = \langle A_k^2\rangle - \langle A_k\rangle^2$. In the Supplementary Material we show that these local correlations on Alice's side give rise to new bounds for the standard CHSH and the multiplicative Bell parameters, which respectively are $\mathrm{CHSH} \leq \sqrt{2}\left(\sqrt{1+\eta_A} + \sqrt{1-\eta_A}\right)$ and $\mathcal{B}_2 \leq 1 + \sqrt{1-\eta_A^2}$. For the special case of maximally entangled states, as the one considered here, the multiplicative Bell parameter is more tightly bounded as follows, $\mathcal{B}_2 \leq 2\sqrt{1-\eta_A^2}$ (for derivation please see the Supplemental Material). For both bounds, the local correlation given by η_A determines the extent of the nonlocal correlations on the right hand side, i.e. upper bound. These inequalities are derived based on Alice's local correlations, but can be similarly derived for Bob's, and hence an even tighter bound is given by their minimum. To experimentally infer these richer bounds on correlations, we selected two vectors a_1, and a_2 on Alice's side that correspond to a particular value of η_A. Then we randomly selected two vectors on Bob's side, and calculated the CHSH and Bell parameters. In Figures 3(a) and (b), we show the results for both parameters when $\eta_A = 0.7$. The observed values all fall within the bound as predicted by $\mathrm{CHSH} \leq \sqrt{2}\left(\sqrt{1+\eta_A} + \sqrt{1-\eta_A}\right)$ and $\mathcal{B}_2 \leq 1 + \sqrt{1-\eta_A^2}$. The local correlations, for example, η_A, also put restrictions on the two particle correlations, which can be defined as,

$$\rho_{ij} = \frac{\langle A_i B_j\rangle - \langle A_i\rangle\langle B_j\rangle}{\Delta_{A_i}\Delta_{B_j}}, \tag{8}$$

. Geometrically, for a particular η_A the correlation vectors $\left(\rho_{0j}, \rho_{1j}\right)$, $j = 0, 1$, lie on the ellipse whose major and minor axes are related to η_A as,

$$e_j = \sqrt{\left(\frac{1 \pm (-1)^j |\eta_A|}{\sqrt{2}}\right)}\begin{bmatrix} 1 \\ (-1)^j \end{bmatrix}. \tag{9}$$

Similar relation holds for the vectors (ρ_{i0}, ρ_{i1}), $i = 0, 1$, defined by the local correlation η_B, on Bob's side. Figure 4 shows the ellipses corresponding to particular values of $\eta_A = 0.7$, and $\eta_A = 0.2$, along with the experimentally measured correlation vectors.

Conclusion.— We derived new classical and quantum bounds for the multiplicative Bell inequalities and experimentally tested them. Our theoretical results mainly stem from the principle of relativistic independence [1] and hence emphasize the significance of correlations.The experimental results show that the multiplicative Bell parameters go beyond their classical limits, thus again falsifying local realism. Additionally, they approach the Tsirelson bound, the upper limit derived from the quantum covariance matrix, and the "relativistic independence" assumption. We were also able to experimentally observe the tighter theoretical bounds on the CHSH and the Bell parameter, $\mathcal{B}_2$, lending support to the claim that quantum correlations arise from the locality of uncertainty relations [1]. An additional practical merit of multiplicative Bell inequalities, is that they elevate the detector efficiency requirement [20] for the test of hidden variable theories. It is challenging for Bell experiments to reach high detection efficiencies, but in principle, multiplicative Bell inequalities, like

those we examined here, provide a simple circumvention of the detector efficiency loophole prevalent in Bell experiments. The authors would like to thank Alessio D'Erico for fruitful discussions. This work was supported by Canada Research Chairs (CRC), Canada Foundation for Innovation (CFI), and Canada First Excellence Research Fund (CFREF). E.C. acknowledges support from the Israel Innovation Authority under project 70002 and from the Quantum Science and Technology Program of the Israeli Council of Higher Education.

* eliahu.cohen@biu.ac.il

[1] D. Paneru *et al.*, Entanglement: quantum or classical?, *Reports on Progress in Physics* **83**, 064001 (2020).
[2] A. Einstein, B. Podolsky, and N. Rosen, Can quantum-mechanical description of physical reality be considered complete?, *Physical Review* **47**, 777 (1935).
[3] M. Genovese, Research on hidden variable theories: A review of recent progresses, *Physics Reports* **413**, 319-396, (2005).
[4] J. S. Bell, On Einstein-Podolsky-Rosen Paradox, *Physics* **1**, 195 (1964).
[5] N. Brunner, D. Cavalcanti, S. Pironio, V. Scarani, and S. Wehner, Bell non-locality, *Reviews of Modern Physics* **86**, 419 (2014).
[6] S.J. Freedman, and J. F. Clauser, Experimental test of local hidden-variable theories, *Physical Review Letters* **28**, (1972).
[7] A. Aspect, P. Grangier, and G. Roger, Experimental tests of realistic local theories via Bell's theorem, *Physical Review Letters* **47**, 460, (1981).
[8] A. Aspect, P. Grangier, and G. Roger, Experimental realization of Einstein-Podolsky-Rosen-Bohm Gedankenexperiment: a new violation of Bell's inequalities, *Physical Review Letters* **49**, 91, (1982).
[9] A. Aspect, J. Dalibard, and G. Roger, Experimental test of Bell's inequalities using time-varying analyzers, *Physical Review Letters* **49**, 1804, (1982).
[10] T. Scheidl *et al.*, Violation of local realism with freedom of choice, *Proceedings of the National Academy of Sciences of the USA* **107**, 19708-19713 (2010).
[11] B. Hensen *et al.*, Loophole-free Bell inequality violation using electron spins separated by 1.3 kilometres, *Nature* **526**, 682 (2015).
[12] M. Giustina *et al.*, Bell violation using entangled photons without the fair-sampling assumption, *Nature* **497**, 227 (2013).
[13] D. Rauch *et al.*, Cosmic Bell test using random measurement settings from high-redshift quasars, *Physical Review Letters* **121**, 080403 (2018).
[14] M. Ansmann *et al.*, Violation of Bell's inequality in Josephson phase qubits, *Nature* **461**, 504 (2009).
[15] M. A. Rowe *et al.*, Experimental violation of a Bell's inequality with efficient detection, *Nature* **409**, 791 (2001).
[16] C. Abellán *et al.*, Challenging local realism with human choices, *Nature* **557**, 212-216 (2018).
[17] B.S. Cirelson, Quantum generalizations of Bell's inequality, *Letters in Mathematical Physics* **4**, 93-100 (1980).
[18] F. Karoly Pl, and T. Vrtesi, Quantum bounds on Bell inequalities. *Physical Review A* **79** 022120 (2009).
[19] D. Frustaglia, J. P. Baltans, C. M. Velzquez-Ahumada, A. Fernndez-Prieto,A. Lujambio, V. Losada, and A. Cabello, Classical physics and the bounds of quantum correlations, *Physical Review Letters* **116**, 250404, (2016).
[20] A. Te'eni, B. Y. Peled, E. Cohen, and A. Carmi, Multiplicative Bell inequalities, *Physical Review A* **99**, 040102, (2019).
[21] A. Carmi, and E. Cohen, On the significance of the quantum mechanical covariance matrix, *Entropy* **20** 500 (2018).
[22] A. Carmi, and E. Cohen, Relativistic independence bounds nonlocality, *Science Advances* **5**, eaav8370, (2019).
[23] N. Brunner, D. Cavalcanti, S. Pironio, V. Scarani and S. Wehner, Bell nonlocality, *Reviews of Modern Physics* **86**, 419–478 (2014).
[24] J.F. Clauser, M.A. Horne, A. Shimony, R.A. Holt, *Physical Review Letters* **23**, 880 (1969).
[25] R. Rangarajan, M. Goggin, and P. Kwiat, Optimizing type-I polarization-entangled photons, *Optics Express* **17** 18920-18933 (2009).

SUPPLEMENTARY MATERIAL FOR EXPERIMENTAL TESTS OF MULTIPLICATIVE BELL INEQUALITIES

Here we derive the richer CHSH and Multiplicative Bell inequalities for $n = 2$. Let us define the Pearson correlations in a standard Bell-CHSH experiment as,

$$\rho_{ij} \stackrel{\text{def}}{=} \frac{\langle A_i B_j\rangle - \langle A_i\rangle\langle B_j\rangle}{\Delta_{A_i}\Delta_{B_j}}, \tag{S1}$$

where the variances are $\Delta^2_{A_i} = \langle A_i^2\rangle - \langle A_i\rangle^2$ and $\Delta^2_{B_j} = \langle B_j^2\rangle - \langle B_j\rangle^2$. In any theory satisfying the generalized uncertainty relation presented in [1], the principle of relativistic causality implies

$$\begin{bmatrix} 1 & \eta_A \\ \eta_A^* & 1 \end{bmatrix} \geq \begin{bmatrix} \rho_{0j} \\ \rho_{1j} \end{bmatrix} \begin{bmatrix} \rho_{0j} & \rho_{1j} \end{bmatrix} \tag{S2a}$$

$$\begin{bmatrix} 1 & \eta_B \\ \eta_B^* & 1 \end{bmatrix} \geq \begin{bmatrix} \rho_{i0} \\ \rho_{i1} \end{bmatrix} \begin{bmatrix} \rho_{i0} & \rho_{i1} \end{bmatrix} \tag{S2b}$$

for $i, j \in \{0, 1\}$, where η_A and η_B are two complex numbers satisfying $|\eta_A| \leq 1$, $|\eta_B| \leq 1$, and η^* denotes the complex conjugate of η. Quantum mechanics satisfies both relativistic causality and the generalized uncertainty relations [1], for

$$\eta_A \stackrel{\text{def}}{=} \frac{\langle A_0 A_1\rangle - \langle A_0\rangle\langle A_1\rangle}{\Delta_{A_0}\Delta_{A_1}}, \quad \eta_B \stackrel{\text{def}}{=} \frac{\langle B_0 B_1\rangle - \langle B_0\rangle\langle B_1\rangle}{\Delta_{B_0}\Delta_{B_1}}. \tag{S3}$$

It was also shown in [1] that following Tsirelson-like bounds stem from (S2) and (S3),:

$$|\text{CHSH}| \leq \min\left\{ \sqrt{2}\left(\sqrt{1+\text{Re}(\eta_A)} + \sqrt{1-\text{Re}(\eta_A)}\right), \ 2\sqrt{2}\sqrt{1-\text{Im}(\eta_A)^2}\right\} \leq 2\sqrt{2} \tag{S4a}$$

$$|\text{CHSH}| \leq \min\left\{ \sqrt{2}\left(\sqrt{1+\text{Re}(\eta_B)} + \sqrt{1-\text{Re}(\eta_B)}\right), \ 2\sqrt{2}\sqrt{1-\text{Im}(\eta_B)^2}\right\} \leq 2\sqrt{2} \tag{S4b}$$

where $\text{CHSH} \stackrel{\text{def}}{=} \rho_{00} + \rho_{10} + \rho_{01} - \rho_{11}$ is the Bell-CHSH parameter.

For real η, Eq. (S4) transforms to,

$$|\text{CHSH}| \leq \sqrt{2}\left(\sqrt{1+\eta_A} + \sqrt{1-\eta_A}\right) \leq 2\sqrt{2} \tag{S5a}$$

$$|\text{CHSH}| \leq \sqrt{2}\left(\sqrt{1+\eta_B} + \sqrt{1-\eta_B}\right) \leq 2\sqrt{2} \tag{S5b}$$

For the multiplicative Bell parameter, $\mathcal{B}_2$, using the inequality of geometric and arithmetic means and using Eq. S5a,

$$|\mathcal{B}_2| = |(\rho_{00} + \rho_{10})(\rho_{01} - \rho_{11})| \leq \left(\frac{\rho_{00} + \rho_{10} + \rho_{01} - \rho_{11}}{2}\right)^2 \tag{S6}$$

$$\begin{aligned} |\mathcal{B}_2| &\leq \frac{1}{2}\left(\sqrt{1-\eta_A} + \sqrt{1+\eta_A}\right)^2 \\ &= 1 + \sqrt{1-\eta_A^2}. \end{aligned} \tag{S7}$$

In [2], it was also proven that,

$$|\rho_{00} + \rho_{01}| \leq \sqrt{2(1+d)} \tag{S8}$$

$$|\rho_{10} - \rho_{11}| \leq \sqrt{2(1-d)}, \tag{S9}$$

where, $d = \langle\{A_0, A_1\}\rangle/2$, and $\{A_0, A_1\}$ is the anti commutator of the local operators A_0, and A_1. For a maximally entangled state like the singlet state, the expectation values of the local operators are zero, and $d = \eta_A$. From Eq. S8, and Eq. S9,

$$|\mathcal{B}_2| = |(\rho_{00} + \rho_{01})(\rho_{10} - \rho_{11})| \leq 2\sqrt{1-\eta_A^2}. \tag{S10}$$

The role of local correlations in determining the non local, Alice-Bob correlations is evident in all these characterizations. Using the above definitions, one may also recognize

$$|\eta_A|^2 = \mathrm{Re}(\eta_A)^2 + \mathrm{Im}(\eta_A)^2 \leq 1, \quad |\eta_B|^2 = \mathrm{Re}(\eta_B)^2 + \mathrm{Im}(\eta_B)^2 \leq 1 \tag{S11}$$

as the Schrödinger uncertainty relations of Alice's A_0 and A_1, and of Bob's B_0 and B_1.

* eliahu.cohen@biu.ac.il

[1] A. Carmi, and E. Cohen, Relativistic independence bounds nonlocality, *Science Advances*, **5**, eaav8370, (2019).
[2] A. Carmi, and E. Cohen, On the significance of the quantum mechanical covariance matrix, *Entropy* **20,7** 500 (2018).

Chapter 4

Conclusion

In conclusion, we provided a comprehensive theoretical study of quantum entanglement and correlations, and presented experimental results on testing the multiplicative Bell inequalities, approaching the quantum limits upto fairly large number of local measurement devices n. We were also able to obtain new tighter inequalities for $n = 2$, and experimentally test them.

In Chapter 2, we presented a broad and comprehensive overview of quantum entanglement, focusing on local, crypto-nonlocal, and non-local hidden variable theories. We discussed some historically interesting and relevant thought experiments that played integral part in the development of quantum physics, and which still continue to be relevant in the studies of quantum foundations. Presenting the proofs of several Bell type inequalities, we attempted to explain and distinguish quantum entanglement with classical theories. Several intriguing concepts, such as quantum contextuality, single particle nonseperability, and N00N states were also discussed. We concluded with the other side of the picture, i.e the extent of the quantum correlations.

In Chapter 3, we picked up on this, by introducing the multiplicative Bell inequalities, a class of inequalities based on the quadratic products of two-point correlators. The Tsirelson or quantum bound for these could be easily obtained from the quantum covariance matrix, and the principle of "relativistic independence" [37]. We also derived new classical and quantum bounds for these multiplicative Bell inequalities and experimentally tested them. We were able to obtain the multiplicative Bell parameters way beyond the classical limits, thus again falsifying local realistic theories. The results also approach the respective Tsirelson bound. We were also able to experimentally observe the tighter theoretical bounds on the CHSH and the Bell parameter, $\mathcal{B}_2$, lending support to the claim that quantum correlations arise from the locality of uncertainty relations [37]. We believe these theoretical and experimental works serve to further enhance the study of quantum correlations. In addition to their theoretical merit in the foundational study, Bell inequalities and their violation, are extremely useful in quantum information science [15], serving as a metric and providing a way of certifying secure quantum communication [17] and randomness [16, 17]. These new class of multiplicative also posses an additional property of being more robust to detector inefficiencies [19], than additive Bell inequalities, thus useful in

closing the detector efficiency loophole and also better suited for the use in cryptographic protocols in such situations. We expect these results to be significant in the fundamental and practical studies of quantum correlations and non locality, quantum game theory and quantum information science.

References

[1] I. N. Levine, D. H. Busch, H. Shull, Quantum chemistry, Upper Saddle River, NJ: Prentice Hall (2000).

[2] A. Szabo, N.S. Ostlund, Modern quantum chemistry: introduction to advanced electronic structure theory Courier Corporation (2012).

[3] A. Halpin *et al.*, Two-dimensional spectroscopy of a molecular dimer unveils the effects of vibronic coupling on exciton coherences, *Nat. Chem.* **6**, 196 (2014).

[4] N. Lambert, Y-N. Chen, Y-C Chen, C-M. Li, G.Y. Chen, and F. Nori, Quantum Biology, *Nat. Phys.* **9**, 10-18 (2013).

[5] H. B. Gray, J. R. Winkler, Electron tunneling through proteins, *Q. Rev. Biophys.* **36**, 341-372 (2003).

[6] G.S. Engel *et al.*, Evidence for wavelike energy transfer through quantum coherence in photosynthetic systems, *Nature* **446**, 782 (2007).

[7] M. A. Nielsen and I. Chuang, Quantum computation and quantum information, Cambridge University Press (2000).

[8] P. Benioff, The computer as a physical system: A microscopic quantum mechanical Hamiltonian model of computers as represented by Turing machines, *J. Stat. Phys.* **22**, 563-591 (1980).

[9] R.P. Feynman, Simulating physics with computers, *Int. J. Theor. Phys.* **21**, 467-488 (1982).

[10] D.P. DiVincenzo, Quantum computation, *Science* **270**, 255-261 (1995).

[11] D. Deutsch, Quantum theory, the Church-Turing principle and the universal quantum computer, *Proc. R. Soc. Lond. A* **400**, 97-117 (1985).

[12] M. Genovese, Research on hidden variable theories: A review of recent progresses, *Phys. Rep.* **413**, 319-396, (2005).

[13] J. S. Bell, On Einstein-Podolsky-Rosen Paradox, *Physics* **1**, 195 (1964).

[14] A. J. Leggett, Nonlocal hidden-variable theories and quantum mechanics: An incompatibility theorem,*Foundations of Physics*, **33**(10), 1469-1493, (2003).

[15] N. Brunner, D. Cavalcanti, S. Pironio, V. Scarani, S. Wehner, Bell nonlocality. Rev. Mod. Phys. 86, 419 (2014).

[16] S. Pironio, *et al.*, Random numbers certified by Bell's theorem, *Nature* 464.7291, 1021-1024 (2010).

[17] A. Acín, N. Brunner, N. Gisin, S. Massar, S. Pironio, and V. Scarani, Device-independent security of quantum cryptography against collective attacks, *Physical Review Letters*, **98(23)**, 230501, (2007).

[18] B. S. Cirel'son, Quantum generalizations of Bell's inequality, *Letters in Mathematical Physics*, **4(2)**, 93-100, (1980).

[19] A. Te'eni, B. Y. Peled, E. Cohen, and A. Carmi, Multiplicative Bell inequalities, *Physical Review A* **99**, 040102, (2019).

[20] A. Einstein, B. Podolsky, and N. Rosen, Can quantum-mechanical description of physical reality be considered complete?, *Physical review*, **47(10)**, 777, (1935).

[21] J.F. Clauser, M.A. Horne, A. Shimony, R.A. Holt, *Phys. Rev. Lett.* **23**, 880 (1969).

[22] D. Paneru, E. Cohen, R. Fickler, R. W. Boyd, and E. Karimi, Entanglement: quantum or classical?. *Reports on Progress in Physics*, **83(6)**, 064001 (2020).

[23] S. D. Bartlett, T. Rudolph, and R. W. Spekkens, Reference frames, superselection rules, and quantum information, *Reviews of Modern Physics*, **79(2)**, 555, (2007).

[24] S. A. Babichev, J. Appel, and A. I. Lvovsky, *Phys. Rev. Lett.* **92**, 193601 (2004).

[25] S.M. Tan, D. F. Walls, and M. J. Collett, Nonlocality of a single photon, *Physical review letters*, **66(3)**, 252, (1991).

[26] L. Hardy, Nonlocality of a single photon revisited, *Physical review letters*, **73(17)**, 2279, (1994).

[27] L. Hardy, Hardy replies, *Physical review letters*, **75(10)**, 2065, (1995).

[28] S.J. Van Enk, Single-particle entanglement, *Physical Review A*, **72(6)**, 064306.

[29] A. Peres, All the Bell inequalities, *Foundations of Physics*, **29(4)**, 589-614, (1999).

[30] D. Paneru *et al.*, Entanglement: quantum or classical?, *Reports on Progress in Physics* **83**, 064001 (2020).

[31] S. Popescu, D. Rohrlich, Quantum nonlocality as an axiom. Found. Phys. 24, 379–385 (1994).

[32] J. Oppenheim, S. Wehner, The uncertainty principle determines the non-locality of quantum mechanics. Science 330, 1072–1074 (2010).

[33] M. Pawlowski, T. Paterek, D. Kaszlikowski, V. Scarani, A. Winter, M. Zukowski, Information causality as a physical principle. Nature 461, 1101–1104 (2009).

[34] N. Linden, S. Popescu, A. J. Short, A. Winter, Quantum nonlocality and beyond: Limits from nonlocal computation. Phys. Rev. Lett. 99, 180502 (2007).

[35] N. Gisin, Quantum measurement of spins and magnets, and the classical limit of PR-boxes. arXiv:1407.8122 [quant-ph] (30 July 2014).

[36] D. Rohrlich, Stronger-than-quantum bipartite correlations violate relativistic causality in the classical limit. arXiv:1408.3125 [quant-ph] (13 August 2014).

[37] A. Carmi, and E. Cohen, Relativistic independence bounds nonlocality, *Science Advances* **5**, eaav8370, (2019).

[38] D. Paneru, A. Te'eni, B.Y. Peled, J. Hubble, Y. Zhang, A. Carmi, E. Cohen, and E. Karimi, Experimental tests of Multiplicative Bell Inequalities, arXiv preprint arXiv:2009.03930, 2020.